JASON MITCHELL BROWN
Studies on the Mechanisms and Significance of Ciliary Biogenesis in *Tetrahymena thermophila*
(Under the Direction of JACEK GAERTIG)

Cilia are microtubule-based organelles adapted to multiple functions in eukaryotic organisms, including locomotion, feeding, movement of extracellular fluid, and various sensory functions. The highly conserved ultrastructure of the cilium is assembled from over 250 proteins which are delivered from the cytoplasm to their sites of incorporation in the growing organelle. This transport is tightly regulated to coincide with the cell cycle, maintain proper ciliary length and number, and ensure that cilia can regenerate if damaged or lost. Intraflagellar transport (IFT), the movement of protein raft particles within cilia and flagella, has been implicated in ciliary assembly in multiple organisms, but the specific function of IFT remains unknown. The results presented here explore the mechanisms and significance of IFT in the ciliate, *Tetrahymena thermophila*. In the first study, genes encoding two motor subunits, *KIN1* and *KIN2*, of the kinesin-II molecular motor, were cloned and disrupted in *Tetrahymena*. Disruption of either subunit alone resulted in mild phenotypic defects. Disrupting both genes led to a complete loss of cilia and an inability to undergo normal cytokinesis. Localization studies revealed that kinesin-II accumulated in actively assembling cilia. Multiple results of this study lead us to propose that the cytokinesis defects in the kinesin mutants were a secondary effect caused by loss of motility. In the second study, the connection between ciliary motility and cytokinesis was examined further. This study describes a type of motility, which we call “rotokinesis”, where the posterior daughter of a dividing cell rotates unidirectionally around the membrane bridge connecting the two daughters. We propose that this rotation increases the efficiency of cytokinesis in cells with wildtype motility. In the final study,

RFT1, a homologue of one of the IFT raft proteins, was cloned and disrupted. The *RFT1* null phenotype is identical to the kinesin-II null phenotype, suggesting these genes are in the same pathway. Excitingly, we isolated *RFT1* suppressors which assemble intermediate length cilia in a temperature-sensitive and cell density-dependent manner, suggesting that RFT1 is not absolutely required for transport of ciliary structural components. This study provides the first evidence that IFT rafts may have a signaling function.

INDEX WORDS: Kinesin-II, Intraflagellar transport, Ciliary assembly, *Tetrahymena*, IFT52, OSM-6, Cytokinesis, Cytoskeleton, Gene disruption

STUDIES ON THE MECHANISMS AND SIGNIFICANCE OF CILIARY BIOGENESIS IN *TETRAHYMENA THERMOPHILA*

by

JASON MITCHELL BROWN

B.S., The University of Georgia, 1994

A Dissertation Submitted to the Graduate Faculty of The University of Georgia in Partial Fulfillment of the Requirements for the Degree

DOCTOR OF PHILOSOPHY

ATHENS, GEORGIA

2001

STUDIES ON THE MECHANISMS AND SIGNIFICANCE OF CILIARY BIOGENESIS IN *TETRAHYMENA THERMOPHILA*

by

JASON MITCHELL BROWN

Approved:

Major Professor: Jacek Gaertig

Committee: Kelly Dawe
Marcus Fechheimer
Claiborne Glover
Edward Kipreos

Electronic Version Approved:

Gordon L. Patel
Dean of the Graduate School
The University of Georgia
December 2001

DEDICATION

The work presented here is dedicated to Gina, Seth, Carlie and Lamont. As anyone who has been through it knows, a successful graduate school experience often means complete immersion in work at the expense of time spent with those we love. Gina, if it were not for your tireless love and support, this work would of course never have been completed. Seth, you are the new joy in my life and I cannot imagine where I would be if you had not arrived. Carlie and Lamont, you never once asked me how I did on a test or whether my experiments were working, you were just always happy to see me without question. For these reasons and many more every other aspect of my life would be meaningless without my family.

ACKNOWLEDGMENTS

I would like to express my deep gratitude to a great number of people that played a part in the completion of this work. First, I would like to thank my major professor and friend, Jacek Gaertig. When we met almost seven years ago I certainly did not know that I would complete a Ph.D. under his guidance, but I knew instantly that before our work together was finished his intellectual excitement would have a major impact on my life. This initial impression has proven true multiple times over. Thanks to Dr. Gaertig for constant encouragement and firm coaxing at just the right times. Thanks also to my committee members Kelly Dawe, Claiborne Glover, Edward Kipreos, and Marcus Fechheimer for their steady guidance and constant advice to set reasonable goals. In addition to his role as a committee member, special thanks must go to Dr. Fechheimer. Without his advice and assistance in more than one time of crisis I certainly would have thrown up my hands in desperation long ago.

My parents Lois and Ted Brown deserve a large measure of the credit for the work presented here. Their constant encouragement to do what I love has sent me on a lifelong quest to find things that stimulate me intellectually and emotionally, one of which perhaps inevitably turned out to be science. Sometimes this quest has led me down difficult paths, but my parents' support has never wavered. Special thanks go also to Roy and Martha Franklin and Tina, Don, Ethan, and Caroline Black. For the past nine years they have never questioned the sometimes crazy turns I have taken with their daughter, sister, sister in-law, and aunt (or at least if they have, they have not let me know it!). Loving thanks also to my grandparents. Although three of them are no longer with

us here on earth, I never cease to feel their presence at important times in my life.

Numerous other people have played direct roles in the work presented here. Some of them are co-authors on the papers presented in this document and some are not, but all made significant contributions. Thanks to Christine Marsala whose experimental contribution to the kinesin-II story played a pivotal role in assuring *Tetrahymena's* place at the IFT table. Christine was responsible for the cloning and characterization of the *KIN2* gene as well setting the stage for the initial characterization of the kinesin-II double knockout phenotype. Special thanks to Frank Hardin, whose keen observation that *Tetrahymena* cells rotate during cell division led us to take a closer look at this process. Frank's enthusiasm as an undergraduate simply working on a class project was infectious and helped teach me that I love to teach. My sincerest gratitude goes to Yan Gao and Rupal Thazhath for their work above and beyond the call of duty to help in the completion of the *RFT1* paper. Yan performed the 2D gel analysis and Rupal performed the quantitative EM. Yan and Rupal in addition to Lu Xia, Kenta Fujiu, Hiroko Kojima, Krzysztof Rogowski, Chengbao Liu, Dorota Wloga and Dylan Burnette were a constant source of friendship and intense scientific inspiration without whose contributions this work would never have progressed this far. Early on, Roman Kosoy provided not only experimental assistance but also intellectual input in the design and assembly of the *KIN1-myc* construct. Several other UGA undergraduates worked diligently at the bench to complete many of the pieces of this project as well as work that did not make it onto these pages. These students include Wood Pope, Brett Margolias, Curtis McNiff, Naishaj Shah and Kelly Fair. Thanks also goes to multiple members of the UGA Cellular Biology Department who were always willing to help, including faculty and fellow graduate students as well as technical and office staff. In addition, my gratitude goes out to multiple faculty, staff and students at Young Harris College. They have been an inspiration during the completion of this dissertation. In particular, I would like to thank

Lynne Nation for her assistance with statistical analysis of the RFT1 data as well as for her constant encouragement.

Finally, as with almost any scientific endeavor, this work was supported by a group of colleagues who kindly provided materials, time, and/or advice. These include Dr. Donna Cassidy-Hanley who helped our lab get up to speed on using the biolistic gun. Thanks to Dr. Mark Farmer and Dr. John Shields (Center for Advanced Ultrastructural Research, University of Georgia) for their constant willingness to provide advice and assistance with all things related to microscopy. Dr. Farmer made a special contribution to some of my early *Tetrahymena* images by showing me how to collect DAPI images on the confocal microscope. I thank Jian Zhao Shen for assistance in preparation of thin sections for electron microscopy in the kinesin-II work. Thanks also to Dr. Mitchell Bernstein, Dr. Peter Satir and Aashir Awan (Albert Einstein College of Medicine) for providing the sequence of the cloned KIN5 gene fragment and numerous discussions regarding the kinesin-II project. Thanks to Dr. Nicolette Levilliers (University Paris-Sud, Paris, France) for providing the TAP952 and AXO49 antibodies, Dr. Marty Gorovsky (University of Rochester, Rochester, NY) for the SG anti-body, Dr. David Allis (University of Virginia, Charlottesville, VA) for the anti-histone hv1 antibodies, Dr. Karl Saxe (Emory University, Atlanta, GA) for providing the bsr plasmid, Dr. Keith Kozminski for providing the Myc construct, and Dr. Aaron Turkewitz for the GFP construct. Thanks to Dr. Joel Rosenbaum and Dr. Doug Cole for numerous discussions, important insights and inspiring published work, all of which constantly made me strive to work better and faster. I am especially grateful to Dr. Ronald Pearlman (York University) for providing the *RFT1* cDNA (*Tetrahymena* EST project clone 213) and agreeing to sideline his own non-IFT-related interests in this gene. Assistance with synthesis of oligonucleotides and DNA sequencing was provided by the UGA Molecular Genetics Instrumentation Facility. Finally, I have saved one of the most important targets for thanks until the end. Of course none of the work we do would be possible without

funding. In particular, this work was supported by grants from the National Institutes of Health and the American Cancer Society to J.G. and by university-wide and teaching assistantships which defray part of the expense of my salary. Sincerest thanks to these funding sources for their support.

TABLE OF CONTENTS

Page

CHAPTER 1

INTRODUCTION

Cilia are complex organelles which have been the subject of research interest since they were first described over three hundred years ago (reviewed by Satir 1995). Organisms which assemble cilia range from protists which use cilia for locomotion and feeding to mammals which have ciliated tissues involved in multiple functions. These functions include respiration, reproduction, and sensory perception, including vision, olfaction, and hearing, as well as determination of left-right asymmetry during early embryonic development. Cilia are composed of over 200 distinct polypeptides, most of which are organized into a central microtubule-based core, the axoneme, which projects from the basal body and is surrounded by the ciliary membrane. The microtubules of the axoneme are arranged in a cylinder with 9 doublet microtubules forming the wall of the cylinder and a pair of singlet microtubules forming a hub in the center. The force necessary for ciliary beating is generated by the molecular motor, dynein, which is organized into two rows of dynein arms attached to the side of each outer doublet. The ciliary beat is regulated by radial spokes bridging the space between the central pair and the outer doublets. Disease states such as the immotile cilia syndrome make it clear that improper assembly of these ciliary structures can have detrimental effects on human health. Because only a small fraction of all ciliary components have been characterized, it is likely that there are additional human diseases resulting from ciliary dysfunction. The assembly of cilia and flagella is a complex process involving synthesis and preassembly of structural subunits inside the cell body, transport of these subunits along the axonemal microtubules, and incorporation at the distal ends. Large protein complexes known as rafts (not to be confused with lipid rafts) are known to move at high speed inside flagella.

This assembly-related motility is known as intraflagellar transport (IFT) and is believed to be responsible for assembly of cilia and flagella.

The objective of my dissertation project was to study the mechanisms of assembly of cilia in the ciliated protozoan model, *Tetrahymena thermophila*. *Tetrahymena* is a nearly ideal organism for studying ciliary assembly since it can be grown to high densities and cilia can be isolated in large quantities for biochemical analyses. *Tetrahymena* can be routinely studied using classical (Mendelian) genetic methods. In addition, the recent development of high frequency DNA-mediated transformation and the discovery that introduced DNA is incorporated exclusively by homologous recombination make gene replacement and knockout routine in this organism.

This dissertation is organized into six chapters. Chapter 2, is a review of the literature covering the structure and function of cilia, the current state of knowledge regarding ciliary assembly, and the roles of cilia in human health. Chapters 3-5 describe my own studies on ciliary assembly in *Tetrahymena*. The third chapter describes the cloning and functional characterization of two members of the kinesin-II family of ciliary molecular motors from *Tetrahymena*. Disruption of both genes led to a dramatic phenotype that included an inability to assemble and maintain cilia and arrest in cytokinesis. Chapter 4 describes a previously unknown type of cytokinesis, named rotokinesis, which involves cilia-dependent whole cell locomotion. This study originated from our analysis of the cytokinesis defects in the kinesin-II mutants, which suggested involvement of whole cell motility in the terminal stage of cell fission during cytokinesis. Chapter 5 describes the cloning and disruption of *RFT1*, a gene encoding a putative kinesin-II cargo protein and the isolation of suppressor strains of mutants lacking *RFT1*. The phenotype of these suppressors suggests a possible signaling function for the *RFT1* gene product, required for maintaining ciliary assembly-associated transport. The final chapter summarizes conclusions drawn from my studies and proposes experiments to further this line of research.

REFERENCES

Satir P: Landmarks in cilia research from Leeuwenhoek to us. *Cell Motil Cytoskel* 1995, 32: 90-94.

CHAPTER 2

REVIEW OF LITERATURE

Axonemal Structure

At the core of all cilia and flagella is a microtubule-based structure known as the axoneme (reviewed by Dutcher 1995). A typical motile axoneme has nine outer doublet and two central singlet microtubules. Each doublet consists of an A tubule with 13 protofilaments and a B tubule with 11 protofilaments. The doublets are arranged in a circle so that when the axoneme is viewed from the base toward the tip, the A tubules face clockwise (Lindemann 1997). This precise circular arrangement appears to be based at least in part on fibrous links between the adjacent outer doublets, known as nexin links, that are visible in axonemal cross sections viewed by transmission electron microscopy (Stephens 1970). In addition, the outer doublets are continuous with the two innermost protofilaments of the basal body triplet microtubules. Attached to the A tubules are two types of structures that are involved in generating and regulating axonemal motility. These are the dynein arms and radial spokes (Lindemann 1997). As I will discuss below, two sets of dynein arms, the inner and outer arms, project from the A tubule toward the adjacent B tubule and provide the force necessary for ciliary bending (Gibbons 1965). The radial spokes are believed to help regulate the ciliary bending pattern by coordinating the activities of the numerous dynein arms throughout the axoneme. They project from the A tubules toward the central pair of singlet microtubules (Goodenough 1985). The central pair microtubules have 13 protofilaments and two types of associated projections that are clearly visible by quick freeze deep etch preparations for electron microscopy. Based on the shape of projections it can be determined that each of the two central tubules is structurally unique (Goodenough 1985). The central pair singlets originate from a structure located above the basal body and thus are not continuous with any basal

body microtubules. This structural arrangement of the central singlets may be critical for their regulatory function (Omoto 1999). Since mutants lacking the central pair are paralyzed, these microtubules are believed to be involved in regulating the activity of dynein arms. This regulation appears to occur through transient connections with the radial spokes perhaps mediated by the central pair projections (Goodenough 1985). In motile cilia and flagella, the activities of all these components must be coordinated in order to generate axonemal motility.

The critical role of microtubules in establishing axonemal structure has been emphasized by ultrastructural studies of *Tetrahymena* and *Chlamydomonas* axonemes that established the longitudinal relationship between different axonemal components (Goodenough 1985). The periodicity of all of the major structures in the axoneme is divisible by the size of the building blocks of microtubules, the α/β tubulin dimers. Each tubulin protein is 4 nm in diameter, making the entire tubulin heterodimer have an 8 nm longitudinal measurement (Lodish 1995). Outer dynein arms and the two types of central pair projections have the simplest repeat patterns. The outer arms have a periodicity of 24 nm and have been described as having a substructure shaped like "a croquet mallet" with the mallet head attached to the A tubule and the handle connecting to the B tubule (Goodenough and Heuser 1982), whereas the C1 and C2 central pair projections have periodicities of 32 and 16 nm, respectively (Goodenough 1985). The inner dynein arms and radial spokes have a more complicated repeat pattern. In *Tetrahymena* axonemes, the radial spokes occur in groups of three spokes which repeat from base to tip in the following pattern: spoke S1-32 nm-spoke S2-24 nm-spoke S3-40 nm-next spoke S1. There is considerable controversy in the literature regarding the substructure and distribution of the inner arms. According to Goodenough and Heuser (1985) *Tetrahymena* inner dynein arms attach near the base of each spoke and therefore have the same 32-24-40 nm repeat pattern. While *Chlamydomonas* cells apparently have inner dynein arms with the same spacing as in *Tetrahymena*, they have only two spokes per 96

nm repeat, which correspond in spacing to the S1 and S2 spokes of *Tetrahymena* (Goodenough 1985). Importantly, Taylor et al (1999) point out that there are at least two other models of inner arm distribution, but that all of the existing models may be reconciled by interpreting the electron microscopic data as two dimensional projections of a three dimensional structure viewed from different angles. The repeat pattern of the inner arms is complicated by the fact that there are at least two different morphological forms of the inner arms. The dynein arms positioned adjacent to spokes S1 and S2 have heads with two globular domains known as dyads and the S3-associated inner arm has a globular triad head region (Goodenough 1985).

A more detailed biochemical and ultrastructural analysis of inner dynein arm isoforms revealed another level of complexity in inner arm distribution (Piperno 1991). Each inner and outer dynein arm is a complex of 2-3 heavy chains (which have motor activity) and a number of additional intermediate and light chains. It has been established that there is heterogeneity in the composition of polypeptide chain types among purified dynein arms. By analyzing inner arm dyneins in *Chlamydomonas* mutants with short flagella as well as normal length flagella at early stages of regeneration, Piperno and Ramanis (1991) found that a subset of inner arm dynein polypeptides were added late during flagellar assembly. It was also found that a subset of inner arm dynein heavy chains were extracted from axonemes under different conditions from the rest of the inner arm heavy chains. Electron microscopic analysis of partially extracted axonemes showed that the inner arms were primarily missing from the distal regions of the axoneme (Piperno 1991). Taken together with earlier structural studies, these results suggest that inner dynein arm isoforms may have very complex distribution patterns along the length of the axoneme. This pattern may be important for controlling the ciliary beat pattern (Piperno 1991).

How does the axoneme generate the ciliary beat?

Dynein was first isolated from *Tetrahymena* cilia by Ian Gibbons (1965). He found that the ATPase activity in cilia could be removed by low salt extraction following digitonin treatment to remove the ciliary membrane and release soluble components of the so-called matrix compartment of cilia. Electron microscopic analysis of axonemes revealed that the dynein arms were removed along with the ATPase activity. When the 30S dynein fraction was recombined with extracted axonemes, the dyneins reattached to the outer doublets and the axonemal ATPase activity of axonemes was restored (Gibbons 1965). Satir (1965) analyzed axonemal tips at different stages of axonemal bending by electron microscopy. He showed that during bending the tips moved relative to each other while the length of ciliary tubules remained constant (Satir 1968). Along with the biochemical analysis of dynein ATPase activity, these results suggested a sliding filament model for ciliary bending in which limited translocation of outer doublets relative to each other is powered by the dynein arms.

Further studies using a combination of partial proteolysis and microscopy supported and extended the sliding filament model. When isolated sea urchin axonemes were treated with a low concentration of trypsin and then exposed to ATP and divalent cations, the axonemes disintegrated primarily into individual doublets (Summers 1971). In this study, the optimal conditions for generating the active sliding were very similar to the conditions previously shown to be optimal for reactivating bending of undigested axonemes. This suggested that the two mechanisms were at least very similar (Summers 1971). More detailed analysis of the effects of trypsin digestion on axonemal structure showed that digestion of nexin links and connections between radial spokes and the central pair correlated most with the level of ATP-induced axonemal disintegration. Groups of two or three doublets were often isolated together unless the axonemes were dialyzed in low salt to remove the dynein arms, supporting the idea that these arms form crossbridges between adjacent doublets (Summers 1973). Analysis of microtubule

polarity in telescoping axonemes showed that the direction of sliding doublets was always the same. One doublet always moved the adjacent doublet toward the tip of the axoneme, indicating that dynein arms attached to an A tubule move toward the base of the adjacent B tubule which corresponds to the microtubule minus end. This was the first demonstration that dynein is a minus-end directed microtubule motor (Sale 1977). Since doublet sliding is always in the same direction, there must be some mechanism of coordination so that all dyneins are not actively sliding all tubules at the same time in the same region of the axoneme.

Insight into the regulation of dynein arm activity came from studies in which *Chlamydomonas* paralyzed flagella mutants lacking either radial spokes or the central pair were mutagenized to look for suppressor mutations (Huang 1982). Suppressor strains that restored some flagellar motility were isolated from both classes of original paralyzed flagella mutants. In no case did the suppressor phenotype result from correction of the original ultrastructural defect. Instead, the suppressor strains either had altered mobility of certain polypeptides on one dimensional SDS polyacrylamide gels or they completely lacked certain polypeptides (Huang 1982). One mutation that was able to suppress either radial spoke or central pair mutants had a deletion in one of the components of the 18S outer arm dynein. Two mutants that completely lacked certain outer arm polypeptides restored function to the radial spoke defective mutants but not the central pair defective mutant. These suppressor mutations suggested that force generation by dynein arms is normally inhibited and that this inhibition is released by interaction of the central pair with the outer doublets through the radial spokes (Huang 1982). Further support for this idea came from reconstitution experiments in which extracted axonemes and dynein-containing axonemal extracts were combined from two different mutants (Smith 1992). The pf28 mutant lacks outer dynein arms, but is motile (Mitchell 1985). This allowed the investigators to focus on the activity of the inner dynein arms which are both necessary and sufficient for motility (see below). The

pf14pf28 double mutant lacks both outer dynein arms and radial spokes. The assay was to measure the velocity of doublet sliding during ATP-induced axoneme disintegration following reconstitution with different combinations of axonemes and extracts (Smith 1992). The sliding velocity of pf28 and pf14pf28 mutant axonemes was 1.3 and 0.5 μm/s, respectively. When the pf28 dynein extract was added to either pf28 or pf14pf28 extracted axonemes, the sliding velocity was indistinguishable from the unextracted pf28 axonemes. This was also the case when pf14pf28 dynein extract was added to pf28 extracted axonemes, suggesting that contact with the pf28 axonemes is able to activate the reconstituted pf14pf28 dynein arms. In contrast, the pf14pf28 extracted axonemes did not activate the pf14pf28 dyneins as shown by a sliding velocity equivalent to the unextracted pf14pf28 axonemes. Since the only difference between these two mutants was the presence or absence of radial spokes these experiments strongly support the hypothesis that radial spokes can activate inner dynein arms (Smith 1992).

Subsequent experiments measuring sliding velocities after reconstitution of spoke-deficient mutant axonemes in the presence of kinase inhibitors showed that inhibition of axonemal kinases was sufficient to restore wildtype sliding velocities to the spoke-less mutant axonemes. This suggests that radial spokes function by inhibiting the axonemal kinase or activating a phosphatase (Howard 1994). Similar studies using phosphatase inhibitors suggest that an axonemal phosphatase is a critical component in the regulation of dynein activity (Habermacher 1995). Importantly, both kinases and phosphatases have been found in the *Chlamydomonas* axoneme near the attachment site for the I1 inner arm dynein (Porter and Sale 2000). Radial spoke protein RSP3, located near the base of the spoke, has been identified as an A-kinase anchoring protein (Gaillard 2001). In addition, casein kinase 1 is located on the outer doublet microtubules and inhibitors of this kinase increase axonemal microtubule sliding in mutants lacking a central pair or radial spokes (Yang and Sale, 2000). In support of the importance of phosphatases in controlling axonemal dynein activity, protein phosphatase type 1 and

protein phosphatase 2A have both been found to be anchored tightly to the outer doublet microtubules, perhaps in position to directly dephosphorylate and activate innner or outer arm dyneins (Yang 2000).

Further regulation of the ciliary beat pattern may also be due to mechanical constraints imposed by axonemal modifications in various organisms. According to the sliding filament model, axonemal bending is created by the torque produced when dynein arms push their associated doublet microtubules against the stationary basal body (Lindemann 1997). The bend in a ciliary beat pattern is typically planar, which suggests that there is a mechanism for restricting the ciliary bending to the beat plane. Two structural features of the axoneme may contribute to restricting the beat plane to varying degrees in different organisms. In some types of axonemes, including those in mammalian sperm flagella, there is evidence that two of the radial spokes are not as free to detach from the central pair as are the rest of the spokes. These stable connections effectively form a bridge across the axoneme perpendicular to the plane of the beat (Lindemann 1992, Lindemann 1997). Also, axonemes in some organisms have an apparently stable connection between outer doublets five and six. This limits the extent to which these two doublets could slide relative to one another and thus limits bending in a plane perpendicular to the normal beat plane (Lindemann 1997). In some organisms, rotation of the central pair may be involved in radial spoke-mediated coordination of dynein arm activity (Omoto 1999). Structural studies suggest that the helical arrangement of radial spokes and central pair projections around the axoneme may act as an axonemal spring that would be deformed by central pair rotation (Goodenough 1985). It remains to be tested whether this proposed spring acts as an additional mechanical constraint on the ciliary beat pattern.

What is the minimal machinery necessary for ciliary/flagellar beating?

Many studies have focused on determining which axonemal components are required for ciliary motility. Screens for *Chlamydomonas* flagellar mutants have lead to

the isolation of mutants in many of these components (Adams 1981, Huang 1977, Huang 1979, Huang 1981, Huang 1982, Kamiya 1991, Mitchell 1985). These include mutants partially or completely lacking either inner or outer dynein arms (Huang 1979, Kamiya 1991, Mitchell 1985), radial spokes (Huang 1981), and all or part of the central pair (Adams 1981). Mutants lacking portions of inner or outer dynein arms suggested that these components may be critical for motility (Huang 1979). Isolation of additional mutants has further clarified the contributions of each type of dynein arm to axonemal motility. First, as described above, the pf28 mutant isolated by Mitchell and Rosenbaum (1985) completely lacked outer dynein arms, but retained a relatively normal flagellar beat shape and swimming pattern. The swimming velocity of these mutants was reduced by approximately 30%, which appeared to be due to a 45% reduction in flagellar beat frequency. These results showed that the inner dynein arms are sufficient for flagellar beating, and therefore the outer dynein arms are not required for beating (Mitchell 1985).

Unlike the outer dynein arms, the inner arms are necessary for flagellar beating. In a screen designed to enrich for inner arm mutants, Kamiya et al (1991) generated two classes of mutants, each of which lack one of two projections of the inner dynein arms. The outer projection points toward the B tubule of the adjacent doublet and is missing in idaA mutants, whereas the inner projection points toward the center of the axoneme and is lacking in idaB mutants. When they analyzed motility, the idaA mutants swam at approximately half the rate of wildtype cells with a beat frequency about half of wildtype. On the other hand, the idaB mutant had motility about two-thirds that of wildtype cells, but with normal beat frequency (Kamiya 1991). Double mutants constructed between idaA and idaB class mutants lacked both the inner and outer projections of the inner dynein arms and were immobile. Therefore, the inner dynein arms consist of two rows of projections and the rows seem to have different functions. In addition, substantial defects in the inner arms can lead to immobility, suggesting that, unlike the inner arms, the outer arms are not sufficient for motility (Kamiya 1991).

As mentioned earlier, the central pair and radial spokes are not absolutely required for flagellar motility since mutants could be isolated which suppress the motility defects of mutants lacking either of these components (Huang 1982). The current model is that modulation of dynein arm activity by the central pair acting through the radial spokes is involved in controlling the beat pattern rather than establishing the beat. This model is supported by the existence of organisms with motile axonemes which completely lack a central pair. The simplest axoneme described to date is in the flagellum of the protozoan, *Diplauxis hatti*. Although this axoneme consists of only three microtubule doublets with no associated central pair, it was found to be motile with a helical beat pattern (Prensier 1980). A similar result was obtained from a comparison between the beat patterns of Asian and American horseshoe crab sperm flagella (Ishijima 1988). This comparison is significant since the flagella from these closely related species seem to differ only in the fact that the American crabs have 9+2 axonemes, whereas the Asian crabs have 9+0 axonemes. Recordings generated by high speed video microscopy allowed the analysis of beat patterns. For the American crab 9+2 axonemes, when the flagellar beat was viewed “from the side” (in a focal plane parallel to the swimming path of the sperm) the entire length of the flagellum was in focus in all images. Also, when the 9+2 flagella were viewed “from the top” the portions of the flagella that came into focus traced a relatively straight line. This indicated that the beat pattern was planar. For the 9+0 Asian axonemes, the beat pattern was a right-handed helix. This is evident because when flagella were recorded with the focal plane parallel to the swimming path of the sperm, that is, either from the top or from the side, only portions of the sperm tail were in focus at any given focal plane. By focusing at different levels from the top to the bottom of the beat envelope and tracing the portions that were in and out of focus with solid and dashed lines, respectively, they found that the beat pattern was a right handed helix (Ishijima 1988). Thus, these results support the conclusions of other studies which have suggested that there is a default helical beat in the absence of a central pair and that

the central pair serves to coordinate the activity of dynein arms to generate the more efficient planar beat. This coordination by the central pair may involve its known high-speed rotation. According to the so-called alternator model, the rotating central pair activates radial spokes which in turn regulate the peripheral dyneins in a sequence controlled by the direction and rate of rotation (Omoto 1999). One important aspect of regulation of the ciliary beat is the previously mentioned fact that all the axonemal dynein arms slide doublets in the same direction. Therefore, if all dynein arms actively moved along outer doublets at the same time there would be no net bending of the axoneme. Satir and his colleagues have proposed a "switch point" model in which only half of the axoneme is active at any one time. Another aspect of this model is that there is a point at which the dynein arms on one side have bent the axoneme as far as it will go in a particular direction (either active or recovery stroke) and at this point the dyneins on the other side of the axoneme would become active. There is some evidence that such a switch could be regulated by alternating contact between the radial spokes and the central pair (Satir 1989).

Ciliary assembly and IFT

Given the complexity of ciliary ultrastructure, an important question is how over 250 different proteins are correctly assembled to form the machinery responsible for the ciliary beat. Early studies of flagellar assembly in *Chlamydomonas* addressed the sites of incorporation of newly translated flagellar proteins (Rosenbaum 1969, Witman 1975). In these experiments, all proteins in the cell were radiolabeled during flagellar regeneration when the regenerating flagella were approximately half-length. It was found that most of the radiolabel was incorporated into the distal region of the flagella (Rosenbaum 1969, Witman 1975). Since protein translation machinery, including ribosomes, has never been observed inside cilia or flagella, these experiments suggested that newly made proteins are transported from the cell body (which is defined here as the part of the cell outside of axonemes) to the flagellar tip. However, since all proteins were labeled, these

experiments did not address the transport and incorporation of specific flagellar components. Over 20 years later, Johnson and Rosenbaum (1992) began to shed some light on this question using a dikaryon technique. This approach takes advantage of the observation that *Chlamydomonas* cells can be induced to mate and therefore share a common cytoplasm, which enables exchange of proteins produced by two distinct genomes before formation of the zygote (Johnson and Rosenbaum 1992). In their experiments, a wildtype cell line was mated with cells expressing an epitope tagged α-tubulin. Using immunofluorescence, these authors found that the tagged tubulin was incorporated into both outer doublet and central pair microtubules at the tip of regenerating flagella. In addition, following formation of dikaryons between wildtype cells and a spokeless mutant, radial spoke proteins were incorporated into mutant flagella at their distal tip (Johnson and Rosenbaum 1992).

In a similar experiment, Piperno et al (1996) studied the incorporation of inner and outer dynein arm proteins into mutant axonemes. They made dikaryons by mating *ida4*, a null mutant for p28, an inner dynein arm light chain, to wildtype cells and staining at different time points with anti-p28 antibodies. The wildtype axonemes were stained early but the mutant axonemes were not. At later time points they first found p28 in basal bodies of mutant cells followed by incorporation into the tip of the mutant axoneme. At even later time points the entire *ida4* axoneme was labeled by the p28 antibody. Surprisingly, when they repeated the experiment with a mutant in IC69, an outer dynein arm intermediate chain, they found that IC69 was incorporated along the entire length of the mutant axoneme instead of being initially concentrated at the tip (Piperno 1996). Taking their results together with those of Johnson and Rosenbaum (1992), these authors suggested that perhaps proteins or complexes, such as radial spokes and inner dynein arms that must bind inside the axoneme, have to be transported to the tip to access their binding sites. On the other hand, proteins such as outer dynein arm proteins, which bind to the outside of the axoneme, could bind along the length of the flagellum without first

going to the tip (Piperno 1996). It is important to consider that axonemal microtubules have uniform polarity, with their plus ends (having a crown of β-tubulin) at the distal tip. This polarity is consistent with the basal body being attached to the proximal end of axonemes and acting as a microtubule nucleation center.

Since proteins apparently are not made within cilia or flagella, the polarity of assembly of certain axonemal components suggests two possible mechanisms of transport and incorporation of components at the distal ends. The first possibility is that components could diffuse from the cell body into the flagellum, but the sites of incorporation could be masked everywhere except at the tip. The second possibility is that there is an active transport mechanism such as a molecular motor that moves components to the tip. Several observations supported the possibility of an active transport mechanism but also do not invalidate the possible importance of masking in addition to active transport. First, Kozminski et. al. (1993) used video enhanced differential interference contrast microscopy to study flagella of a *Chlamydomonas* paralyzed flagella mutant. Surprisingly, they observed bidirectional movement of particles under the flagellar membrane. This motility was named intraflagellar transport or IFT and the particles were named rafts (Kozminski 1993, 1995). A year later, two studies suggested that one or more kinesin-related proteins might be involved in IFT and that IFT might be required for flagellar assembly. Fox et al (1994) showed, using pan-kinesin antibodies to probe western blots of flagellar proteins, that there is a small group of kinesin-like proteins in *Chlamydomonas* flagella. Second, Walther et al (1994) showed that the previously isolated flagellar assembly ts mutant, *fla10*, had a point mutation in a kinesin related protein. Homologs of FLA10 in other organisms form a subgroup of kinesins named kinesin-II. Further analysis of the role of FLA10 kinesin-II in IFT and flagellar assembly convincingly showed the following: 1) the IFT particles observed by DIC correspond to protein rafts observed by electron microscopy between the outer doublets and the flagellar membrane; 2) induction of the *fla10* ts phenotype

leads to a reduction in the number of rafts and a cessation of IFT immediately prior to the onset of flagellar resorption; 3) by immunoEM it was found that the FLA10 protein was located between the outer doublet microtubules and the flagellar membrane, placing it in the proper location to transport the IFT particles toward the flagellar tip (Kozminski 1995). Despite the fact that FLA10 has not been found to be directly associated with rafts, it is possible that available fixation methods do not preserve the motor-raft linkages sufficiently for detection.

The motors driving IFT

Kinesin-II has been purified as a heterotrimeric microtubule-associated motor complex from several organisms (Cole 1999) and is composed of two motor subunits and a third nonmotor subunit. In fact, it remains the only heterotrimeric kinesin discovered thus far. Individual motor subunits of kinesin-II have an N-terminal motor domain, a central region in which the two non-identical motor subunits of the complex interact by forming coiled-coils, and a C-terminal tail domain that is believed to be involved in cargo interactions. As in most other kinesins, the motor domain of kinesin-II contains the ATPase activity of the motor as well as stretches of amino acids involved in microtubule binding (Marszalek and Goldstein 2000). The third subunit of the heterotrimer, known as KAP115 in sea urchin, interacts with the tail domains of the motor subunit heterodimer (Wedaman 1996).

Convincing evidence has mounted over the last few years indicating that kinesin-II is required for the assembly of cilia and flagella in multiple organisms and cell types, and that its role is most likely in moving cargo toward the distal end of axonemes (anterograde transport). As described above, in the ts *Chlamydomonas* kinesin-II mutant, *fla10*, a loss of IFT at the restrictive temperature is followed by the shortening and disappearance of flagella (Kozminski 1995). In sea urchin, injection of anti-kinesin-II antibodies led to shortening of cilia on the developing embryo (Morris and Scholey 1997). In *Tetrahymena* and mouse, gene knockouts demonstrated a requirement for

kinesin-II to assemble motile cilia (see Chapter 3 of this study: Brown 1999, Nonaka 1998). Kinesin-II is also required for normal assembly and function of non-motile cilia in sensory organs of both *Caenorhabditis elegans* and mouse (Perkins 1986, Shakir 1993, Marszalek 2000). In addition, GFP-tagging experiments in *C. elegans* showed that a putative IFT cargo protein and the kinesin-II accessory subunit, KAP, moved at the same rate in cilia, supporting the hypothesis that kinesin-II transports rafts within cilia (Orozco 1999).

In addition to its apparent function in transporting IFT rafts, several studies have shown the importance of kinesin-II in the transport of membrane-bounded vesicles in a variety of cell types. Axon ligation experiments in mouse sciatic nerves showed that the kinesin-II homologues KIF3A and KIF3B accumulate on the proximal side of the ligation along with membrane bounded vesicles (Kondo 1994, Yamazaki 1995). Injection of anti-KIF3B antibody Fab fragments into neurons in the mouse decreased the frequency of membrane-bounded vesicle transport through the axons of these cells. Several lines of evidence showed that KIF3B and the kinesin-II non-motor subunit transport vesicles that are associated with the membrane skeleton protein, fodrin, (Takeda 2000). In *Xenopus*, expression of a dominant negative GFP-kinesin-II fusion protein blocked the association between both mutant and wildtype kinesin-II and vesicles in the intermediate compartment between the ER and Golgi (Le Bot 1998). The same construct expressed in *Xenopus* melanophore cells blocked the normal dispersion of membrane-bounded pigment granules (Tuma 1998) that had previously been shown to copurify with kinesin-II and a dynein motor. Thus, it is clear that kinesin-II is not restricted in its function to assembly of cilia and flagella and appears to have the capability of transporting both membranous vesicles and protein complexes (rafts).

As mentioned above, IFT has both anterograde and retrograde components. Once a plus end-directed motor was identified that seemed to power anterograde transport, it appeared likely that a minus end-directed motor would be identified that powered the

retrograde movement. Several recent studies have confirmed this hypothesis for *Chlamydomonas* and *C. elegans*. Pazour et al (1998) identified a deletion mutant of the gene encoding the *Chlamydomonas* protein LC8, which had short immotile flagella and strikingly had a massive accumulation of IFT rafts under the flagellar membrane. The mutated protein is a light chain of both cytoplasmic dynein and outer arm dynein, and thus the mutant phenotype suggested that cytoplasmic dynein might be the motor for retrograde IFT (Pazour 1998). In support of this hypothesis, DHC1b, a cytoplasmic dynein heavy chain was also found to be required for flagellar assembly in Chlamydomonas and had a similar accumulation of rafts in the short flagella (Pazour 1999, Porter 1999). Therefore, a cytoplasmic dynein homologue appears to be the motor for retrograde IFT.

Raft structure and possible functions

The results described above suggested that the rafts could act as adaptors to link axonemal structural components to a motor that could transport them to the tip. The next major question to be addressed was what proteins make up the rafts. Piperno and Mead (1997) reasoned that the rafts would constitute a large protein complex which would disappear in *fla10* cells after a shift to the restrictive temperature, but before the onset of flagellar resorption. They also hypothesized that this complex could be responsible for transport of inner dynein arms to the flagellar tip. By looking for an association between proteins with the expected behavior in *fla10* cells and inner dynein arm components they found a 17S complex that cofractionated with the inner dynein arm protein, p28. By a similar strategy, Cole et al (1998) characterized a 16S protein complex from the flagellar membrane plus matrix fraction that could be resolved into two subcomplexes. They were able to resolve 15 raft polypeptides by a combination of one- and two-dimensional gel electrophoresis. Database searches using microsequences derived from 2D gel-purified IFT particle polypeptides revealed that at least two of the raft polypeptides share sequence homology with genes in *C. elegans* and humans. The *C. elegans* genes, OSM-

1, and OSM-6, have both been found to have mutant alleles that prevent normal assembly and function of chemosensory neurons that contain immotile 9+0 axonemes (Cole 1998). Time lapse fluorescence video microscopy of GFP-labeled kinesin-II, OSM-1 and OSM-6 revealed that all three proteins are transported in both the anterograde and retrograde directions along axonemes of chemosensory neurons (Signor 1999). Thus, these studies in *C. elegans* show for the first time that kinesin-II and at least portions of its cargo are returned to the cell body by retrograde IFT.

Several additional studies have now suggested that the requirement for kinesin-II function to maintain cilia and flagella may be the transport of rafts. In addition to *C. elegans osm-1* and *osm-6* genes, mutations in additional genes lead to defects in ciliary assembly. In *Chlamydomonas,* mutation of the raft component, IFT88 leads to cells completely lacking flagella. Interestingly, the mouse homolog of IFT88, *Tg737,* was previously shown to cause a mouse version of the human polycystic kidney disease. Analysis of these mice revealed that primary cilia normally present in the kidneys were shortened to less than half their normal length in the raft protein mutant (Pazour 2000). Similarly, mutants in the *C. elegans* homologue of IFT88 have defective sensory cilia. More recently, a mutation in IFT52, the *Chlamydomonas* homologue of *C. elegans* OSM-6, has been shown to cause a loss of flagella (Brazelton 2001)**.**

What is not clear is how rafts relate to the structural components of axonemes that are being transported during assembly. Strikingly, biochemical studies have not shown convincingly that raft particles are associated with any type of structural component of cilia and flagella. It has been postulated that raft particles act as movement platforms powered by kinesin-II and cytoplasmic dynein and are associated only weakly with the "structural cargo" like tubulin, dynein arms, or spoke components. Cole et al argued that such weak association may be important in releasing the structural cargo at the distal end (Cole 1998). However, we can not escape the impression that this hypothesis attempts to explain the lack of a detectable direct association which may not even exist. At the

current state of knowledge, in my opinion it is still possible that the bulk of structural components of cilia and flagella are transported by a mechanism separated from rafts and kinesin-II/cytoplasmic dynein. The disassembly of axonemes in kinesin-II mutants demonstrates that the motor movement and rafts are required for assembly, but they do not establish that they actually move the structural components.

While multiple studies continue to emphasize the importance of IFT for ciliary/flagellar maintenance, until very recently no serious progress has been made toward determining the mechanism by which IFT supports the maintenance of these organelles. Two recent studies addressed this issue by looking at the turnover of flagellar proteins under various conditions. Song and Dentler (2001) labeled *Chlamydomonas* flagellar proteins by exposing cells to ^{35}S under various conditions to address the question of whether flagellar proteins turnover in intact flagella. While maintaining synchronized cells under conditions that promote flagellar length stability, they found that at least 80 flagellar polypeptides become labeled with ^{35}S during a 4 hr labeling period. This suggests that even in “non-assembling” flagella, multiple flagellar proteins are exchanged for newly synthesized proteins. In a similar set of experiments using HA-tagged tubulin transferred to cells lacking the tagged tubulin by the dikaryon technique, Marshall and Rosenbaum (2001) have shown that tubulin subunits do turn over in flagella. One simple possibility is that the subunits of flagella undergo treadmilling: preferential addition at the plus (distal) ends and loss at the minus ends (in the transition zone near the basal body). However, Marshall and Rosenbaum's data indicate that in *Chlamydomonas*, tubulin turnover is limited to the tip of the flagellum, and loss at the flagellar base was not detected. Combining the dikaryon techniques with the flagellar assembly, short flagella, and long flagella mutants, these authors further suggest that the primary function of IFT in morphostatic (nonassembling) flagella is to balance the turnover of tubulin subunits (Marshal and Rosenbaum 2001). Interestingly, Song and Dentler found by treating cells with colchicine to prevent the incorporation of new tubulin subunits that the exchange of

several proteins in the flagellum does not require tubulin turnover, suggesting a complex mechanism of regulation (Song and Dentler 2001). While these two studies come to slightly different conclusions they both agree that simple balancing of flagellar protein turnover by IFT transport may not be the only mechanism of flagelar length control.

A few studies over the last several years have begun to lend some support to the idea that kinesin-II and/or raft components interact with signaling components. Colocalization and yeast two-hybrid studies have suggested an association between kinesin-II and Smg GDS, a regulator of small G-protein activity (Shimizu 1996) and between kinesin-II and a stress-activated MAP kinase kinase kinase (Nagata 1998). Additional recent links between IFT and signal transduction have emerged by studying flagellar length control or mating behavior of *Chlamydomonas*. In a primarily pharmacological study of flagellar length control, Tuxhorn, et al (1998) found several agents that affect flagellar length. Lithium was able to stabilize and in some cases increase flagellar length in the presence of concentrations of cAMP that normally promote flagellar shortening. This is interesting since lithium has been shown to affect signaling pathways in a variety of cell types. Agents that prevent calcium uptake actually also promote flagellar assembly, suggesting that a low level of calcium must be present to maintain the axoneme at steady state, perhaps by acting in a signaling pathway involving calmodulin (Tuxhorn 1998).

Another process in flagella that may link IFT to signaling pathways is gamete activation during mating in *Chlamydomonas*. Gamete activation is a complex series of tightly regulated events in the cell that are all triggered when flagella of gametes with different mating types adhere to each other. Interestingly, one of the first changes that occurs upon a shift of *fla10* cells to the restrictive temperature is a loss of the ability to mate successfully (which occurs prior to disassembly of flagella), and this appears to be due to a defect in gamete activation (Pan and Snell 2000). These results suggest the possibility that at the restrictive temperature *fla10* cells fail to deliver one or more

signaling components that are necessary for gamete activation. Another intriguing potential link between IFT and signaling is that a human homologue of *Chlamydomonas* IFT52 was originally identified by cloning a cDNA that is down-regulated in a neuroblastoma cell line following long-term opioid treatment (Wick 1995). This link could potentially be important in the interpretation of the results presented in Chapter 5 of this document since an opiate receptor has been found in *Tetrahymena* (O'neill 1988). Additionally, β-endorphin, an opiate receptor agonist, has been localized to *Tetrahymena* cilia (Csaba and Kovacs 1999). The interactions between IFT components and signal transduction could be very complex. First, it is possible that IFT moves components of the signaling pathways as cargo to the tips of flagella. Second, it is possible that signaling pathways regulate the rate of IFT, possibly coupling the mechanisms that regulate the length of organelles to IFT and coordinating anterograde and retrograde pathways.

To conclude, it is clear that IFT is one of the best characterized motile systems, exceeding even the studies on axonal transport in neurons in the identification of components and reconstruction of the mechanism. However, still many fundamental questions remain to be answered.

A simple model for ciliary/flagellar assembly

Taken together, all of the results presented above suggest the following model of ciliary assembly (Fig. 1). Axonemal structural components accumulate near the basal bodies along with the rafts and kinesin-II motors that may be involved in transporting them. Somehow they bind to each other and then begin their movement toward the tip of the flagellum along the outer doublet microtubules. Our work suggests that there is some signal that distinguishes mature from immature cilia at this point (see Chapter 3). Then the motor travels along the length of the flagellum to the tip where the new components are released and assembled onto axonemes perhaps by a higher affinity interaction between the site of assembly and a low affinity binding site on the rafts. To avoid accumulation of the rafts at the tip, cytoplasmic dynein is required for transporting the

rafts as well as kinesin-II back to the cell body where they may be recycled for another round of transport. Furthermore, it can be postulated that kinesin-II moves cytoplasmic dynein to the tip as well. Some of the studies mentioned above as well as our own work presented in Chapter 5 suggest that rafts may be the targets of one or more signaling pathways that may alter raft function and therefore alter the assembly state of cilia or flagella. Many interesting and important questions remain regarding kinesin-II and its role in IFT and ciliary assembly. These remaining questions and future directions are discussed in Chapter 6.

The Significance of Cilia for Human Health

Cilia are found in various tissues throughout the human body. These tissues include ciliated epithelia lining the nasal cavity (Menini 1999), sinuses, respiratory tract (Houtmeyers 1999), as well as ependymal cilia lining brain ventricles and spinal cord (Rieke 1987). In addition, motile cilia function in normal human reproduction by lining the oviducts and cervix in females (Vann 1982), and in males, lining the efferent ducts and providing the motile apparatus for spermatozoa (Lindemann 1997). Furthermore, some specialized types of cilia with modified structure appear to play critical roles in both the formation and function of sensory systems in mammals and in early mammalian development. These include the connecting cilia in vertebrate photoreceptor cells (Barber 1974, Liu 1999) and sensory cilia such as those involved in olfaction (Barber 1974, Menini 1999), as well as the 9+0 embryonic nodal cilia, which are essential for determination of left-right visceral asymmetry (Nonaka 1998). These nodal cilia are one example of the so-called primary cilia that are present in many types of tissues. Until recently it was assumed that all primary cilia are immotile, but recent studies have shown that this is not universally true and have renewed interest in these unusual cilia (Nonaka 1998). Despite this renewed interest, the function of primary cilia in contexts other than early development remains largely a mystery (Wheatley 1996).

Ciliary motility does not appear to be absolutely required for survival in humans (Afzelius 1995). This is suggested by the occurrence of a genetically heterogeneous group of diseases known collectively as either immotile cilia syndrome (ICS) or more broadly as primary ciliary dyskinesia (Bush 1998). ICS was first described in 1976 by Afzelius who studied the disease in four male patients. All four men had live but paralyzed sperm cells whose axonemes lacked both inner and outer dynein arms. For this reason most males with ICS are sterile (Afzelius 1995). The four originally described ICS patients also had frequent respiratory, sinus, and ear infections (Afzelius 1976). Using the clearance of inhaled radioactive tracer particles from lungs as an assay for the function of the respiratory epithelium, Afzelius found that all of the patients lacked mucociliary clearance. A biopsy from one of the four individuals revealed a lack of motility in respiratory cilia and an abnormal ciliary ultrastructure, including an almost complete lack of dynein arms (Afzelius 1976). Perhaps the most interesting finding was that three out of the four patients had a developmental malformation known as *situs inversus*, the complete reversion of the normal left-right asymmetry of the visceral organs. Interestingly, the one patient that did not have situs inversus was the brother of one of the three who did, suggesting that the determination of disease symptoms may not be genetically straightforward (Afzelius 1976).

A syndrome encompassing some of the symptoms exhibited by the four patients studied by Afzelius had been described earlier by Kartagener (1933). Kartagener's syndrome is characterized by situs inversus, sinusitus, and bronchiectasis (chronic infection and inflammation of the bronchioles). The study of the four patients with immotile cilia suggested a biological explanation for the association of symptoms in Kartagener's triad (Afzelius 1976). In fact, Afzelius speculated that the situs inversus was directly caused by immotility of some cilia functioning in the developing embryo. He suggested that these cilia are directly responsible for the dextral rotation of the viscera during development and that when the ciliary beat stops, the rotation might occur

improperly (Afzelius 1976). Studies of families with members having Kartagener's syndrome suggested that the disease is inherited as an autosomal recessive trait. These studies also revealed that patients with the other two symptoms of Kartagener's triad were equally as likely to have normal or inverted visceral asymmetry. These studies, together with the work of Afzelius, suggested that while the lack of axonemal motility was genetically transmitted, "chance alone will determine whether the viscera will take up the normal or reversed position" (Afzelius 1976).

The observations of Afzelius and others regarding immotile cilia syndrome have lead to a search for animal models of this disease. Two mutations in rodents partially recapitulate the symptoms of Kartagener's syndrome. The recessive mouse mutation known as hydrocephalic-polydactyl (*hpy*) leads to complete sterility in homozygous males due to incomplete formation of sperm axonemes (Bryan 1983). In addition, *hpy* homozygotes of both sexes develop hydrocephalus, suggesting possible abnormal function of ependymal cilia. Despite these similarities, the *hpy* mice do not appear to be a good model for the immotile cilia syndrome. First, there was no evidence that *hpy* mice displayed situs inversus. In addition, all epithelia that were examined had motile cilia with only subtle and infrequent ultrastructural defects. Thus, it appears that a distinct subset of all cilia is affected in the hpy mouse, as compared to human patients with ICS. A second potential rodent model of immotile cilia syndrome is the WIC-Hyd rat. WIC-Hyd mutant males lack motile respiratory and ependymal cilia and develop severe hydrocephalus leading to death soon after birth (Torikata 1991). As in Kartagener's syndrome, about 50% of male WIC-Hyd mutants have situs inversus. On the other hand, while mutant females also develop hydrocephalus, they are much less severely affected than males (Torikata 1991). Thus, the WIC-Hyd rats may be a more appropriate model for human immotile cilia syndrome. However, unlike the cases of ICS observed in humans so far, though, the severity of the phenotype of WIC-Hyd rats appears to be X chromosome-linked (Torikata 1991). Since both of these rodent mutants are

hydrocephalic and do not appear to suffer from respiratory distress, it is possible that the ependymal cilia are relatively more important and the respiratory cilia relatively less important compared with the same cilia in humans. Alternatively, the two types of cilia may be affected to different extents in humans with ICS compared with the rodent mutants. Some dogs have been described which presented with an almost perfect phenocopy of ICS in humans, but these cases have not been pursued as potential animal models (Afzelius 1995).

The connection between abnormalities of ciliary function and reversal of left-right asymmetry has only recently begun to be elucidated. In fact, as late as a review published in the October 1998 issue of *Thorax*, Afzelius proclaimed, "a more knotty problem is to establish how body symmetry is determined, and thus to find out how a particular gene will cause the heart to go to the left side while its allele will let chance alone decide its position" (Afzelius 1998). A series of papers published in the last few years have begun to solve this "knotty problem". Chen et al (1998), made a mouse knockout of the winged helix family transcription factor, Hfh4. This gene had previously been shown to be expressed preferentially in ciliated tissues during their differentiation, suggesting a role in the induction of expression of genes encoding ciliary components. The Hfh4 knockout mice had frequent prenatal deaths and post-natal deaths before day four. About half of these mice had situs inversus and half were hydrocephalic. In addition, the mice that did survive to maturity were infertile (Chen 1998). Histology revealed a complete lack of cilia on the respiratory epithelium, oviduct, sperm cells, and choroid plexus (portion of brain producing cerebrospinal fluid). RT-PCR analysis revealed that the one of the dynein genes (later named left-right dynein) (*lrd*) gene was not expressed in lung tissue from *hfh4*-/- mice. The *lrd* gene encodes a dynein homologue that is mutated in a mouse mutant with situs inversus known as *inversus viscerum* (*iv*). While Chen et al (1998) acknowledged a possible connection between Hfh4 control over *lrd* expression, a possible lack of primary cilia of the embryonic node,

and randomized left-right asymmetry in their *hfh4* knockout mice, earlier studies suggesting that nodal cilia were immotile and lacked dynein arms lead them to suggest that lrd protein is involved in carrying some intracellular cargo that determines left-right polarity in the embryo (Chen 1998).

Two recent papers from Hirokawa's lab have made great progress toward explaining the connection between cilia and left-right asymmetry. Nonaka et al (1998) found that mouse embryos in which the kinesin-II gene, KIF3B, was disrupted exhibited a randomization of left-right asymmetry and died between 9.5 and 12.5 days post coitum. Two observations regarding the KIF3B null mice suggested a role for cilia in left-right determination. First, expression of one of the earliest genes in the left-right determination pathway, *lefty-2*, was abnormally distributed in the KIF3B -/- embryos. This places KIF3B upstream of *lefty-2* in this pathway. Second, monocilia which are normally present on cells in the embryonic node did not form in the KIF3B knockout mice (Nonaka 1998). Embryonic nodal cilia had previously been presumed to be immotile since they lack an axonemal central pair and appear to lack dynein arms. Despite this earlier assumption, Nonaka et. al. (1998) made video recordings of these nodal cilia in wildtype cells. They found that the nodal cilia exhibited a uniform vortical beat pattern. In addition, using fluorescently labeled beads, they made the somewhat surprising observation that there was a leftward laminar flow of extraembryonic fluid through the node (Nonaka 1998). When they made the same type of video recordings of the nodal region of KIF3B knockout embryos, they found that the fluorescent beads only underwent random fluctuations corresponding to Brownian motion. These observations lead to a model of left-right determination in which the leftward nodal flow is generated by vortexing action of nodal cilia which in turn concentrates an unknown secreted morphogen toward the left side of the embryo where it could bind to its receptor and set off a signaling cascade leading to leftness (Nonaka 1998). These authors propose that the shape of the node is critical in controlling the leftward flow of extraembryonic fluid. The

node is roughly triangular, with the base of the triangle toward the posterior end of the embryo. When viewed from the ventral side, the nodal cilia swirl in a counterclockwise motion (Nonaka 1998). Because the flow in the anterior part of the node is restricted by the shape of the node, the primary direction of flow would correspond to the posterior portion of the ciliary beat. This would tend to cause a flow toward the left side of the embryo (Nonaka 1998).

A second recent study made a direct experimental connection between nodal flow hypothesis and left-right determination (Okada 1999). These authors made video recordings of nodal flow in two mouse mutants with well characterized defects in body situs determination. The mutation in *inversus viscerum* (*iv*) mice leads to a randomization of left-right asymmetry, whereas the *inversion of embryonic turning* (*inv*) mutation causes a complete inversion of body situs. In addition, both of these genes had been shown to act upstream of *lefty-2*, similar to the findings with KIF3B. As mentioned previously, the *iv* mutation is in the *lrd* gene which encodes a dynein homologue, so it is not entirely surprising that observations of *iv* nodes showed that nodal cilia in these embryos are completely paralyzed and appeared rigid (Okada 1999). Accordingly, there was no nodal flow in *iv* embryos. Since nodal cilia fail to be assembled in the KIF3B knockout, this original study left open the possibility that the presence of nodal cilia rather than their beating action was the critical factor in left-right determination. On the contrary, the lack of nodal flow in *iv* embryos which have nodal cilia, strongly supported the importance of ciliary beating for this pathway (Okada 1999). The gene mutated in *inv* mice is not characterized, but recordings of *inv* nodes showed that the nodal cilia beat as fast as in wildtype cells. In contrast, the nodal flow in these embryos was not normal. Although flow was still toward the left side of the embryo, it was much more turbulent and thus slower than in wildtype embryos. The reason for this abnormal flow was not investigated closely, but a possible explanation is that the shape of the nodes in the *inv* embryos was often not triangular. This may interfere with translation of the ciliary beat

into smooth leftward flow (Okada 1999). Thus, mutations in three different types of genes leads to interference with nodal flow in three different ways, but all three mutations lead to abnormal determination of body situs. These studies strongly support the importance of smooth leftward nodal flow created by vortical beating of nodal cilia and the triangular shape of the node for normal determination of sidedness in the embryo (Okada 1999). While it is unclear whether a similar mechanism operates in humans, the strong connection between immotile cilia and situs inversus in humans makes it seem likely.

Tetrahymena thermophila as a model organism for studying ciliary assembly.

This work describes studies of ciliary assembly in the ciliated protozoan, *Tetrahymena thermophila.* We have chosen to study ciliary assembly and IFT in *Tetrahymena* for several reasons. First, *Tetrahymena* is covered with several hundred cilia per cell, each of which must be duplicated to ensure that the subsequent daughter cells receive a full complement of cilia. These cilia can be removed from the cell in large quantities for biochemical analyses. Second, robust techniques have been developed in recent years for gene disruption in *Tetrahymena* cells. These methods are based on the observation that DNA introduced into cells replaces endogenous sequences exclusively by homologous recombination. Finally, *Tetrahymena* has two types of nuclei in each cell, each with a different function. The macronucleus is a transcriptionally active, somatic nucleus, whereas the micronucleus is a transcriptionally silent germline nucleus. As described in detail in Chapter 3 (Materials and Methods), the properties of these two types of nuclei have been harnessed to yield powerful genetic tools for the study of genes with lethal phenotypes.

There are also some important limitations of *Tetrahymena* of which we are painfully aware. First, cilia although numerous, are much shorter compared to flagella, and therefore less suitable for quantitative studies on parameters of IFT in living cells. Second, very few ciliary mutants have been isolated to date, and notably there are

currently no mutants with paralyzed cilia that would be suitable for studies of IFT. Third, *Tetrahymena* is a complex organism, with multiple types of cilia (oral, locomotory, caudal) and complicated development which is repeated during each cell cycle. Finally, forward genetic approaches are currently very limited in *Tetrahymena,* making gene discovery slow and often not feasible. However, on the positive side, *Tetrahymena* cilia more closely resemble ciliated epithelia of mammalian cells in their metachronal movements than do the flagella of *Chlamydomonas*. Also, for unknown reasons, attempts at using the green fluorescent protein (GFP) in *Chlamydomonas* have failed so far while GFP is highly fluorescent in *Tetrahymena* (and can be used to label components of IFT as I will show below). While both *Tetrahymena* and *Chlamydomonas* have their distinct drawbacks, there is a striking methodological synergy between these organisms. New gene types can be identified based on desired phenotypes in *Chlamydomonas* (with the limitation that they cannot be essential for survival, which is usually not a factor for flagellar components), but it is currently not possible to eliminate function of genes identified solely by biochemical approaches or genes that are essential for survival. However, any gene, essential or nonessential, can be easily mutated in *Tetrahymena*. *Tetrahymena* is a powerful reverse genetic system resembling yeast in many methodological respects. Of course, yeast genetics is still more powerful, but yeast cells do not have axonemes and do not assemble centrioles.

REFERENCES

Adams GMW, Huang B, Piperno G, and Luck DJL: The central pair microtubular complex of *Chlamydomonas* flagella: polypeptide composition as revealed by analysis of mutants. *J Cell Biol* 1981, 91: 69-76.

Afzelius BA: A human syndrome caused by immotile cilia. *Science* 1976, 193: 317-319.

Afzelius BA: Role of cilia in human health. *Cell Motil Cytoskel* 1995, 32: 95-97.

Afzelius BA: Immotile cilia syndrome: past, present, and prospects for the future. *Thorax* 1998, 53: 894-897.

Barber VC: Cilia in sense organs. *In: Cilia and Flagella* (MA Sleigh ed.) 1974, Academic Press. London.Brazelton WJ, Amundsen CD, Silflow CD, Lefebvre PA: The bld1 mutation identifies the *Chlamydomonas* osm-6 homolog as a gene required for flagellar assembly. *Curr Biol* 2001, 11: 1591-1594.

Brown JM, Marsala C, Kosoy R, Gaertig J: Kinesin-II is preferentially targeted to assembling cilia ans is required for ciliogenesis and normal cytokinesis is *Tetrahymena*. *Mol Biol Cell* 1999, 10: 3081-3096.

Bryan JHD: The immotile cilia syndrome mice versus man. *Virchows Arch [Pathol Anat]* 1983, 399: 265-275.

Bush A, Cole P, Hariri M, Mackay I, Phillips G, O'Callaghan C, Wilson R, Warner JO: Primary ciliary dyskinesia: diagnosis and standards of care. *Eur Respir J* 1998, 12: 982-988.

Cole DG: Kinesin-II, coming and going. *J Cell Biol* 1999, 147: 463-6.

Cole DG, Diener DR, Himelblau AL, Beech PL, Fuster JC, Rosenbaum JL: *Chlamydomonas* kinesin-II-dependent intraflagellar transport (IFT): IFT particles contain proteins required for ciliary assembly in *Caenorhabditis elegans* sensory neurons. *J Cell Biol* 1998, 141: 993-1008.

Chen J, Knowles HJ, Hebert JL, Hackett BP: Mutation of the mouse hepatocyte nuclear factor/forkhead homologue 4 gene results in absence of cilia and random left-right asymmetry. *J Clin Invest* 1998, 102: 1077-1082.

Csaba G, Kovacs P: Localization of beta-endorphin in *Tetrahymena* by confocal microscopy. Induction of the prolonged production of the hormone by hormonal imprinting. *Cell Biol Int* 1999, 23: 695-702.

Dutcher SK: Flagellar assembly in two hundred and fifty easy-to-follow steps. *Trend Genet* 1995, 11: 398-404.

Fox LA, Sawin KE, Sale WS: Kinesin-related proteins in eukaryotic flagella. *J Cell Sci* 1994, 107: 1545-1550.

Gaillard AR, Diener DR, Rosenbaum JL, Sale WS: Flagellar radial spoke protein 3 is an A-kinase anchoring protein (AKAP). *J Cell Biol* 2001, 153: 443-448.

Gibbons IR, Rowe AJ: Dynein: a protein with andenosine triphosphatase activity from cilia. *Science* 1965, 149: 424-425.

Goodenough UW, Heuser JE: Substructure of inner dynein arms, radial spokes, and the central pair/projection complex of cilia and flagella. *J Cell Biol* 1985, 100: 2008-2018.

Goodenough UW, Heuser JE: Substructure of the outer dynein arm. *J Cell Biol* 1982, 95: 798-815.

Habermacher G, Sale WS: Regulation of dynein-driven microtubule sliding by an axonemal kinase and phosphatase in *Chlamydomonas* flagella. *Cell Motil Cytoskel* 1995, 32: 106-109.

Houtmeyers E, Gosselink R, Gayan-Ramirez, Decramer M: Regulation of mucociliary clearance in health and disease. *Eur Respir J* 1999, 13: 1177-1188.

Howard DR, Habermacher G, Glass DB, Smith EF, Sale WS: Regulation of *Chlamydomonas* flagellar dynein by an axonemal protein kinase. *J Cell Biol* 1994, 127: 1683-1692.

Huang B, Piperno G, Luck DJL: Paralyzed flagella mutants of *Chlamydomonas reinhardtii* defective for axonemal doublet microtubule arms. *J Biol Chem* 1979, 254: 3091-3099.

Huang B, Piperno G, Ramanis Z, Luck DJL: Radial spokes of *Chlamydomonas* flagella: genetic analysis of assembly and function. *J Cell Biol* 1981, 88: 80-88.

Huang B, Ramanis Z, Luck DJL: Suppressor mutations in *Chlamydomonas* reveal a regulatory mechanism for flagellar function. *Cell* 1982, 28: 115-124.

Huang B, Rifkin MR, Luck DJL: Temperature-sensitive mutations affecting flagellar assembly and function in *Chlamydomonas reinhardtii*. *J Cell Biol* 1977, 72: 67-85.

Ishijima S, Koichi S, Hiramoto Y: Comparitive study of the beat patterns of American and asian horseshoe crab sperm: evidence for a role of the central pair complex in forming planar waveforms in flagella. *Cell Motil Cytoskel* 1988, 9: 264-270.

Johnson KA, Rosenbaum JL: Polarity of flagellar assembly in *Chlamydomonas*. *J Cell Biol* 1992, 119: 1605-1611.

Kamiya R, Kurimoto E, Muto E: Two types of *Chlamydomonas* flagellar mutants missing different components of inner-arm dynein. *J Cell Biol* 1991, 112: 441-447.

Kartagener M. *Beitr Klin Erforsch* 1933, 83: 489.

Kondo S, Sato-Yoshitake R, Noda Y, Aizawa H, Nataka T, Matsuura Y, Hirokawa N: KIF3A is a new microtubule-based anterograde motor in the nerve axon. *J Cell Biol* 1994, 125:1095-1107.

Kozminski KG, Johnson KA, Forscher P, Rosenbaum JL: A motility in the eukaryotic flagellum unrelated to flagellar beating. *Proc Natl Acad Sci USA* 1993, 90: 5519-5523.

Kozminski KG, Beech PL, Rosenbaum JL: The *Chlamydomonas* kinesin-like protein FLA10 is involved in motility associated with the flagellar membrane. *J Cell Biol* 1995, 131: 1517-1527.

Le Bot N, Antony C, White J, Karsenti I, Vernos I: Role of Xklp3, a subunit of the *Xenopus* kinesin II heterotrimeric complex, in membrane transport between the endoplasmic reticulum and the Golgi apparatus. *J Cell Biol* 1998, 143: 1559-1573.

Lee S, Wisniewski JC, Dentler WL, Asai DJ: Gene knockouts reveal separate functions for two cytoplasmic dyneins in *Tetrahymena thermophila*. *Mol Biol Cell* 1999, 10: 771-784.

Lindemann CB, Kanous KS: A model for flagellar motility. *Internat Rev Cytol* 1997, 173: 1-72.

Lindemann CB, Orlando A, Kanous KS: The flagellar beat of rat sperm is organized by the interaction of two functionally distinct populations of dynein bridges with a stable central axonemal partition. *J Cell Sci* 1992, 102: 249-260.

Liu X, Udovichenko IP, Brown SDM, Steel KP, Williams DS: Myosin VIIa participates in opsin transport through the photoreceptor cilium. *J Neurosci* 1999, 19: 6267-6274.

Lodish H, Baltimore D, Berk A, Zipursky SL, Matsudaira P, Darnell J (eds.) Molecular Cell Biology, 3rd ed. Scientific American Books, Inc. New York, 1995: Pp 1052-1053.

Marshall WF, Rosenbaum JL. Intraflagellar transport balances continuous turnover of outer doublet microtubules: implications for flagellar length control. *J Cell Biol* 2001, 155: *in press*.

Marszalek JR, Goldstein LS. Understanding the functions of kinesin-II: *Biochim Biophys Acta* 2000, 1496: 142-50.

Marszalek JR, Liu X, Roberts EA, Chui D, Marth JD, Williams DS, Goldstein LS: Genetic evidence for selective transport of opsin and arrestin by kinesin-II in mammalian photoreceptors. *Cell* 2000, 102: 175-87.

Menini A: Calcium signaling and regulation in olfactory neurons. *Curr Opin Neurobiol* 1999, 9: 419-426.

Mitchell DR, Rosenbaum JL: A motile *Chlamydomonas* flagellar mutant that lacks outer dynein arms. *J Cell Biol* 1985, 100: 1228-1234.

Morris RL, Scholey JM: Heterotrimeric kinesin-II is required for the assembly of motile 9+2 ciliary axonemes on sea urchin embryos. *J Cell Biol* 1997, 138: 1009-1022.

Nagata K, Puls A, Futer C, Aspenstrom P, Schaefer E, Nakata T, Hirokawa N, Hall A: The MAP kinase kinase kinase MLK2 co-localizes with activated JNK along microtubules and associates with kinesin superfamily motor KIF3. *EMBO J* 1998, 17: 149-158.

Nonaka S, Tanaka Y, Okada Y, Takeda S, Harada A, Kanai Y, Kido M, Hirokawa N: Randomization of left-right asymmetry due to loss of nodal cilia generating leftward flow of extraembryonic fluid in mice lacking KIF3B motor protein. *Cell* 1998, 95: 829-837.

Okada Y, Nonaka S, Tanaka Y, Saijoh Y, Hamada H, Hirokawa N: Abnormal nodal flow precedes situs inversus in *iv* and *inv* mice. *Molec Cell* 1999, 4: 459-468.

Omoto CK, Gibbons IR, Kamiya R, Shingyoji C, Takahashi K, Witman GB: Rotation of

the central pair microtubules in eukaryotic flagella. *Molec Biol Cell* 1999, 10: 1-4.

O'Neill JB, Pert CB, Ruff MR, Smith CC, Higgins WJ, Zipser B. Identification and characterization of the opiate receptor in the ciliated protozoan, *Tetrahymena*. *Brain Res* 1988, 450: 303-15.

Orozco JT, Wedaman KP, Signor D, Brown H, Rose L, Scholey JM: Movement of motor and cargo along cilia. *Nature* 1999, 398: 674.

Pan J, Snell WJ. Signal transduction during fertilization in the unicellular green alga, *Chlamydomonas*: *Curr Opin Microbiol* 2000, 3: 596-602.

Pazour GJ, Wilkerson CG, Witman GB: A dynein light chain is essential for the retrograde particle movement of intraflagellar transport (IFT). *J Cell Biol* 1998, 141: 979-992.

Pazour GJ, Dickert BL, Witman GB: The DHC1b (DHC2) isoform of cytoplasmic dynein is required for flagellar assembly. *J Cell Biol* 1999, 144: 473-481.

Pazour GJ, Dickert BL, Vucica Y, Seeley ES, Rosenbaum JL, Witman GB, Cole DG: *Chlamydomonas* IFT88 and its mouse homologue, polycystic kidney disease gene tg737, are required for assembly of cilia and flagella. *J Cell Biol* 2000, 151: 709-18.

Perkins LA, Hedgecock EM, Thomson JN, Culotti JG: Mutant sensory cilia in the nematode *Caenorhabditis elegans*. *Dev Biol* 1986, 117: 456-87.

Piperno G, Ramanis Z: The proximal portion of *Chlamydomonas* flagella contains a distinct set of inner dynein arms. *J Cell Biol* 1991, 112: 701-709.

Piperno G, Mead K, Henderson S: Inner dynein arms but not outer dynein arms require the activity of kinesin homologue protein KHP1^{FLA10} to reach the distal part of flagella in *Chlamydomonas*. *J Cell Biol* 1996, 133: 371-379.

Piperno G, Mead K: Transport of a novel complex in the cytoplasmic matrix of *Chlamydomonas* flagella. *Proc Natl Acad Sci USA* 1997, 94: 4457-4462.

Porter ME, Bower R, Knott JA, Byrd P, Dentler W: Cytoplasmic dynein heavy chain 1b is required for flagellar assembly in *Chlamydomonas*. *Mol Biol Cell* 1999, 10: 693-712.

Porter ME and Sale WS: The 9+2 axonemeanchors multiple inner arm dyneins and a network of kinases and phosphatases that control motility. *J Cell Biol* 2000, 151: F37-F42.

Prensier G, Vivier E, Goldstein S, Schrevel J: Motile flagellum with a "3+0" ultrastructure. *Science* 1980, 207: 1493-1494.

Rieke GK, Jordan FL, Wynder HJ, Thomas WE: Ultrastructure of ependymal cells in primary cultures of cerebral cortex. *J Neurosci Res* 1987, 18: 484-92.

Rosenbaum JL, Moulder JE, Ringo DL: Flagellar elongation and shortening in *Chlamydomonas.* The use of cycloheximide and colchicine to study the synthesis and assembly of flagellar proteins. *J Cell Biol* 1969, 41: 600-619.

Sale WS, Satir P: Direction of active sliding of microtubules in *Tetrahymena* cilia. *Proc Natl Acad Sci USA* 1977, 74: 2045-2049.

Satir P: Studies on cilia: II. Examination of the distal region of the ciliary shaft and the role of filaments in motility. *J Cell Biol* 1965, 26: 805-834.

Satir P: Studies on cilia. *J Cell Biol* 1968, 39: 77-94.

Shakir MA, Fukushige T, Yasuda H, Miwa J, Siddiqui SS: *C. elegans* osm-3 gene mediating osmotic avoidance behaviour encodes a kinesin-like protein. *Neuroreport* 1993, 4: 891-4.

Shimizu K, Kawabe H, Minami S, Honda T, Takaishi K, Shirataki H, Takai Y: SMAP, an Smg GDS-associating protein having arm repeats and phosphorylated by Src tyrosine kinase. *J Biol Chem* 1996, 271: 27013-7.

Signor D, Wedaman KP, Orozco JT, Dwyer ND, Bargmann CI, Rose LS, Scholey JM: Role of a class DHC1b dynein in retrograde transport of IFT motors and IFT raft particles along cilia, but not dendrites, in chemosensory neurons of living *Caenorhabditis elegans*. *J Cell Biol* 1999, 147: 519-530.

Smith EF, Sale WS: Regulation of dynein-driven microtubule sliding by the radial spokes in flagella. *Science* 1992, 257: 1557-1559.
Song L, Dentler WL: Flagellar protein dynamics in *Chlamydomonas*. *J Biol Chem* 2001, 276: 29754-63.

Stephens RE: Isolation of nexin-the linkage protein responsible for maintenance of the nine-fold configuration of flagella axonemes. *Biol Bull (Woods Hole)* 1970, 139: 438.

Summers KE, Gibbons IR: Adenosine triphosphate-induced sliding of tubules in trypsin-treated flagella of sea urchin sperm. *Proc Natl Acad Sci USA* 1971, 68: 3092-3096.

Summers KE, Gibbons IR: Effects of trypsin digestion on flagellar structures and their relationship to motility. *J Cell Biol* 1973, 58: 618-629.

Takeda S, Yamazaki H, Seog D, Kanai Y, Terada S, Hirokawa N: Kinesin superfamily protein 3 (KIF3) motor transports fodrin-associating vesicles important for neurite budding. *J Cell Biol* 2000, 148: 1255-1265.

Taylor HC, Satir P, Holwill MEJ: Assessment of inner dynein arm structure and possible function in ciliary and flagellar axonemes. *Cell Motil Cytoskel* 1999, 43: 167-177.

Torikata C, Kijimoto C, Koto M: Ultrastructure of respiratory cilia of WIC-Hyd male rats an animal model for human immotile cilia syndrome. *Amer J Pathol* 1991, 138: 341-347.

Tuma MC, Zill A, Le Bot N, Vernos I, Gelfand V: Heterotrimeric kinesin II is the microtubule motor protein responsible for pigment dispersion in *Xenopus* melanophores. *J Cell Biol* 1998, 143: 1547-58.

Tuxhorn J, Daise T, Dentler WL: Regulation of flagellar length in *Chlamydomonas*. *Cell Motil Cytoskeleton* 1998, 40: 133-46.

Vann PG, Blake JR: Mechanics of ovum transport in the oviduct. *Prog Clin Biol Res (suppl)* 1982, 80: 53-57.

Walther Z, Vashishtha M, Hall J: The *Chlamydomonas FLA10* gene encodes a novel kinesin-homologous protein.

Wedaman KP, Meyer DW, Rashid DJ, Cole DG, Scholey JM: Sequence and submolecular localization of the 115-kD accessory subunit of the heterotrimeric kinesin-II (KRP85/95) complex. *J Cell Biol* 1996, 132: 371-80.

Wheatley DN, Wang AM, Strugnell GE: Expression of primary cilia in mammalian cells. *Cell Biol Internat* 1996, 20: 73-81.

Wick MJ, Ann DK, Loh HH: Molecular cloning of a novel protein regulated by opioid treatment of NG108-15 cells. *Brain Res Mol Brain Res* 1995, 32: 171-5.

Witman GB: The site of *in vivo* assembly of flagellar microtubules. *Ann NY Acad Sci* 1975, 253: 178-191.

Yamazaki H, Nakata T, Okada Y, Hirokawa N: KIF3A/B: A heterdimeric kinesin superfamily protein that works as a microtubule plus end-directed motor for membrane organelle transport . *J Cell Biol* 1995, 130: 1387-1399

Yang P, Fox L, Colbran RJ, Sale WS: Protein phosphatases PP1 and PP2A are located in distinct positions in the *Chlamydomonas* flagellar axoneme. *J Cell Sci* 2000, 113: 91-102.

Yang P and Sale WS: Casein kinase I is anchored on axonemal doublet microtubules and regulates flagellar dynein phosphorylation and activity. *J Biol Chem* 2000, 275: 18905-18912.

FIGURE LEGENDS

Figure 2.1. Cartoon depiction of axonemal ultrastructure (as referenced in the text). (A) Transverse section (B) Longitudinal section. Sections are color-coded as follows: red, A-tubule of outer microtubule doublet; blue, B-tubule of outer microtubule doublet; black, central pair of microtubules and associated projections; green, inner and outer dynein arms; yellow, radial spokes. The basal body (open rectangles in transverse section) anchors axoneme to the cell body. Microtubules of the axoneme are oriented with their minus ends near the cell body and their plus ends at the ciliary tip.

2.2. Kinesin-II is a heterotrimeric motor protein (as referenced in the text). Each of two motor subunits has an N-terminal motor domain and a C-terminal globular tail as well as a central region where the two subunits interact by forming a coiled-coil. A non-motor KAP subunit associates with the tail.

Figure 2.3. Model of ciliary assembly. (1) Kinesin-II, cytoplasmic dynein, and IFT raft particles are concentrated in a pool near the basal bodies. (2 and 3) Both types of motor become associated with rafts. Raft-associated kinesin-II binds to axonemal outer doublet microtubules and moves rafts and dynein toward the ciliary tip. (4-6) Some axonemal structural components, which may be weakly bound to rafts, dock at their binding sites. Kinesin-II becomes inactive, and cytoplasmic dynein becomes active. Cytoplasmic dynein then moves the remaining rafts and kinesin-II back to the cell body. (7) Rafts and motors may re-enter the pool for use in another round of transport. Our results (Chapter 5) suggest that signaling pathways regulate raft transport.

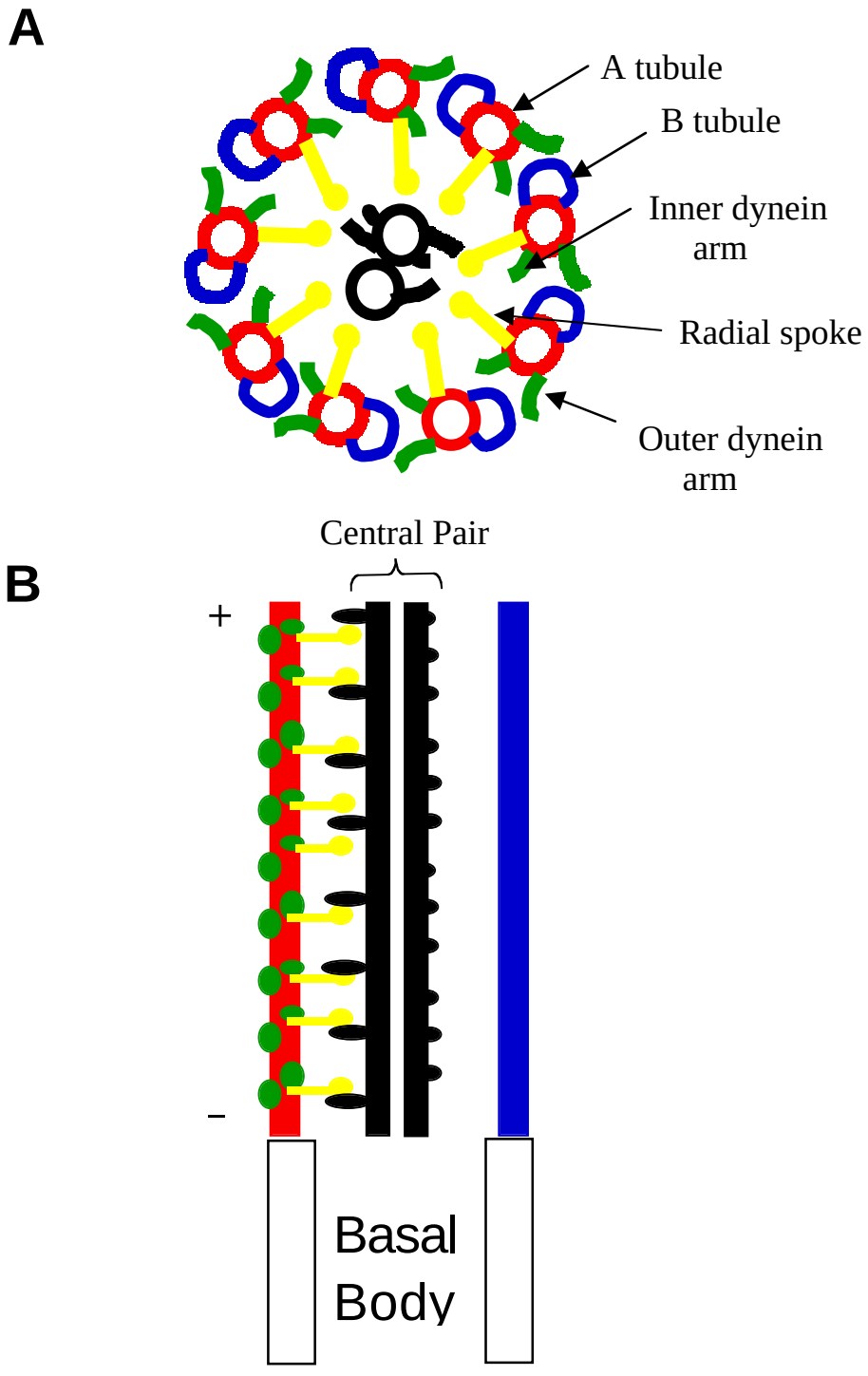
A
A tubule
B tubule
Inner dynein arm
Radial spoke
Outer dynein arm
B
Central Pair
+
–
Basal Body

Figure 2.1

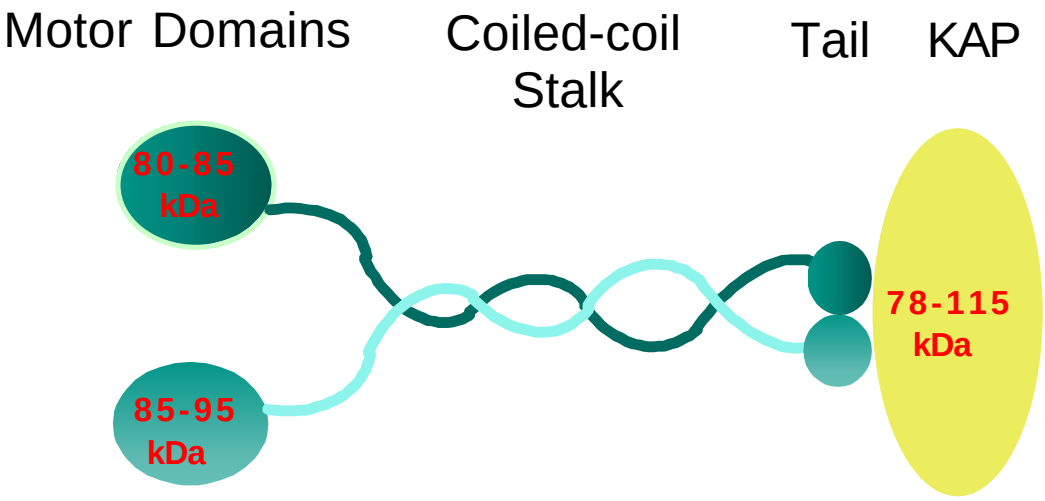
Motor Domains
Coiled-coil Stalk
Tail
KAP
80-85 kDa
85-95 kDa
78-115 kDa

Figure 2.2

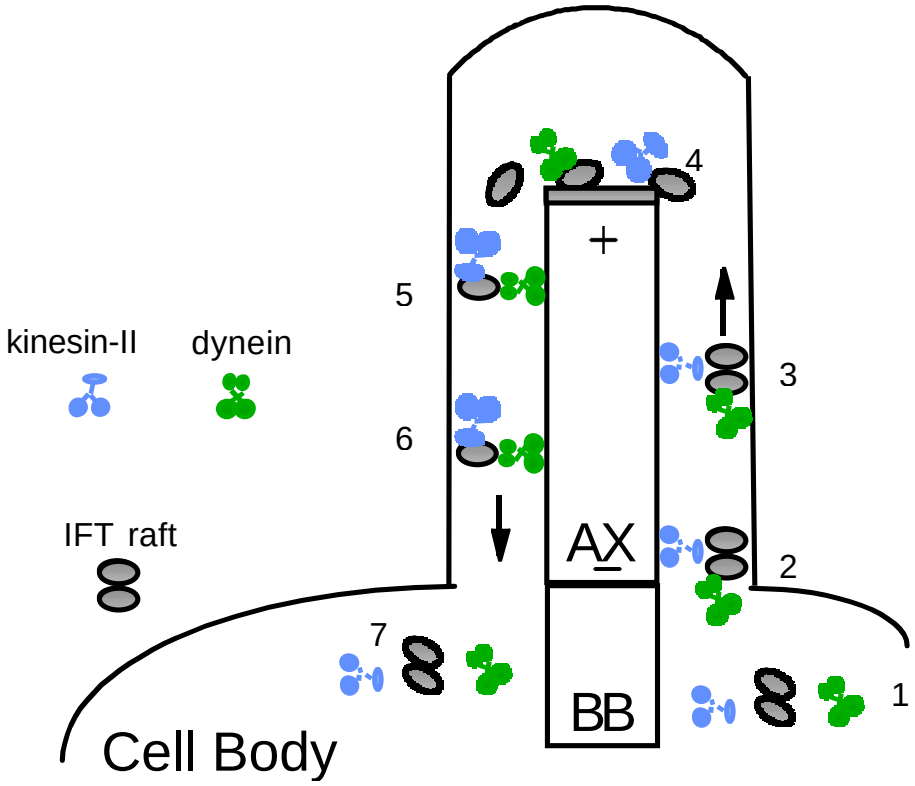

Figure 2.3

CHAPTER 3

KINESIN-II IS PREFERENTIALLY TARGETED TO ASSEMBLING CILIA AND IS REQUIRED FOR CILIOGENESIS AND NORMAL CYTOKINESIS IN *TETRAHYMENA* [1]

[1] Jason M. Brown, Christine Marsala, Roman Kosoy, and Jacek Gaertig. Reprinted from Molecular Biology of the Cell, (1999, volume 10, 3081-3096), with permission by the American Society for Cell Biology.

ABSTRACT

We cloned two genes, *KIN1* and *KIN2*, encoding kinesin-II homologues from the ciliate *Tetrahymena thermophila* and constructed strains lacking either *KIN1* or *KIN2* or both genes. Cells with a single disruption of either gene showed partly overlapping sets of defects in cell growth, motility, ciliary assembly, and thermoresistance. Deletion of both genes resulted in loss of cilia and arrests in cytokinesis. Mutant cells were unable to assemble new cilia or to maintain preexisting cilia. Double knockout cells were not viable on a standard medium but could be grown on a modified medium on which growth does not depend on phagocytosis. Double knockout cells could be rescued by transformation with a gene encoding an epitope-tagged Kin1p. In growing cells, epitope-tagged Kin1p preferentially accumulated in cilia undergoing active assembly. Kin1p was also detected in the cell body but did not show any association with the cleavage furrow. The cell division arrests observed in kinesin-II knockout cells appear to be induced by the loss of cilia and resulting cell paralysis.

INTRODUCTION

Kinesins-II are microtubule-dependent motors that exist as heterotrimeric complexes in diverse organisms (Cole et al., 1993, 1998; Yamazaki et al., 1995). Members of the kinesin-II family have been implicated in axonal transport, assembly of cilia and flagella, and transport of pigment granules (Walther et al., 1994; Yamazaki et al., 1995; Morris and Scholey, 1997; Rogers et al., 1997). Kinesin-II is essential for assembly of cilia and flagella. A mutation in the *Chlamydomonas* kinesin-II motor, FLA10, resulted in a loss of flagella (Walther et al., 1994). Injection of anti-kinesin-II antibodies into blastula-stage sea urchin embryos partially blocked assembly of cilia (Morris and Scholey, 1997). Furthermore, a knockout of essential murine kinesin-II genes leads to a complete block in the assembly of monocilia on embryonic nodal cells (Nonaka et al., 1998; Marszalek et al., 1999; Takeda et al., 1999). In *Chlamydomonas*, video-enhanced microscopy showed

bidirectional movement of particles inside flagella. These membraneless particles, named rafts, were proposed to be involved in delivery of flagellar subunits from the cell body to the tips of growing flagella (Kozminski et al., 1993; Rosenbaum et al., 1999). Importantly, FLA10 activity is required to maintain intraflagellar transport (Kozminski et al., 1995). Kinesin-II motor subunits supported microtubule plus end-directed motility in vitro (Cole et al., 1993; Kondo et al., 1994), and kinesin-II was found highly enriched in cilia and flagella (Walther et al., 1994; Cole et al., 1998; Nonaka et al., 1998). Recently, a green fluorescent protein (GFP)-tagged subunit of a kinesin-II complex was observed to move inside the chemosensory cilia of living *Caenorhabditis elegans*, primarily in the anterograde direction toward the distal tips of axonemes (Orozco et al., 1999). Because incorporation of new axonemal subunits is known to take place at the tips of assembling flagella, which correspond to the plus ends of axonemal microtubules (Johnson and Rosenbaum, 1992), kinesin-II is a strong candidate for an anterograde motor transporting flagellar components, possibly in association with rafts, from the cell body to the tips of flagella. The retrograde flagellar movement appears to be essential for flagellar assembly (Piperno et al., 1998) and is most likely powered by a cytoplasmic dynein complex (Pazour et al., 1998; Porter et al., 1999).

In nerve cells kinesin-II is associated with membrane-bounded organelles (Yamazaki et al., 1995; Muresan et al., 1998; Yang and Goldstein, 1998). Thus, it is most likely that kinesin-II complexes transport different types of cellular cargo in axons and flagella. Most kinesin-II motors exist as heterotrimeric complexes containing two non-identical motor subunits and a third accessory nonmotor subunit. Because kinesin-II is the only kinesin-related protein complex known to contain nonidentical motor subunits, heterodimerization may be used to create combinatorial motors that have different cargo specificities. In mouse and rat, kinesin-II was found in two complexes containing one common motor subunit (KIF3A) and one of two variable motor subunits (KIF3B or KIF3C) (Muresan et al., 1998; Yang and Goldstein, 1998). Furthermore, three isoforms

of the kinesin-II-associated subunit KAP3 were identified in mouse (Yamazaki et al., 1995, 1996). In *C. elegans* three kinesin-II motor subunits were identified, which form at least one heterotrimeric complex and one dimeric complex (Signor et al., 1999). Combinatorial kinesin-II complexes could be formed by mixing and matching of different motor and nonmotor subunits that produce functionally distinct motors in different cells.

We and others have recently identified three kinesin-II homologous genes (*KIN1*, *KIN2*, and *KIN5*) in the unicellular organism the ciliate *Tetrahymena thermophila* (this study; Bernstein, personal communication). Thus, combinatorial interactions may be used to generate multiple, functionally distinct variants of kinesin-II within a single cell. Here we describe the cloning and functional analysis of two members of the kinesin-II family of *T. thermophila*, *KIN1* and *KIN2*. Our analyses show that *KIN1* and *KIN2* genes have overlapping but nonidentical functions. Either *KIN1* or *KIN2* is required for assembly and maintenance of cilia, and kinesin-II encoded by the *KIN1* gene preferentially accumulates in cilia that undergo active assembly. Surprisingly, the mutants lacking both *KIN1* and *KIN2* genes frequently fail to complete cytokinesis. Multiple lines of evidence indicate that the cytokinesis phenotype in kinesin-II mutants is induced by the loss of cilia and resulting cell paralysis.

MATERIALS AND METHODS

Strains, Culture Growth, and Conjugation

Strains used are described in Table 3.1. Tetrahymena cell cultures were grown in 50 ml of either SPP (1% proteose peptone, 0.2% glucose, 0.1% yeast extract, 0.003% EDTA·ferric sodium salt) (Gorovsky, 1973) or MEPP medium (2% proteose peptone, 2 mM Na_3 citrate·$2H_2$ O, 1 mM ferric chloride, 12.5 μM cupric sulfate, 1.7 μM folinic acid, Ca salt) (Orias and Rasmussen, 1976) supplemented with 100 U/ml penicillin, 100 μg/ml streptomycin, and 0.25 μg/ml amphotericin B in 250-ml Erlenmayer flasks with moderate shaking at 30°C. To induce conjugation, two strains of different mating types were grown

to midlogarithmic phase, and 50 ml of each strain were washed two times and left in the starvation medium (10 mMTris-Cl, pH 7.5) in the original volume. After 16–20 h, equal numbers of cells (1.5×10^7 cells of each strain) were mixed in a total volume of 100 ml in a 2-l Erlenmeyer flask and left unshaken at 30°C.

Gene Cloning and Sequence Analysis

PCR was used to amplify kinesin-related protein (KRP) sequences of *T. thermophila*. Total genomic DNA isolated using the fast urea extraction method (Gaertig et al., 1994b) was used as a template. Three types of degenerate primers were used to amplify sequences encoding the most conserved peptides of motor domains present in other KRPs. Primer A, 5'-AT(T/C)TT(T/C)GC(T/C)TA(T/C)GG(T/A)(T/C)A(A/G)AC-3', encodes a sense strand of IFAYGQT. Primer B, 5'-G(A/T)(A/T)CC(A/G)GC(T/A) A(A/G)(A/G)TC(A/G)AC-3', encodes an antisense sequence of LVDLAGSE. Primer C, 5'-CTTAGA(G/A)T(T/C)TCT(G/A)(T/A)A(G/A)GG(A/G)AT(G/A)TG-3', encodes an antisense sequence of the peptide HIP(Y/F)RDSK. Total genomic DNA was amplified using primers A and C and amplified again with primers A and B. Final products of ~400 bp were cloned. To clone genomic fragments of *KIN1* and *KIN2*, total *T. thermophila* DNA was digested with restriction endonucleases and used to prepare a Southern blot. The PCR-generated *KIN1* and *KIN2* fragments were labeled with [α^{32}P]dATP using random hexamer primers and used as probes. The *KIN1* gene was cloned as a 3.5-kb HindIII fragment and a partially overlapping 2.5-kb EcoRI–XbaI fragment. The majority of *KIN2* was cloned as partly overlapping 2.5-kb HindIII and 2-kb Csp45 I–BglII restriction fragments. The 3' end of the *KIN2* gene was cloned using rapid amplification of cDNA ends (Frohman, 1990). Protein secondary structure was predicted using NNPREDICT (Kneller et al., 1990). The probability of coiled coil formation was calculated using COILS (Lupas et al., 1991). Sequence homology searches were done using BLAST from the National Center for Biotechnology Information (Bethesda, MD; Altschul et al., 1990). Protein sequence comparison was done using BESTFIT,

COMPARE, and DOTPLOT programs of the University of Wisconsin Genetics Computer Group (UWGCG; Madison, WI) Wisconsin Package. Alignments of multiple sequences were prepared using PILEUP; evolutionary distances between sequences were calculated using DISTANCES; and an evolutionary tree was made using GROWTREE of the UWGCG package (Devereux et al., 1984).

Germ Line and Somatic Gene Knockouts

To construct a targeting fragment for disruption of the *KIN1* gene, plasmid pKIN17-7 containing the 3.5-kb HindIII fragment of *KIN1* was linearized at its single BglII site within the region encoding a motor domain. The protruding BglII ends were filled in using T4 DNA polymerase. The *neo2* disruption cassette (Gaertig et al., 1994a) was inserted into the BglII site of pKIN17-7 to give pKIN17-7neo. To construct a gene disruption fragment for *KIN2*, plasmid pCS4, containing a 5-kb fragment of *KIN2*, was linearized at the Csp45 I site present in the coding region. The *bsr1* gene cassette was inserted into the Csp45 I site. This cassette is a derivative of the *neo2* gene cassette in which a blasticidin S (bs) resistance gene (Sutoh, 1993) is inserted between the *Tetrahymena* histone *HHF1* promoter and the *BTU2* transcription terminator (Gaertig et al., 1994a). To disrupt either the *KIN1* or *KIN2* gene in the germline micronucleus (MIC) we introduced transforming DNA into early mating cells using the biolistic gun (Cassidy-Hanley et al., 1997). For disruption of *KIN1*, 4 μg of pKIN17-7neo DNA that had been digested with HindIII were used to coat 1 mg of tungsten M10 (Bio-Rad, Hercules, CA) particles (Sanford et al., 1991). For disruption of *KIN2*, 4 *m*g of pCS4bsr1 plasmid DNA that had been linearized with KpnI and SacI were used to coat gold particles (1 μm, Bio-Rad). Strains CU428.1 and B2086.1 were allowed to conjugate for 2.5–3.5 h before bombardment. For *KIN1* disruption, bombarded cells were incubated in SPP for 12 h at room temperature, and transformants were selected in SPP with 120 *m*g/ml paromomycin. For *KIN2* disruption, bombarded cells were incubated for 7 h at 30°C in SPP, left for 14–16 h at room temperature, and selected in SPP with 60 *m*g/ml bs.

Transformants heterozygous for *KIN1/kin1::neo2* or *KIN2/kin2::bsr1* were identified and brought to homozygosity in the MIC as described (Cassidy-Hanley et al., 1997). To construct strains lacking all copies of both *KIN1* and *KIN2* in their MICs, we crossed a strain homozygous for the *kin1::neo2* gene to a strain homozygous for the *kin2::bsr1* gene and selected double heterozygotes resistant to both paromomycin and bs. These were crossed to the B*VII strain (Orias and Bruns, 1976) to generate micronuclear homozygotes, and the exconjugants from this cross were reisolated, grown, and crossed to a CU427.3 strain. Double knockout heterokaryons strains were identified (UG13 and UG14) that have different mating types.

Phenotypic Analyses

Growth rates were measured in SPP medium without shaking by counting cells periodically using a Coulter Electronics (Hialeah, FL) model ZF counter. Dead cells were identified by trypan blue exclusion test by adding 30 μl of 0.4% trypan blue (Sigma, St. Louis, MO) to 70 μl of cells in culture medium. To measure the rate of cell movement, 40 μl of cells from a growing culture were placed on a slide and analyzed in a hanging drop, using an Olympus Optical (Tokyo, Japan) inverted microscope and 4× phase-contrast objective. Images of moving cells were recorded using a video camera and image capture software. Distances traveled by moving cells were measured using NIH Image version 1.62. To analyze the rate of ciliary regeneration, cells were grown to a density of 3×10^5 cells/ml, starved for 24 h in 10 mM Tris-HCl, pH 7.5, and deciliated (Calzone and Gorovsky, 1982). Cilia regeneration was monitored by determining the fraction of motile cells. To bring the double knockout phenotype to expression, heterokaryon strains UG13 and UG14 were crossed to each other. Nine to 10 h after mixing, individual pairs were isolated into drops of SPP or MEPP medium and left for 13–15 h at room temperature. As controls, wild-type exconjugants or parental cells were isolated. The cell number in each drop was determined by counting live cells under an inverted microscope. Observations of live dividing cells were done on the Zeiss (Thornwood, NY)

Axioscope microscope using differential interference contrast optics with the Plan-NeoFluar 40× (numerical aperture, 0.75) lens. The images were recorded on the DAGE-MTI (Michigan City, IN) DC330 charge-coupled device camera. The s-video output of the camera was fed directly into the Macintosh G3/AV All-in-one computer using the Apple (Cupertino, CA) Video Player software.

Immunocytochemistry and Electron Microscopy

For staining double knockout cells, ~500–1000 cells were isolated into 30 μl of 10 mM Tris, pH 7.5, on a coverslip. An equal volume of 2% paraformaldehyde, 0.5% Triton X-100, and 1 μM paclitaxel in PHEM (60 mM PIPES, pH 6.9, 25 mM HEPES, 10 mM EGTA, 2 mM MgCl2) was added, and samples were air dried at 30°C. Coverslips were processed for immunofluorescent labeling as described (Gaertig et al., 1995), using rabbit polyclonal SG serum raised against *Tetrahymena* total tubulin (Guttman and Gorovsky, 1979) at 1:100 dilution. Cells expressing the epitope-tagged Kin1p were double labeled using the TAP952 mouse monoclonal antibodies directed against the monoglycylated isoforms of tubulins (Callen et al., 1994) and the anti-GFP rabbit polyclonal antibodies (Clontech, Palo Alto, CA) at 1:100 and 1:400 dilution, respectively. Secondary antibodies were goat anti-mouse FITC (Sigma), goat anti-rabbit-Cy3, and goat anti-rabbit-FITC (Zymed, San Francisco, CA) conjugates, and all were used at 1:100 dilution. Cells were viewed using a Bio-Rad MRC 600 confocal microscope. The length of axonemes either on cells or isolated was determined on confocal sections using NIH Image software version 1.62. To increase the consistency of analysis of ciliary axoneme lengths on whole cells, for each cell analyzed a single confocal section was chosen, which included the widest cross-section of the macronucleus that could be found in that z-series.

For electron microscopy, Cells were washed with 10 mM Tris, pH 7.5, and fixed in 2% glutaraldehyde in 100 mM cacodylate buffer at 4°C for 1 h, incubated in 2.5% sucrose in 100 mM cacodylate for 20 min, and postfixed in 1% osmium tetroxide in 100

mM cacodylate for 1.5 h at 4°C. Cells were embedded in Epon after dehydration in graded steps from 30 to 100% ethanol. Sections were stained with uranyl acetate and lead citrate and were visualized on a JEOL (Tokyo, Japan) 100CXII transmission electron microscope.

Construction of Epitope-tagged Targeting Fragments and Rescue Transformation

The Muta-Gene phagemid in vitro mutagenesis kit (Bio-Rad) was used to create MluI (5') and NcoI (3') sites near the N terminus of the *KIN1* coding sequence on the plasmid pKIN17-7 to construct pKIN17NM. The sequence of the mutagenic oligonucleotide, KINL-MC, is 5'-TTT ACT ATT TTT TTC CAT GGC TTC TAC GCG TTT GCT CAT TAT ACT T-3'. The 5xMyc insert was prepared by amplifying the plasmid pJR1265 (kindly provided by Dr. K. Kozminski, University of California, Berkeley, CA) with the primers MYC-ML, 5'-GGA CGC GTC TTT AAA GCT ATG GAG CAA AAG-3', and SK, 5'-TCT AGA ACT AGT TGG ATC-3'. After digesting with MluI and NcoI it was inserted into the corresponding sites of pKIN17NM to construct pKIN17myc-6. To prepare a GFP-tagged Kin1 gene, the GFP sequence was amplified from pH4.GFP1 plasmid (kindly provided by Dr. A. Turkewitz, University of Chicago, Chicago, IL; Haddad and Turkewitz, 1997) using primers GFP5'Ml, 5'-GAC GCG TAA TGA GTA AAG GAG AAG AAC-3', and GFP3'Bsp, 5'-GTC ATG ATT TTG TAT AGT TCA TCC ATG C. The PCR product was digested with MluI and BspHI and subcloned between the MluI and NcoI sites of the pKIN17myc-6 in place of the Myc epitope tag to give pKIN17gfp plasmid. For preparation of rescuing DNA, pKIN17-7, pKIN17myc-6, and pKIN17gfp were digested with HindIII, and pCS4 was digested with SacI and KpnI. Double knock-out heterokaryon strains UG13 and UG14 were starved, mixed, and transformed by biolistic bombardment at 10 h after mating. Rescued conjugation progeny were selected with 15 mg/ml 6-methylpurine.

Cell Fractionation and Western Blotting

Cells were grown to 4×10^5 /ml at 30°C in 300 ml of SPP, washed once with 10 mM Tris, pH 7.5, and suspended in 15 ml of 10 mM Tris, pH 7.5, containing protease inhibitors (1 mM PMSF, 1 μg/ml pepstatin A, 1 μg/ml leupeptin, 10 μg/ml chymostatin, 10 μg/ml antipain, 5 μg/ml E-64; all inhibitors from Sigma). Dibucaine (Sigma) was added at a final concentration of 3 mM. When most cells had stopped moving (~2 min), 5 vol of ice-cold 10 mM Tris, pH 7.5, were added. All subsequent procedures were performed at 4°C. Cell bodies were sedimented by centrifugation at $1100 \times$ g for 5 min. The supernatant was collected, and the centrifugation was repeated. Cilia were collected by centrifugation at $14{,}000 \times$ g for 20 min, washed once in wash buffer (10 mM HEPES, pH 7.4, 100 mM NaCl, 4 mM $MgCl_2$, 0.1 mM EGTA) containing protease inhibitors, and recentrifuged at $14{,}000 \times$ g. Cell bodies were washed once in 10 mM Tris, pH 7.5, and recentrifuged at $1100 \times$ g. Pellets containing cell bodies or cilia were weighed and resuspended at 100 mg of wet pellet/ml in either 10 mM Tris, pH 7.5, plus protease inhibitors (cell bodies) or wash buffer plus protease inhibitors (cilia). To obtain axonemes, 10 mg of cilia were extracted with wash buffer containing 0.5% NP-40 on ice for 10 min and centrifuged at $14{,}000 \times$ g. The supernatant, containing membranes, was retained. The axonemal fraction was resuspended in the original volume of wash buffer plus protease inhibitors. Either 500 μg of cilia or axonemes or NP-40-soluble fraction (each obtained from 500 μg of cilia) were subjected to 8% SDS-PAGE and transferred onto a 0.45- μm Trans-Blot nitrocellulose membrane (Bio-Rad) by semidry electroblotting using the Trans-Blot SD cell (Bio-Rad) at 20 V for 2 h. Filters were blocked in 5% dry milk, 0.1% Tween 20, and $1\times$ PBS for 1.5 h and incubated overnight at 4°C in reaction buffer (1% dry milk, 0.1% Tween 20 in $1\times$ PBS) with anti-Myc hybridoma supernatant (clone 9E10; American Type Culture Collection, Manassas, VA) at 1:2.5 dilution, rabbit anti-histone hv1 serum at 1:10,000 dilution, or mouse AXO49 anti-bodies at 1:3000 dilution. Membranes were washed in PBST (13PBS, 0.1% Tween

20) at room temperature, incubated in reaction buffer with 1:1500 dilution of either anti-mouse immunoglobulin G or anti rabbit immunoglobulin HRP-linked goat antibodies (Amersham, Arlington Heights, IL) for 1.5 h, and washed once for 15 min, two times for 5 min each in PBST, and then three times for 5 min each in 1× PBS. Blots were developed using the ECL Western blotting analysis system (Amersham).

RESULTS

Cloning of KIN1 and KIN2, Members of the Kinesin-II Family, in T. thermophila

We identified fragments of four putative KRP genes (*KIN1–KIN4*) using PCR of total genomic DNA of *T. thermophila*.We cloned genomic restriction fragments of *KIN1* and *KIN2*, and sequence analysis revealed open reading frames encoding proteins of 735 and 697 amino acids, respectively, that were most similar to kinesin-II. The predicted *KIN1*-encoded protein (Kin1p) has a calculated molecular mass of 85.04 kDa and a pI of 7.61, whereas Kin2p has a calculated molecular mass of 82 kDa and a pI of 6.88. By comparing genomic sequences with the corresponding cDNAs, we identified three small introns in each gene. Two of the three introns of *KIN1* and *KIN2* are located at the same positions within the coding sequences (Figure 3.1A). The two genes are genetically linked in the micronuclear genome (our unpublished results). Both predicted proteins have an expected structure of a kinesin-II heavy chain, with a central region of α-helical coiled coil flanked by globular N- and C-terminal motor and tail regions, respectively (Figure 3.1A). By comparing the Kin1p and Kin2p sequences with kinesin heavy chain of *Drosophila melanogaster* (Yang et al., 1989), we identified a kinesin motor domain within the N-terminal globular domains of both proteins. Phylogenetic analysis showed that the motor domains of Kin1p and Kin2p are more related to each other (67% identical) than to any other known kinesin-II (60 –63%) (Figure 3.1B). *KIN1* and *KIN2* also showed significant homology (54%) between their rod domains and lower levels of homology with the rod domains of other kinesins-II (Figure 3.1C). The tails of *KIN1* and

KIN2 are very basic but showed only weak homology to each other (32% sequence identity).

Cells Lacking Either KIN1 or KIN2 Show Deficiencies in Cell Growth, Motility, Ciliary Assembly, and Thermoresistance

Tetrahymena cells, like most other ciliates have two nuclei, the germ line, transcriptionally silent MIC and the somatic, transcriptionally active macronucleus (MAC). To disrupt *KIN1* in both the MIC and MAC, we used a fragment in which the *neo2* gene was inserted into the motor domain. We biolistically transformed the MICs of early conjugating cells (Figure 3.2A; see MATERIALS AND METHODS). Southern blotting showed that one transformant contained a disrupted *KIN1* gene (Figure 3.2B), whereas in the second transformant, the *kin1::neo2* fragment integrated into the 3' flanking region of *KIN1*. Homozygotes for the disrupted allele in the MIC and MAC were constructed using two rounds of "genomic exclusion" (Figure 3.2A; see MATERIALS AND METHODS). We used essentially the same strategy to disrupt *KIN2*, except that we used the *bsr1* gene as a disruption cassette instead of *neo2* (Figure 3.2C).

Strains lacking either *KIN1* or *KIN2* were viable, morphologically normal, and motile but multiplied more slowly than wild-type (WT) strains, with the doubling times that were 23 and 86% longer than WT, respectively (Table 3.2). Furthermore, single knockout strains showed decreased survival rate when exposed to higher temperatures. After 45–47 h of incubation at 39–40°C, ΔKIN1 and ΔKIN2 cells had viabilities that were 50 and 73% of WT viabilities, respectively (Table 3.2).

ΔKIN1 cells swim more slowly than control WT cells (Table 3.2). When grown for 1 d before measurement at 30°C, the average speed of ΔKIN1 was 67% of WT. ΔKIN2 cells did not show any defect in motility rate (Table 3.2). At 30°C, ΔKIN1 cells showed a nearly normal rate of cilia formation after deciliation (Table 3.2). However, at 38–40°C, ΔKIN1 cells regenerated cilia with a half-time of recovery almost twice that of WT cells. ΔKIN2 showed no difference from WT at 30 or 39°C.

Either KIN1 or KIN2 Is Required for Assembly of Cilia and Normal Cytokinesis

To test for synthetic interactions between *KIN1* and *KIN2,* we created double knockout heterokaryons lacking *KIN1*and *KIN2* in their MICs and having WT alleles in their MACs. To bring the double knockout (ΔKIN1ΔKIN2) phenotype to expression in the MACs, we crossed heterokaryon strains to each other. As a control, we also mated cells having only WT copies. ΔKIN1ΔKIN2 pairs separated at the proper time, indicating that zygotic expression of neither Kin1p nor Kin2p is required for the completion of conjugation. When refed ΔKIN1ΔKIN2 cells multiplied more slowly than WT controls. By 36 h after pair isolation, the average number of cells per drop (cells derived from a single mating pair) was 27.9 ± 32.0 and 91.6 ± 25.0 for ΔKIN1ΔKIN2 and WT cells, respectively (n = 41 and 47, respectively). On a standard culture medium (SPP), WT cells continued to grow to maximal density, whereas after 84 h, all ΔKIN1ΔKIN2 cells failed to multiple further and died out within a few days.

The most striking difference in the ΔKIN1ΔKIN2 cells compared with single knockouts was their progressive loss of motility. By 36 and 84 h after pair isolation, 71.4 and 100% of ΔKIN1ΔKIN2 drops (n = 41) contained no motile cells, respectively, compared with only 2% of control isolates at 84 h (n =47). Confocal analysis revealed that ΔKIN1ΔKIN2 cells contained fewer normal-length ciliary axonemes (Figure 3.3), with most of the decrease occurring between 12 and 36 h (Figure 3.4E). During the *Tetrahymena* cell cycle, locomotory cilia are not resorbed before cell division. Instead, full-length cilia are retained, whereas new cilia are assembled from new basal bodies that appear near the existing basal bodies (Dippell, 1968). At 22 h after pair isolation we observed ΔKIN1ΔKIN2 cells with axonemes that were highly heterogeneous in length (Figure 3.3D). Further axoneme shortening occurred between 22 and 84 h, leading to axon-emes with a mean length of 7.7% of the length in WT (Figures 3.3, E–H, and 4E). By 29 h most cells have undergone only zero to four cell divisions and therefore would normally

contain 100–6.25% of the preexisting cilia transmitted from the exconjugants. However, at 29 h, many cells already completely lacked cilia of normal length (Figure 3.3, E and F). Thus, kinesin-II is required for both assembly of new cilia and maintenance of preexisting cilia. Transmission electron micrographs revealed that at 84 h most cilia contained only extremely short remnants of outer doublets and were covered by a small bulge of the plasma membrane (Figure 3.4, A and B). Cross-sections, in contrast, showed normal structure of basal bodies in mutants (Figure 3.4, C and D).

Surprisingly, many ΔKIN1ΔKIN2 cells grew large in size and had increased numbers of nuclei. A WT cell undergoing cytokinesis is shown in Figure 3A. Many ΔKIN1ΔKIN2 cells contained multiple "subcells" and multiple nuclei, indicating that they failed to complete cytokinesis after nuclear division (Figure 3.3, F–H). At 60 h in the standard SPP medium 58.5% of ΔKIN1ΔKIN2 cells had more than one subcell, compared with 3% of WT cells (Figure 3.5A). Along with the increase in the number of subcells, we observed an increase in the number of nuclei in ΔKIN1ΔKIN2 cells (Figure 3.5, B and C). Importantly, the two major phenotypic traits of ΔKIN1ΔKIN2 mutants, cell paralysis and arrest in cytokinesis, have different times of onset. Specifically, the cell paralysis appears to occur before the cytokinesis arrests. For example, at 22 h, the majority of double knockout isolates already contained paralyzed cells, whereas only a few percent of cells contained multiple subunits or nuclei (Figure 3.5D). Furthermore, virtually all live multinucleated "monsters" that we observed were completely paralyzed. These observations raise the intriguing possibility that the observed cytokinesis defects are caused by the loss of cilia or simply by the loss of cell motility.

Double Knockout Cells Can Be Rescued by Reintroduction of a Wild-Type *KIN1* or *KIN2* Gene

If the absence of both *KIN1* and KIN2 is the cause of the phenotypes of ΔKIN1ΔKIN2 cells, reintroduction of either WT *KIN1* or *KIN2* should rescue the mutant cells. We mated cells that were not only double knockout heterokaryons but that also have the

mpr1-1 gene in their MICs and not their MACs. The mpr1-1 gene confers resistance to 6-methylpurine (mp). Because the drug resistance allele is in the MIC and not in the MAC, only conjugation progeny cells can survive in the presence of mp, whereas all nonmating cells as well as cells that abort mating without developing a new MAC are killed (Orias and Bruns, 1976). When these were crossed and plated on SPP medium containing mp, no surviving cells were recovered in multiple experiments despite using large numbers of mating cells (1×10^7 cells per experiment; $n = 4$). In contrast, viable and motile clones were recovered (at a frequency of 1–50 per experiment) when ΔKIN1ΔKIN2 heterokaryons were bombarded with particles coated by either *KIN1* or *KIN2* fragments.

Epitope-tagged Kin1p Preferentially Accumulates in Cilia That Undergo Active Assembly

We subsequently rescued mating ΔKIN1ΔKIN2 heterokaryons using a genomic fragment of *KIN1* modified by addition of a 5xMyc epitope tag to the N terminus of predicted Kin1p. The mechanism of rescue is based on replacement of the disrupted macronuclear copies of the target gene by the rescuing fragment, mediated by homologous recombination (Hai and Gorovsky, 1997). Thus, using the heterokaryon rescue approach, the epitope-tagged Kin1p is expressed at its normal locus using its own promoter. Using anti-Myc antibodies we detected a protein of the expected molecular mass of ~100 kDa in cells rescued by a gene encoding 5xMyc-Kin1p but not in cells rescued by a WT *KIN1* gene (Figure 3.6A). Western blotting analysis showed the presence of 5xMyc-Kin1p in the ciliary fraction, but no signal was detected in the equivalent amount of the cell bodies (Figure 3.6A). Purity of cell fractions was verified using anti-macronuclear histone, hv1 antibodies (Stargell et al., 1993), and AXO49 antibodies directed against hyperglycylated tubulin isoforms known to be specific to cilia (Bre et al., 1996). On Western blots, the anti-hv1 histone antibodies detected a single band of expected size in the cell body fraction but not in the ciliary fraction (Figure 3.6B), whereas the AXO49 cross-reacted only with the ciliary fraction (Figure 3.6C). Extraction of cilia with NP-40 showed that

approximately half of 5xMyc-Kin1p was present in the membrane plus soluble matrix fraction, and half was in the insoluble axonemal fraction (Figure 3.6A). When fixed and permeabilized cells expressing 5xMyc-Kin1p were processed for immunofluorescence with anti-Myc antibodies, we repeatedly failed to detect any signal above the background observed in control cells.

In an attempt to increase the sensitivity of detection of Kin1p, we rescued ΔKIN1ΔKIN2 cells with a gene encoding Kin1p fused to GFP. The GFP-Kin1p transformants grew well and were motile. Although we could not detect any GFP autofluorescence in live transformant cells, we detected the GFP-Kin1p signal in fixed cells by immunofluorescence using polyclonal anti-GFP antibodies. In WT nondividing (Figure 3.7A) and dividing cells (Figure 3.7M), anti-GFP antibodies produced only a weak background staining in the cell body, whereas cilia were not stained. In cells rescued by a GFP-KIN1 fragment, a weak GFP signal was detected in cilia, and there was an increase of signal in the cell body relative to negative control cells (Figure 3.7G). Most locomotory cilia were weakly labeled, except a few cilia, which were labeled more strongly and were generally shorter and therefore could be immature cilia in the process of their assembly (Figure 3.7, G and H boxed areas). Strong GFP labeling was observed in oral cilia in the developing oral apparatus in dividing cells (Figure 3.7O, arrows), and only weak labeling was detected in mature oral cilia of nondividing cells (Figure 3.7G, arrows). Thus, it appears that Kin1p preferentially accumulates in locomotory and oral cilia, which undergo active assembly. To test this hypothesis, we analyzed the localization of GFP-Kin1p in nongrowing cells (incubated in a starvation medium overnight), which were deciliated and allowed to regenerated cilia. These cells were double labeled using anti-GFP antibodies and the TAP952 monoclonal antibodies, which recognize monoglycylated tubulins (Bre etal., 1996).

In starved cells before deciliation, the TAP952 antibody primarily labeled the tips of cilia (Figure 3.8B). However, in regenerating cells, newly assembled cilia were labeled

more uniformly by TAP952 (Figure 3.8, D and F). Thus, the uniform labeling with the TAP952 antibody can be used as a marker for newly assembled cilia. In starved cells before deciliation, the pattern of distribution of GFP-Kin1p was similar to the pattern seen in vegetatively growing cells, with most of the GFP signal present in cilia and some staining of the cell body (Figure 3.8A). Twenty minutes after deciliation, short cilia were already present, and virtually all cilia were labeled heavily by anti-GFP and uniformly by TAP952 antibodies (Figure 3.8, C and D). At 45 min most cilia were also stained brightly by anti-GFP antibodies and uniformly by the TAP952 antibodies (Figure 3.8, E and F). Negative control cells did not show any ciliary labeling by anti-GFP antibodies at 45 min (our unpublished results). By 180 min, most cilia in cells expressing GFP-Kin1p were already fully assembled, as indicated by the pattern of labeling of TAP952 (mainly tips of cilia), and there was a dramatic decrease in the staining intensity of cilia by anti-GFP antibodies (Figure 3.8, G and H). Thus, in cilia regenerating starved cells, Kin1p preferentially accumulates in cilia that actively assemble, and its abundance decreases dramatically after ciliary assembly is completed.

Strikingly, in vegetatively growing cells individual locomotory cilia, which were labeled strongly with anti-GFP, antibodies were also labeled uniformly by the TAP952. In most cases, scattered single growing cilia (more uniform TAP952 labeling) were strongly labeled by anti-GFP antibodies and were immediately adjacent to mature cilia (tip labeling by TAP952), which were only very weakly labeled by anti-GFP antibodies (Figure 3.7, I–L). Negative control cells lacking GFP-Kin1p showed no anti-GFP labeling in both mature and growing cilia (Figure 3.7, C–F). Newly developed oral cilia, which were labeled heavily by anti-GFP antibodies, were also uniformly labeled by TAP952 antibodies (Figure 3.7, O and P). Thus, Kin1p is preferentially targeted to a subset of cilia that undergo active assembly in both vegetatively growing and cilia regenerating cells. The targeting mechanism appears to operate at the resolution level of a single cilium.

Loss of Viability of Double Knockout Cells Is Caused by Inability to Phagocytose

In *Tetrahymena* cells a subset of specialized cilia is organized into four oral membranelles that surround the oral cavity. Coordinated beating of oral cilia is required for directing food particles into the phagocytic vacuoles formed at the bottom of the oral cavity. At 41–60 h, (Figure 3.3, G and H) most ΔKIN1ΔKIN2 cells appeared to lack any oral membranelles, which were easily identified in WT cells (Figure 3.3A) or in ΔKIN1ΔKIN2 cells at earlier time points (Figure 3.3, C–F). Microscopic observations of live ΔKIN1ΔKIN2 cells showed absence of any food vacuoles inside the cell body. Thus, the ΔKIN1ΔKIN2 cells lose their ability to phagocytose, likely because they lack oral cilia. This observation raises the possibility that ΔKIN1ΔKIN2 cells die on the standard medium (SPP) because they are unable to feed. Although *Tetrahymena* cells require phagocytosis to grow on the SPP medium used so far in this study, mutants of *Tetrahymena* that lack a functional oral apparatus, can be grown in a modified medium (MEPP). Presumably, this medium stimulates alternative routes for nutrient uptake, such as micropinocytosis (Orias and Rasmussen, 1976). Strikingly, unlike in SPP medium, in MEPP most ΔKIN1ΔKIN2 cells remained viable and divided with a doubling time of ~8.5 h. Thus, the cause of lethality of double knockout cells in SPP is the inability to perform phagocytosis, resulting from the loss of oral cilia. Although ΔKIN1ΔKIN2 cells continued to grow and divide in the MEPP medium, they remained completely paralyzed, and many remained multinucleated (Figures 3.3I and 3.5).

Cell Division Phenotype in Double Knockout Cells Is Most Likely Induced by Cell Paralysis

To assess how the absence of Kin1p and Kin2p affects the course of cytokinesis, we analyzed live WT and ΔKIN1ΔKIN2 cells during cell division using video microscopy. In *T. thermophila*, initially the cleavage furrow is formed asymmetrically on one side of the cell. We isolated early dividers having a unilateral cleavage furrow from WT

and ΔKIN1ΔKIN2 populations and analyzed the course of cytokinesis (Figure3.9). It took ~20 min for WT cells to complete cell division starting from the unilateral cleavage stage (Figure 3.9, A–F). Mutant cells showed a nearly normal cleavage furrow ingression (Figure 3.9, G–K), but many failed to separate at the final stage of cytokinesis. Figure 3.9 shows a ΔKIN1ΔKIN2 cell that had almost a complete cleavage furrow ingression at 25 min (Figure 3.9K) but failed to separate completely and after 6 h showed signs of cortical integration, with the cytoplasmic content of the posterior cell being absorbed by the anterior cell (Figure 3.9L).

As already mentioned, the temporal analysis of phenotypic traits indicated that the cell division arrests occur after cells become paralyzed. Furthermore, we did not see any Kin1p in association with the cleavage furrow (Figure 3.7O). All these observations taken raised a possibility that the arrests at cytokinesis in ΔKIN1ΔKIN2 cells are caused by lack of ciliary motility. Thus, *Tetrahymena* cells may require cell locomotion to complete cytokinesis. Dividing WT cells are generally less motile compared with nondividing cells and tend to sit at the bottom of a culture dish. However, a video analysis of a number of WT cells revealed that within ~2 min before cell separation the posterior daughter cell often rotates along its longitudinal axis, and virtually all daughter cells briefly pull apart immediately before their final separation (our unpublished results). It is likely that the rotations create a strain within the membranous channel connecting the daughter cells, which facilitate its breakage when the cells pull apart. The detailed analysis of the motile activity of dividing cells will be published elsewhere (Brown, Hardin, and Gaertig, unpublished data). The dividing double knockout cells remain completely paralyzed in the course of cell division. Thus, it appears that the arrests in cytokinesis frequently seen in ΔKIN1ΔKIN2 cells are induced by cell paralysis.

DISCUSSION

To investigate the function of kinesin-II *in vivo*, we constructed strains of *T. thermophila*, which lack the kinesin-II-encoding genes *KIN1* and *KIN2*. Cells lacking either *KIN1* or

KIN2 exhibited several subtle phenotypes. Some of these, such as slow growth and temperature sensitivity were observed in cells lacking either of the two genes. However, only cells lacking *KIN1* showed reduced cell motility and impaired assembly of cilia. The reduction in growth rate was more severe in the *KIN2* null cells. Thus, although the phenotypes caused by deletion of either gene partly overlap, *KIN1* appears to be more important for ciliary functions, whereas *KIN2* is more important for cell multiplication.

Three lines of evidence indicate that *KIN1* and *KIN2* arose relatively recently as a result of the duplication of a common ancestor kinesin-II gene: 1) sequences of *KIN1* and *KIN2* are more similar to each other than to any other known kinesins-II; 2) positions of two of three introns are conserved; and 3) the two genes are genetically linked and thus are located not far from each other on the same micronuclear chromosome. To address the possibility of overlapping functions between *KIN1* and *KIN2*, we created cells lacking all copies of both genes, using a novel approach based on construction of heterokaryon strains lacking specific genes in the germ line micronucleus and having normal gene copies in the somatic macronucleus (Hai and Gorovsky, 1997). The heterokaryons are phenotypically normal, because only the macronuclear genes are expressed during the vegetative life of *Tetrahymena*. However, when two heterokaryons mate, they form new MACs from the micronuclei, which lack all functional copies of the targeted genes. This approach effectively produces an inducible gene knockout. Double knockout cells showed two major defects: 1) extreme shortening of locomotory and oral cilia and 2) frequent failure in cytokinesis. Double knockout cells were not viable on a standard medium but could grow on a modified medium on which *Tetrahymena* cells do not require phagocytosis for their survival (Orias and Rasmussen, 1976). Thus, the lethality observed on the standard medium is most likely caused by the loss of oral cilia, which are essential for phagocytosis in *Tetrahymena*. Consequently, *Tetrahymena* cells do not require *KIN1* and *KIN2* for their survival under conditions in which cells are not dependent on phagocytosis.

The most dramatic phenotypic change in double knockout *Tetrahymena* cells is the almost complete loss of cilia. Similarly, mutation of the *Chlamydomonas* kinesin-II *FLA10* leads to complete resorbtion of existing flagella (Lux and Dutcher, 1991; Walther et al., 1994). Knockout of the kinesin-II gene in mouse, KIF3B, caused death of embryos before midgestation. However, the nodal cells in the KIF3B-deficient embryos completely failed to assemble cilia (Nonaka et al., 1998). This phenotype is essentially identical to the phenotype caused by elimination of both Kin1p and Kin2p in *Tetrahymena*. Thus, kinesin-II genes function universally in ciliary assembly.

We show that in addition to its role in the assembly of new cilia, kinesin-II is also essential for ciliary maintenance. In wild-type *Tetrahymena*, most if not all locomotory cilia are never resorbed during the vegetative life cycle. Strikingly, we found that after induction of the knockout phenotype, mutant cells not only failed to assemble new cilia but also resorbed all of their preexisting cilia. Moreover, an epitope-tagged Kin1p was found along the full length of cilia in nongrowing (starved) cells, consistent with the involvement of kinesin-II in ciliary maintenance. These data are consistent with a high level of turnover of axonemal subunits reported for morphostatic cilia and flagella (Rosenbaum and Child, 1967; Nelsen, 1975; Stephens, 1997) and suggest that the subunit turnover is driven by kinesin-II and possibly other molecular motors.

Although kinesin-II is required for both assembly and maintenance of cilia, we found that epitope-tagged motor proteins preferentially accumulate in cilia that undergo assembly. This phenomenon was observed in regenerating cilia and in a subset of oral and locomotory cilia that assemble in vegetative cells. *Tetrahymena* cells appear to use a mechanism that preferentially directs kinesin-II to the newly assembled cilia or causes its preferential retention by assembling cilia. Because in *Tetrahymena* new cilia are formed immediately adjacent to the preexisting cilia, the proposed targeting and retention mechanism must operate at the resolution level of a single cilium. Interestingly, immunofluorescence studies in *Chlamydomonas* showed that the kinesin-II epitopes were

more concentrated near the basal bodies and in the proximal part of the axoneme (Vashishtha et al., 1996; Cole et al., 1998). Thus, initially, kinesin-II may be targeted to the basal bodies and later move to the adjacent axoneme.

The molecular nature of kinesin-II involvement in ciliogenesis and ciliary maintenance is not well understood. In *Chlamydomonas*, FLA10 activity is required to maintain intraflagellar transport, the motility of raft particles detected beneath the flagellar membrane (Kozminski et al., 1995). Induction of the *fla10* mutant phenotype caused loss of rafts and the loss of two types of 16S protein complexes from flagella, suggesting that 16S complexes are both components of rafts and the FLA10 cargo (Piperno and Mead, 1997; Cole et al., 1998). One of the components of the 16S complex in *Chlamydomonas* is a protein homologous to the OSM-6 protein of *C. elegans*, which plays an essential role in the function of chemosensory ciliary neurons (Cole et al., 1998; Collet et al., 1998). Recently, fluorescent OSM-6-GFP protein was observed to move inside the chemosensory cilia of living *C. elegans* worms at the same rate as the rate of movement of the KAP subunit of the kinesin-II complex (Orozco et al., 1999). The 16S complexes are most likely components of rafts seen in live cells by differential interference contrast microscopy and are proposed to function in transport of flagellar subunits (Rosenbaum et al., 1999). Consistent with this hypothesis, induction of the *fla10* phenotype blocked transport of an inner dynein arm polypeptide but allowed for transport of an outer dynein arm component (Piperno et al., 1996), suggesting that the inner but not outer arm components are one of the cargoes of kinesin-II. It seems unlikely, however, that a failure to transport inner dynein arm components by kinesin-II would result in a complete block in axonemal assembly, because numerous mutants lacking specific axonemal components (dynein arms and radial spokes) have been described that still assemble axonemes (Dutcher, 1995). It is likely that kinesin-II in addition to its role in the transport of dynein arm components is also involved in the transport of some structural components required for the initial elongation of the axoneme such as

microtubule subunits or ciliary membranes. Interestingly, longitudinal sections of basal bodies on ΔKIN1ΔKIN2 cells showed that many of the very short axonemal fragments are covered by a bulge of ciliary membrane, suggesting that membranes are properly delivered to the growing axoneme. It appears that kinesin-II is involved in the delivery of a basic structural component of cilia that is essential for elongation of axonemal microtubules, such as tubulin dimers or oligomers.

The most unexpected result of our study was the frequent failure of double knockout cells to complete cytokinesis. Some previous studies suggested that kinesin-II plays a direct role in cell division. Immunofluorescent studies in sea urchin embryos showed an accumulation of kinesin-II proteins in the interzone of the mitotic spindle during anaphase before the formation of the cleavage furrow (Henson et al., 1995). Also, the *fla10* mutation results in synthetic defects in the cell cycle when combined with another mutation (Lux and Dutcher, 1991), and FLA10 protein transiently associates with the centrioles in *Chlamydomonas* (Vashishtha et al., 1996). However, despite dramatic cytokinesis defects in our kinesin-II mutants, we did not find any evidence that would support direct involvement of kinesin-II in cytokinesis. First, immunolocalization studies showed that epitope-tagged Kin1p is highly concentrated in cilia. Although some Kin1p was detected in the cell body by immunofluorescence, this pool did not show any clear association with the cleavage furrow or changes in the distribution during the cell cycle. More likely, the cell body pool of Kin1p represents the newly synthesized motor subunits before their delivery to cilia. Furthermore, the double KIN mutants appear not to be affected in the initiation and ingression of the cleavage furrow until the final stage of cytokinesis when the daughter cells break the cytoplasmic connection. At that time in wild-type cells we found that the posterior daughter cells often rotate along their longitudinal axis, and both daughters pull apart. These observations suggest that *Tetrahymena* cells use mechanical force generated by ciliary beating to culminate

cytokinesis. This hypothesis is consistent with the earlier onset of the cell paralysis phenotype compared with the cell division arrest phenotype (Figure 3.6D). Although cell locomotion is not absolutely required for cell division, it appears to be an evolutionary adaptation to support the unusually high rate of culture growth of Tetrahymena.

ACKNOWLEDGMENTS

We are grateful to Dr. Donna Cassidy-Hanley for assistance with the use of the biolistic gun. We are most grateful to University of Georgia Athens undergraduates Curtis McNiff, Brett Margolias, Wood Pope, and Clyde Hardin for contribution in analyses of knockout phenotypes and Naishaj Shah for construction of the GFP-KIN1 plasmid. We thank Dr. Mark Farmer (Center for Advanced Ultrastructural Research, University of Georgia) for help with the use of the video imaging system and for suggestions regarding capture of DAPI images on the confocal microscope. We thank Jian Zhao Shen for assistance in preparation of thin sections for electron microscopy and Yan Gao for assistance with Western blots. We also thank Dr. Mitchell Bernstein (Albert Einstein College of Medicine) for providing the sequence of the cloned KIN5 gene fragment, Dr. Nicolette Levilliers (University Paris-Sud, Paris, France) for providing the TAP952 and AXO49 antibodies, Dr. Marty Gorovsky (University of Rochester, Rochester, NY) for the SG anti-body, Dr. David Allis (University of Virginia, Charlottesville, VA) for the anti-histone hv1 antibodies, Dr. Karl Saxe (Emory Univer-sity, Atlanta, GA) for providing the bsr plasmid, Dr. Keith Kozminski for providing the Myc construct, and Dr. Aaron Turkewitz for the GFP construct. We also thank Dr. Marty Gorovsky and Dr. Joseph Frankel (University of Iowa, Iowa City, IA) for reading the manuscript and for helpful suggestions. The biolistic bombardment experiment for the disruption of the *KIN1* gene was performed at the biolistic facility of the Plant Science Center at Cornell University. This work was supported by US Public Health Service grant GM-54017 from the National Institutes of Health to J.G.

REFERENCES

Altschul, S.F., Gish, W., Miller, W., Myers, E.W., and Lipman, D.J. (1990). Sequence homology searches done using BLAST. J. Mol. Biol. *215*, 403–410.

Bre, M.-H., et al. (1996). Axonemal tubulin polyglycylation probed with two monoclonal antibodies: widespread evolutionary distribution, appearance during spermatozoan maturation and possible function in motility. J. Cell Sci. *109*, 727–738.

Callen, A.-M., et al. (1994). Isolation and characterization of libraries of monoclonal antibodies directed against various forms of tubulin in *Paramecium*. Biol. Cell *81*, 95–119.

Calzone, F.J., and Gorovsky, M.A. (1982). Cilia regeneration in *Tetrahymena*. Exp. Cell Res. *140*, 474–476.

Cassidy-Hanley, D., Bowen, J., Lee, J., Cole, E.S., VerPlank, L.A., Gaertig, J., Gorovsky, M.A., and Bruns, P.J. (1997). Germline and somatic transformation of mating *Tetrahymena thermophila* by particle bombardment. Genetics *146*, 135–147.

Cole, D.G., Chinn, S.W., Wedaman, K.P., Hall, K., Vuong, T., and Scholey, J.M. (1993). Novel heterotrimeric kinesin-related protein purified from sea urchin eggs. Nature *366*, 268–270.

Cole, D.G., Diener, D.R., Himelblau, A.L., Beech, P.L., Fuster, J.C., and Rosenbaum, J.L. (1998). *Chlamydomonas* kinesin-II-dependent intraflagellar transport (IFT): IFT particles contain proteins required for ciliary assembly in *Caenorhabditis elegans* sensory neurons. J. Cell Biol. *18*, 993–1008.

Collet, J., Spike, C.A., Lundquist, E.A., Shaw, J.E., and Herman, R.K. (1998). Analysis of osm-6, a gene that affects sensory cilium structure and sensory neuron function in *Caenorhabditis elegans*. Genetics *148*, 187–200.

Devereux, J., Haeberli, P., and Smithies, O. (1984). A comprehensive set of sequence analysis programs for the VAX. Nucleic Acids Res. *12*, 387–395.

Dippell, R.V. (1968). The development of basal bodies in *Paramecium*. Proc. Natl. Acad. Sci. USA *61*, 461–468.

Dutcher, S.K. (1995). Flagellar assembly in two hundred and fifty easy-to-follow steps. Trends Genet. *11*, 398–404.

Frohman, M.A. (1990). RACE: rapid amplification of cDNA ends. In: PCR Protocols, ed. M.A. Innis, D.H. Gelfand, J.J. Sninsky, and T.J. White, San Diego: Academic Press, 28–38.

Gaertig, J., Cruz, M.A., Bowen, J., Gu, L., Pennock, D.G., and Gorovsky, M.A. (1995). Acetylation of lysine 40 in alpha-tubulin is not essential in *Tetrahymena thermophila*. J. Cell Biol. *129*, 1301–1310.

Gaertig, J., Gu, L., Hai, B., and Gorovsky, M.A. (1994a). High frequency vector-mediated transformation and gene replacement in *Tetrahymena*. Nucleic Acids Res. *22*, 5391–5398.

Gaertig, J., Thatcher, T.H., Gu, L., and Gorovsky, M.A. (1994b). Electroporation-mediated replacement of a positively and negatively selectable b-tubulin gene in *Tetrahymena thermophila*. Proc. Natl. Acad. Sci. USA *91*, 4549–4553.

Gorovsky, M.A. (1973). Macro- and micronuclei of *Tetrahymena pyriformis*: a model system for studying the structure and function of eukaryotic nuclei. J. Protozool. *20*, 19–25.

Guttman, S.D., and Gorovsky, M.A. (1979). Cilia regeneration in starved *Tetrahymena*: an inducible system for studying gene expression and organelle biogenesis. Cell *17*, 307–317.

Haddad, A., and Turkewitz, A.P. (1997). Analysis of exocytosis mutants indicates close coupling between regulated secretion and transcription activation in *Tetrahymena*. Proc. Natl. Acad. Sci. USA *94*, 10675–10680.

Hai, B., and Gorovsky, M.A. (1997). Germ-line knockout heterokaryons of an essential alpha-tubulin gene enable high-frequency gene replacement and a test of gene transfer from somatic to germ-line nuclei in *Tetrahymena thermophila*. Proc. Natl. Acad. Sci. USA *94*, 1310–1315.

Henson, J.H., Cole, D.G., Terasaki, M., Rashid, D., and Scholey, J.M. (1995). Immunolocalization of the heterotrimeric kinesin-related protein KRP(85/95) in the mitotic apparatus of sea urchin embryos. Dev. Biol. *171*, 182–194.

Johnson, K.A., and Rosenbaum, J.L. (1992). Polarity of flagellar assembly in Chlamydomonas. J. Cell Biol. 119, 1605–1611.

Kneller, D.G., Cohen, F.E., and Langridge, R. (1990). Improvements in protein secondary structure prediction by an enhanced neural network. J. Mol. Biol. *214*, 171–182.

Kondo, S., Sato Yoshitake, R., Noda, Y., Aizawa, H., Nakata, T., Matsuura, Y., and Hirokawa, N (1994). KIF3A is a new microtubule-based anterograde motor in the nerve axon. J. Cell Biol. *125*, 1095–1107.

Kozminski, K.G., Beech, P.L., and Rosenbaum, J.L. (1995). The *Chlamydomonas* kinesin-like protein FLA10 is involved in motility associated with the flagellar membrane. J. Cell Biol. *131*, 1517–1527.

Kozminski, K.G., Johnson, K.A., Forscher, P., and Rosenbaum, J.L. (1993). A motility in the eukaryotic flagellum unrelated to flagellar beating. Proc. Natl. Acad. Sci. USA *90*, 5519–5523.

Lupas, A., Van Dyke, M., and Stock, J. (1991). Predicting coiled coils from protein sequences. Science *252*, 1162–1164.

Lux, F., III, and Dutcher, S.K. (1991). Genetic interactions at the FLA10 locus: suppressors and synthetic phenotypes that affect the cell cycle and flagellar function in *Chlamydomonas reinhardtii*. Genetics *128*, 549–561.

Marszalek, J.R., Ruiz-Lozano, P., Roberts, E., Chien, K.R., and Gold-stein, L.S. (1999). Situs inversus and embryonic ciliary morphogenesis defects in mouse mutants lacking the KIF3A subunit of kinesin-II. Proc. Natl. Acad. Sci. USA *27*, 5043–5048.

Morris, R.L., and Scholey, J.M. (1997). Heterotrimeric kinesin-II is required for the assembly of motile 9 + 2 ciliary axonemes on sea urchin embryos. J. Cell Biol. *138*, 1009–1022.

Muresan, V., Abramson, T., Lyass, A., Winter, D., Porro, E., Hong, F., Chamberlin, N.L., and Schnapp, B.J. (1998). KIF3C is a novel neuronal kinesin that interacts with KIF3A and associates with membrane vesicles. Mol. Biol. Cell *9*, 637–652.

Nelsen, E.M. (1975). Regulation of tubulin during ciliary regeneration of nongrowing *Tetrahymena*. Exp. Cell Res. *94*, 152–158.

Nonaka, S., Tanaka, Y., Okada, Y., Takeda, S., Harada, A., Kanai, Y., Kido, M., and Hirokawa, N. (1998). Randomization of left-right asymmetry due to loss of nodal cilia generating leftward flow of extraembryonic fluid in mice lacking KIF3B motor protein. Cell *95*, 829–837.

Orias, E., and Bruns, P.J. (1976). Induction and isolation of mutants in *Tetrahymena*. In: Methods in Cell Biology, ed. D.M. Prescott, New York: Academic Press, 247–282.

Orias, E., and Rasmussen, L. (1976). Dual capacity for nutrient uptake in *Tetrahymena*. IV. Growth without food vacuoles. Exp. Cell Res. *102*, 127–137.

Orozco, J.T., Wedaman, K.P., Signor, D., Brown, H., Rose, L., and Scholey, J.M. (1999). Movement of motor and cargo along cilia. Nature *398*, 674.

Pazour, G.J., Wilkerson, C.G., and Witman, G.B. (1998). A dynein light chain is essential for the retrograde particle movement of intraflagellar transport (IFT). J. Cell Biol. *141*, 979–992.

Piperno, G., and Mead, K. (1997). Transport of a novel complex in the cytoplasmic matrix of *Chlamydomonas* flagella. Proc. Natl. Acad. Sci. USA *94*, 4457–4462.

Piperno, G., Mead, K., and Henderson, S. (1996). Inner dynein arms but not outer dynein arms require the activity of kinesin homologue protein KHP1(FLA10) to reach the distal part of flagella in *Chlamydomonas*. J. Cell Biol. *133*, 371–379.

Piperno, G., Siuda, E., Henderson, S., Segil, M., Vaananen, H., and Sassaroli, M. (1998). Distinct mutants of retrograde intraflagellar transport (IFT) share similar morphological and molecular defects. J. Cell Biol. *143*, 1591–601.

Porter, M.E., Bower, R., Knott, J.A., Byrd, P., and Dentler, W. (1999). Cytoplasmic dynein heavy chain 1b is required for flagellar assembly in *Chlamydomonas*. Mol. Biol. Cell *10*, 693–712.

Rogers, S.L., Tint, I.S., Fanapour, P.C., and Gelfand, V.I. (1997). Regulated bidirectional motility of melanophore pigment granules along microtubules in vitro. Proc. Natl. Acad. Sci. USA *94*, 3720–3725.

Rosenbaum, J.L., and Child, F.M. (1967). Flagellar regeneration in protozoan flagellates. J. Cell Biol. *34*, 345–364.

Rosenbaum, J.L., Cole, D.G., and Diener, D.R. (1999). Intraflagellar transport: the eyes have it. J. Cell Biol. *144*, 385–388.

Sanford, J.C., DeVit, M.J., Russell, J.A., Smith, F.D., Harpending, P.R., Roy, M.K., and Johnston, S.A. (1991). An improved, helium-driven biolistic device. Technique 3, 3–16.

Signor, D., Wedaman, K.P., Rose, L.S., and Scholey, J.M. (1999). Two heteromeric kinesin complexes in chemosensory neurons and sensory cilia of *Caenorhabditis elegans*. Mol. Biol. Cell *10*, 345–360.

Stargell, L.A., Bowen, J., Dadd, C.A., Dedon, P.C., Davis, M., Cook, R.G., Allis, C.D., and Gorovsky, M.A. (1993). Temporal and spatial association of histone H2A variant hv1 with transcriptionally competent chromatin during nuclear development in *Tetrahymena thermophila*. Genes & Dev. *7*, 2641–2651.

Stephens, R.E. (1997). Synthesis and turnover of embryonic sea urchin ciliary proteins during selective inhibition of tubulin synthesis and assembly. Mol. Biol. Cell *8*, 2187–2198.

Sutoh, K. (1993). A transformation vector for *Dictyostelium discoideum* with a new selectable marker bsr. Plasmid *30,* 150–154.

Takeda, S., Yonekawa, Y., Tanaka, Y., Okada, Y., Nonaka, S., and Hirokawa, N. (1999). Left-right asymmetry and kinesin superfamily protein KIF3A: new insights in determination of laterality and mesoderm induction by kif3A-/- mice analysis. J. Cell Biol. *145*, 826–835.

Vashishtha, M., Walther, Z., and Hall, J.L. (1996). The kinesin-homologous protein encoded by the *Chlamydomonas* FLA10 gene is associated with basal bodies and centrioles. J. Cell Sci. *109*, 541–549.

Walther, Z., Vashistha, M., and Hall, J.L. (1994). The *Chlamydomonas* FLA10 gene encodes a novel kinesin-homologous protein. J. Cell Biol. *126*, 175–188.

Yamazaki, H., Nakata, T., Okada, Y., and Hirokawa, N. (1995). KIF3A/B: a heterodimeric kinesin suparfamily protein that works as a microtubule plus end-directed motor for membrane organelle transport. J. Cell Biol. *130*, 1387–1399.

Yamazaki, H., Nakata, T., Okada, Y., and Hirokawa, N. (1996). Cloning and characterization of KAP3: a novel kinesin superfamily-associated protein of KIF3A/3B. Proc. Natl. Acad. Sci. USA *93,* 8443–8448.

Yang, J.T., Layman, R.A., and Goldstein, L.S.B. (1989). A three-domain structure of kinesin heavy chain revealed by DNA sequence and microtubule binding assays. Cell *56,* 879–889.

Yang, Z., and Goldstein, L.S.B. (1998). Characterization of the KIF3C neural kinesin-like motor from mouse. Mol. Biol. Cell *9,* 249–261.

Table 3.1. Strains used in this study

Strain	Micronuclear genotype	Macronuclear genotype	Macronuclear phenotype (known drug resistances, mating types)
B2086.1	WT	WT	II
CU427.3	*chx1-1/chx1-1*	WT	cy-s, VI
CU428.1	*mpr1-1/mpr1-1*	WT	mp-s, VII
B*VII	nonfunctional mic (star)	WT	VII
UG1	*kin1::neo2/kin1::neo2*	*kin1::neo2*	pm-s
UG2	*kin1::neo2/kin1::neo2*	*kin1::neo2*	pm-s
UG3	WT	WT	
UG4	WT	WT	
UG7	*kin2::bsr1/kin2::bsr1*	*kin2::bsr1*	bs-r
UG8	*kin2::bsr1/kin2::bsr1*	*kin2::bsr1*	bs-r
UG9	WT	WT	
UG10	WT	WT	
UG11	WT	*kin2::neo2*	pm-r
UG12	WT	*kin2::neo2*	pm-r
UG13	*kin1::neo2/kin1::neo2, kin2::bsr1/kin2::bsr1*	*KIN2/kin2::bsr1*	bs-r, pm-s, mp-s
UG14	*kin1::neo2/kin1::neo2, kin2::bsr1/kin2::bsr1, mpr1-1/mpr1-1*	WT	bs-s, pm-s, mp-s

Strains B2086.1, CU428.1, and CU427.3 were kindly provided by Dr. P. Bruns (Cornell University, Ithaca, NY). UG1 and UG2 strains are germline transformation derivatives which have disruption of the KIN1 gene. Please note that although all copies of KIN1 in the MAC are disrupted with the neo2 gene, these cells are sensitive to pm because of apparent silencing of neo2 gene (our unpublished observations). However, when UG1 and UG2 are crossed, their progeny cells temporarily express dominant pm resistance allowing for genetic identification of the neo2 gene. The UG3 and UG4 strains are wild-type controls derived from the same parental strains that were used to construct UG1 and UG2. UG7 and UG8 are germ line transformation derivatives, which have disruption of the KIN2 gene. UG9 and UG10 strains are wild-type controls derived from the same parental strains (heterozygous for KIN2/kin2<bsr1) that were used to construct UG7 and UG8.

Table 3.2. Analysis of Single Knockout Phenotypes.

Phenotype	Δ*KIN1*	Control	Δ*KIN2*	Control
Doubling Time 30° C (min)*	447 ± 36	362 ± 31	608 ± 144	327 ± 50
Viability 38-40° C (percent)	27 ± 8	53 ± 22	69 ± 8	94 ± 4
Swimming rate 30° C (μm/sec)	93 ± 29	139 ± 39	158 ± 38	166 ± 38
Swimming rate 38-40° C	52 ± 15	103 ± 22	119 ± 24	103 ± 22
Cilia regeneration $t_{1/2}$ 30° C (min)	86 ± 17	74 ± 22	50 ± 20	52 ± 30
Cilia regeneration $t_{1/2}$ 30° C	128 ± 23	70 ± 13	71 ± 37	60 ± 32

* Only germline knockouts were examined for doubling times. Numbers for all other phenotypes represent data from somatic and germline knockouts. All experiments were performed at least 3 times except cilia regeneration at 30° C which was performed twice. For swimming rates 150-200 individual pathlengths were measured per experiment and data for one representative experiment is shown. All values are ± standard deviation.

FIGURE LEGENDS

Figure 3.1. *KIN1* and *KIN2* are kinesin-II homologous genes in *Tetrahymena.*(A) Diagram of the alignment of predicted *KIN1* and *KIN2* encoded protein sequences. Domains are indicated as follows: stripes, motor domain; gray, coiled coil stalk; white, globular tail. Percent identity between Kin1p and Kin2p in each domain is indicated. Triangles represent positions of introns in the corresponding genomic DNA. (B) Phylogram of kinesin-II proteins. Alignments of multiple sequences were prepared using PILEUP; evolutionary distances between sequences were calculated using DISTANCES; and an evolutionary tree was made using GROWTREE of the UWGCG system (Devereux et al., 1984). (C) Sequence comparison between *KIN1* and *KIN2* and between *KIN2* and Chlamydomonas reinhardtii FLA10 (Walther et al., 1994). Dot matrix analysis was done using COMPARE and DOTPLOT programs of UWGCG. Sequence data used for comparisons are available from European Molecular Biology Laboratory, GenBank, and DNA Data Bank of Japan under accession numbers AJ244020 (*KIN1*), AJ244021 (*KIN2*), L33697 (Crfla10), D14968 (Ceosm3), AB002357 (Hskiaa0359), A57107 (Mmkif3b), C48835 (Xlklp3), AF013116 (Mmkif3c), U00996 (Spkrp95), U15974 (Dmklp68d), D12645 (Mmkif3a), and L16993 (Spkrp85). The sequence of Ttkin5 was provided by M. Bernstein (personal communication). The Cekrp85 and Cekrp95 sequences were identified by the *C. elegans* sequencing project (Signor et al., 1999).

Figure 3.2. Germ line disruption of *KIN1* and *KIN2*.(A). Genetic scheme for creation of homozygous single knockout strains. (1 and 2) During mating between two wild-type strains the targeted gene is disrupted in the MIC by biolistic transformation. The resulting progeny are heterozygous for the null allele in both the MAC and the MIC. (3) During vegetative growth heterozygous clones become homozygous for the wild-type allele in the MAC because of random segregation of alleles in the amitotic MAC (phenotypic assortment). (4 – 6) A strain heterozygous for the disrupted allele in the MIC is crossed to

a star strain lacking a functional MIC, resulting in the transfer of a haploid MIC containing only a disrupted allele of the target gene. Endoreplication produces a diploid MIC yielding knockout heterokaryon cells. (7 and 8) Conjugation of two knockout heterokaryons leads to formation of a new MAC containing only disrupted copies of the targeted gene. (B) Analysis of germ line *KIN1::neo2* transformants. Left panel, Southern blot of total genomic DNAs digested with EcoRI and BglII and probed with a radiolabeled *KIN1* fragment. Right panel, diagram of the *KIN1* locus. Lane 1, control strain DNA; lanes 2 and 3, independent germline transformants. The endogenous locus gives two fragments of 2.8 and 4 kb. A gene knockout is expected to give a single 8.2-kb fragment, and a 3' integration should give 2.8- and 8.9-kb fragments. Note that the restriction patterns of transformant DNA analyzed in lane 3 is consistent with gene replacement, whereas in the transformant DNA analyzed in lane 2 the *KIN1::neo2* fragment integrated into the 3' flanking region of *KIN1* gene. The endogenous 4.0-kb fragment is found in the original germ line transformants, indicating that these clones are heterozygous for *KIN1/kin1::neo2*.(C) Left panel, Southern blot of total genomic DNAs digested with Csp45 I and probed with a radiolabeled *KIN2* genomic fragment. Right panel, diagram of the *KIN2* locus. Lane 1, a transformant strain homozygous for *KIN2::bsr1* gene; lane 2, wild-type control. The endogenous *KIN2* gives a fragment of 3.0 kb. Disrupted *KIN2* gives a fragment of 3.7 kb. The minor upper band present in both lanes most likely represents an incompletely digested *KIN2* fragment.

Figure 3.3. Cytological analysis ofΔKIN1ΔKIN2. The phenotype was brought to expression by mating of double knockout heterokaryon strains (UG13 and UG14). Cells shown in A–H were grown in SPP medium, whereas the cell shown in I was grown in MEPP medium. Individual conjugation progeny cells were isolated and prepared for immunofluorescent confocal microscopy by staining with anti-tubulin antibodies (SG) and DAPI. (A) Dividing WT control 12 h after pair isolation. (B) WT control (84 h). (C)

ΔKIN1ΔKIN2 cell (12 h) undergoing an early stage of cell division. The oral apparatus is already duplicated. (D) ΔKIN1ΔKIN2 cell (22 h) showing cilia heterogeneous in length. (E) ΔKIN1ΔKIN2 cell (29 h) at a final stage of cytokinesis. (F) ΔKIN1ΔKIN2 cell (29 h) with unseparated daughter cells and two sets of nuclei. (G and H) ΔKIN1ΔKIN2 cells (41 and 60 h) with uniformly short cilia, multiple nuclei, and multiple cortical subcells. (I) ΔKIN1ΔKIN2 cell 15 d after isolation of pairs grown in MEPP medium. Bars, 25 mm (bar in A shows scale for A–H). OA, oral apparatus.

Figure 3.4. (A–D) Electron microscopic analysis of WT and ΔKIN1ΔKIN2 cells. (A) Longitudinal section through WT axoneme. (B) Longitudinal section through axonemal remnant of a ΔKIN1ΔKIN2 cell. (C and D) Cross-sections through WT and double knockout basal bodies, respectively. Cells were processed for thin-section electron microscopy 84 h after pair isolation. (E) Analysis of the length of ciliary axonemes in ΔKIN1ΔKIN2 and WT cells, measured on confocal sections of cells labeled for tubulin by the SG serum using the NIH Image software package. Values are mean 6 SD (n 5 110 and 120 for wild-type and DKIN1DKIN2 cells, respectively).

Figure 3.5. Quantitative analysis of cell morphology and subunit composition. ΔKIN1ΔKIN2 and WT cells were prepared by mating of appropriate parental strains and isolation of individual mating pairs into either SPP or MEPP medium. Cells prepared for immunofluorescence microscopy were scored for the number of cortical subcells (A), number of MACs (B), and number of MICs (C). Wild-type and ΔKIN1ΔKIN2 cells grown in SPP were scored 60 h after isolation of pairs. ΔKIN1ΔKIN2 cells grown in MEPP were scored 15 d after pair isolation. Histograms show percentages of cells with the indicated numbers of cortical subunits or nuclei (n = 135). (D) Compiled data from observations on living cells and parallel immunofluorescence studies. Paralysis is measured as the percentage of drops containing paralyzed cells (n = 41), and cytokinesis

failures are estimated as the percentage of cells prepared as in A–C containing multiple subunits (n = 10–135).

Figure 3.6. (A) Double knockout heterokaryon strains (UG13 and UG14) were crossed to express the ΔKIN1ΔKIN2 phenotype and rescued with gene fragments of either *KIN1*(2)or *KIN1* containing an N-terminal 5xMyc epitope tag (1). Cells were selected with mp on SPP medium, and surviving, motile clones were analyzed by Western blotting of fractions prepared from cells rescued with either construct. The blot was probed with a monoclonal anti-myc antibody. A band of appropriate size (~100 kDa) for 5xMyc-Kin1p is present only in ciliary fractions of cells transformed with epitope-tagged *KIN1*. (B and C) To verify the effectiveness of cell fractionation procedures, blots were probed with antibodies that recognize the macronuclear histone hv1 (B) or the AXO49 antibodies (C) directed against hyperglycylated tubulin isoforms, which are restricted to cilia (Bre et al., 1996).

Figure 3.7. Wild-type (A–F, M, and N) and GFP-kin1p rescued (G–L, O, and P) cells were isolated from exponentially growing cultures and processed for confocal analysis using anti-GFP antibodies and TAP952 anti-tubulin antibodies. GFP and tubulin were detected using secondary antibodies coupled to Cy3 and FITC, respectively. For individual cells corresponding images of GFP (A, C, E, G, I, K, M, and O) and tubulin (B, D, F, H, J, L, N, and P) are shown. (A and B) Negative control cell. Some background staining with GFP antibodies is present in the cell body (A). (C–F) higher magnifications of the boxes shown in panels A and B. (G and H) Nondividing cell expressing GFP-Kin1p. Note weak staining of cilia by anti-GFP antibodies. Some cilia shown in boxed areas are labeled more strongly by anti-GFP antibodies (G). These cilia are shorter and label more uniformly by the TAP952 antibodies (H). (I–L) Higher magnifications of the boxes shown in G and H. Arrowheads show shorter immature cilia,

which label uniformly with TAP952 antibodies and also show more of GFP signal. Stars indicate mature cilia in which the TAP952 labeling is restricted to ciliary tips, and there is relatively less GFP signal. (M and N) Negative control dividing cell. Two oral apparatuses are present. (O and P) Dividing cell expressing GFP-Kin1p. The oral cilia are labeled heavily by anti-GFP antibodies (O) and uniformly by TAP952 antibodies (P). Note relatively weak staining for GFP in the oral apparatus of a nondividing cell (G). Bars: A and M, 15 mm; C, 1 mm. OA, oral apparatus; LM, longitudinal microtubule bundle.

Figure 3.8. Cells expressing GFP-Kin1p were starved for 24 h, deciliated, and allowed to regenerate cilia. At various times, samples of cells were processed for immuno-fluorescence using anti-GFP antibodies plus secondary antibodies coupled to Cy3 and TAP952 anti-tubulin antibodies plus secondary antibodies coupled to FITC. Pairs of corresponding GFP (A, C, E, and G) and tubulin (B, D, F, and H) images are shown for individual cells. Bars, 15 mm.

Figure 3.9. Comparison of cleavage furrow progression in WT (A–F) and ΔKIN1ΔKIN2 (G–L) cells. Single cells were isolated and analyzed using differential interference contrast video microscopy.

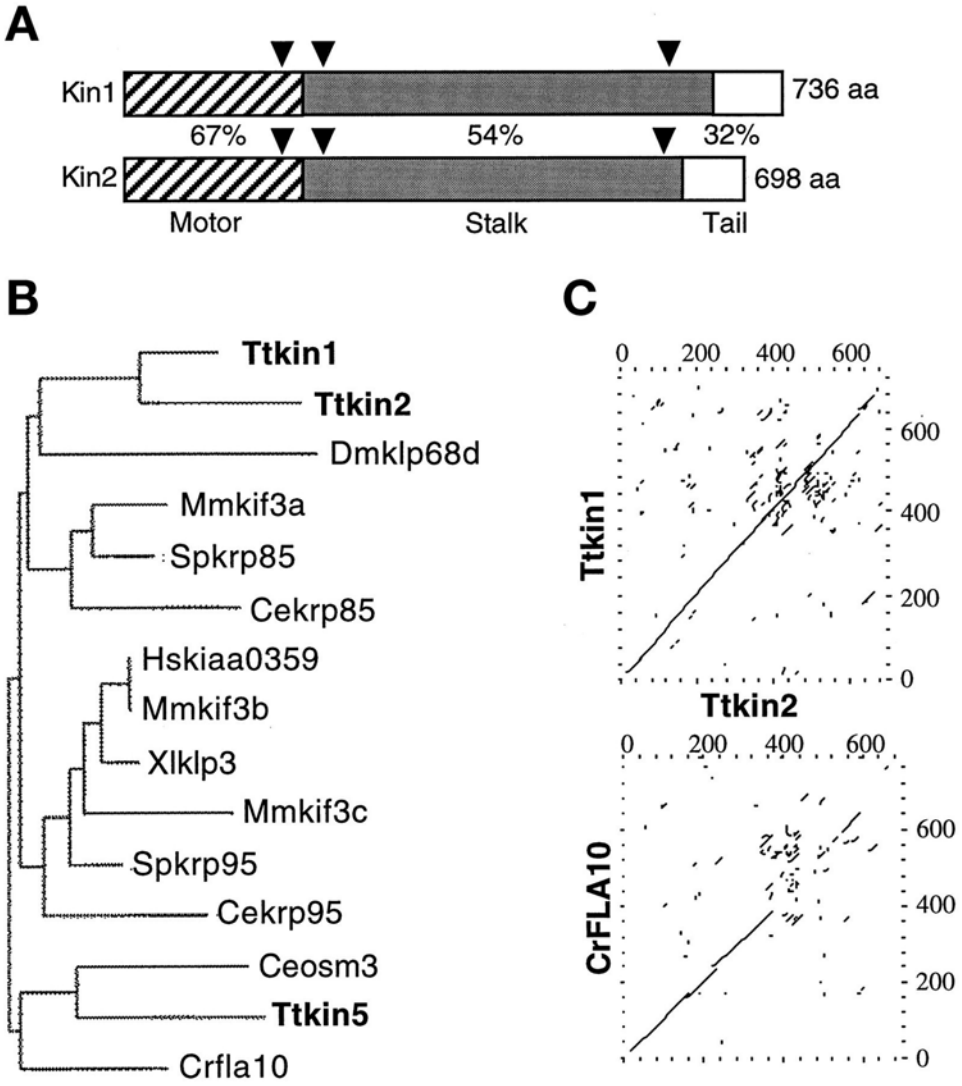
A
Kin1
736 aa
67%
54%
32%
Kin2
698 aa
Motor
Stalk
Tail
B
Ttkin1
Ttkin2
Dmklp68d
Mmkif3a
Spkrp85
Cekrp85
Hskiaa0359
Mmkif3b
Xlklp3
Mmkif3c
Spkrp95
Cekrp95
Ceosm3
Ttkin5
Crfla10
C
0
200
400
600
Ttkin1
Ttkin2
CrFLA10

Figure 3.1

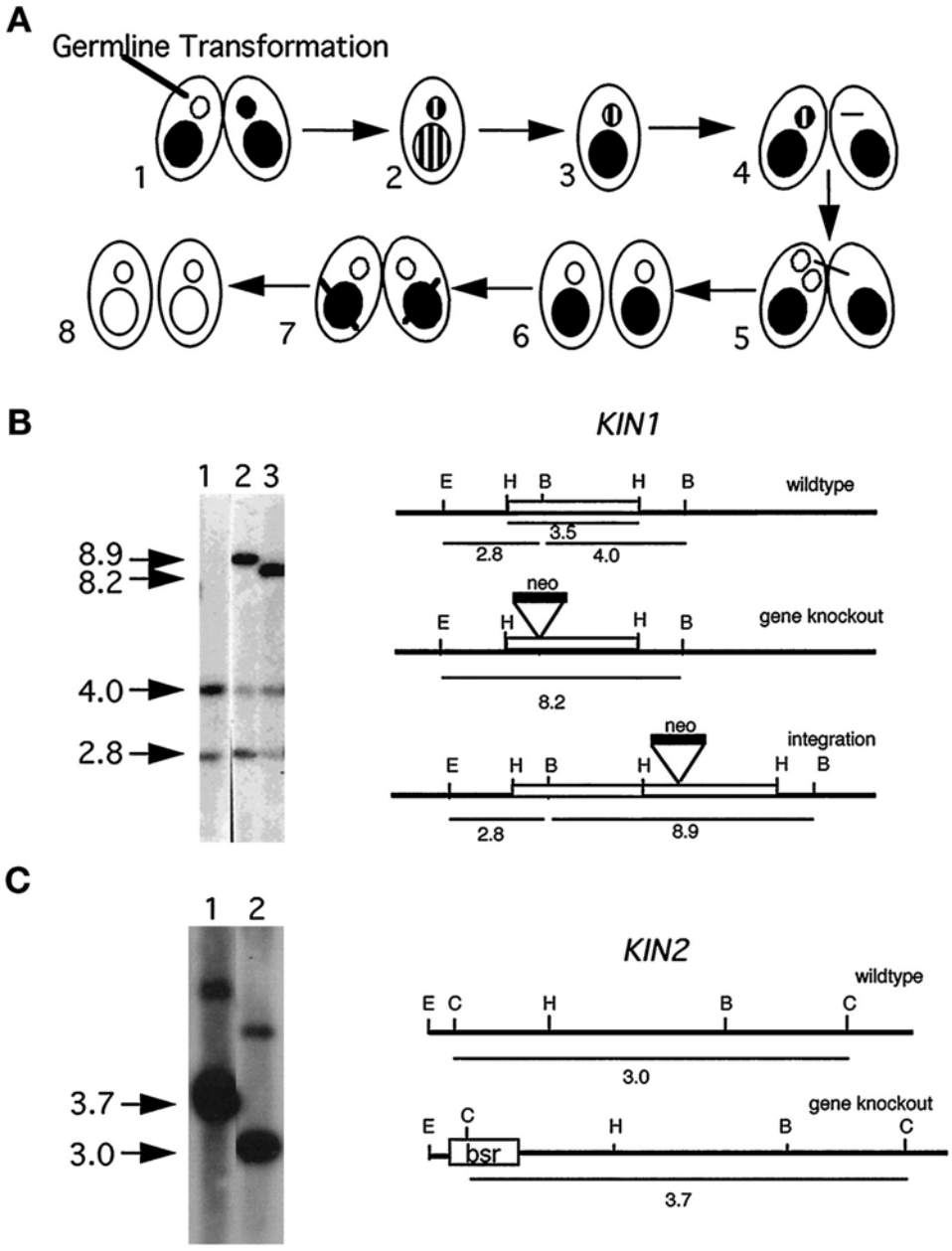
A
Germline Transformation
1
2
3
4
5
6
7
8
B
KIN1
1 2 3
8.9
8.2
4.0
2.8
E H B H B
wildtype
3.5
2.8
4.0
neo
gene knockout
8.2
integration
2.8
8.9
C
1 2
3.7
3.0
KIN2
wildtype
E C H B C
3.0
gene knockout
bsr
3.7

Figure 3.2

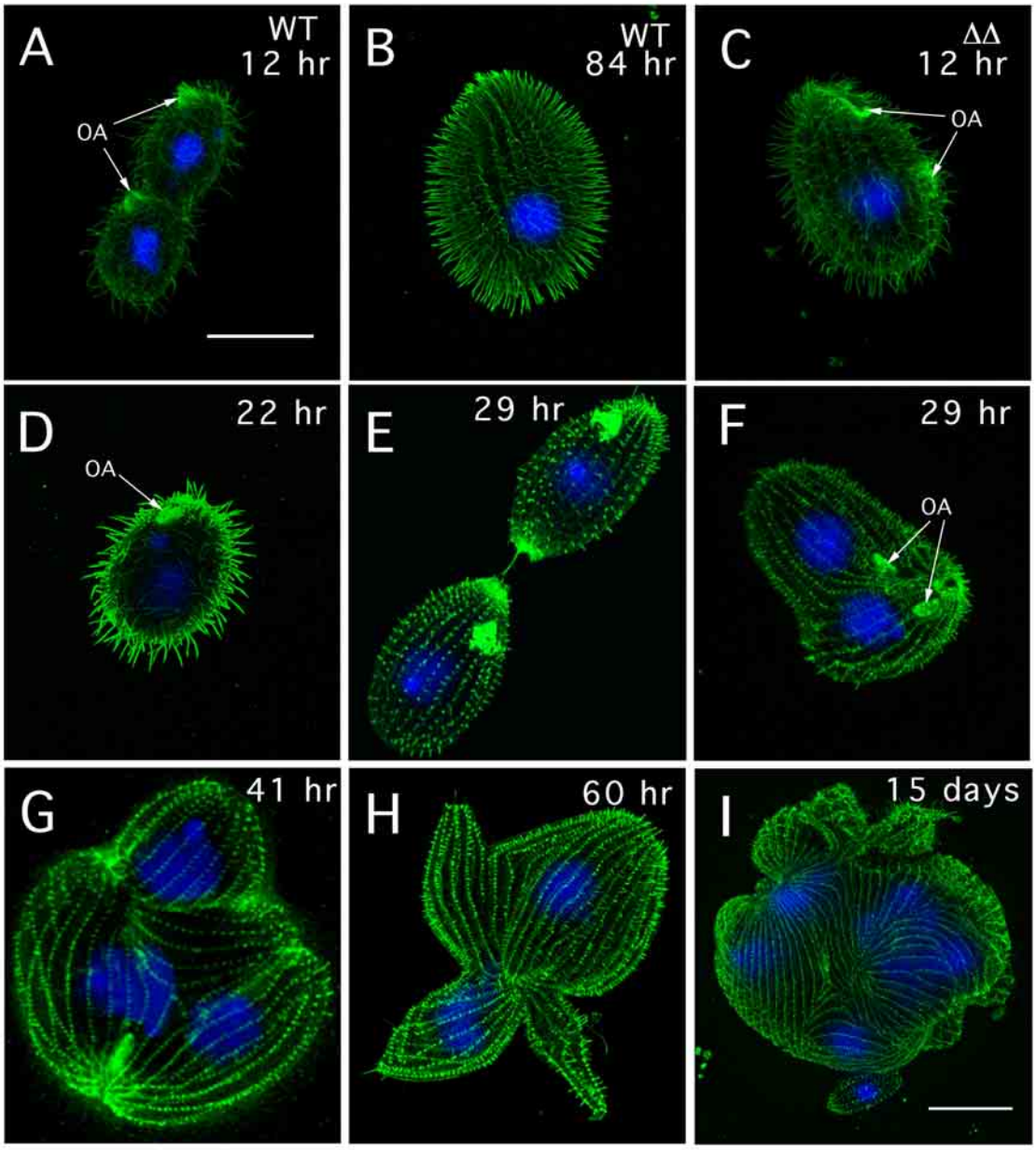
A
WT
12 hr
OA
B
WT
84 hr
C
ΔΔ
12 hr
OA
D
22 hr
OA
E
29 hr
F
29 hr
OA
G
41 hr
H
60 hr
I
15 days

Figure 3.3

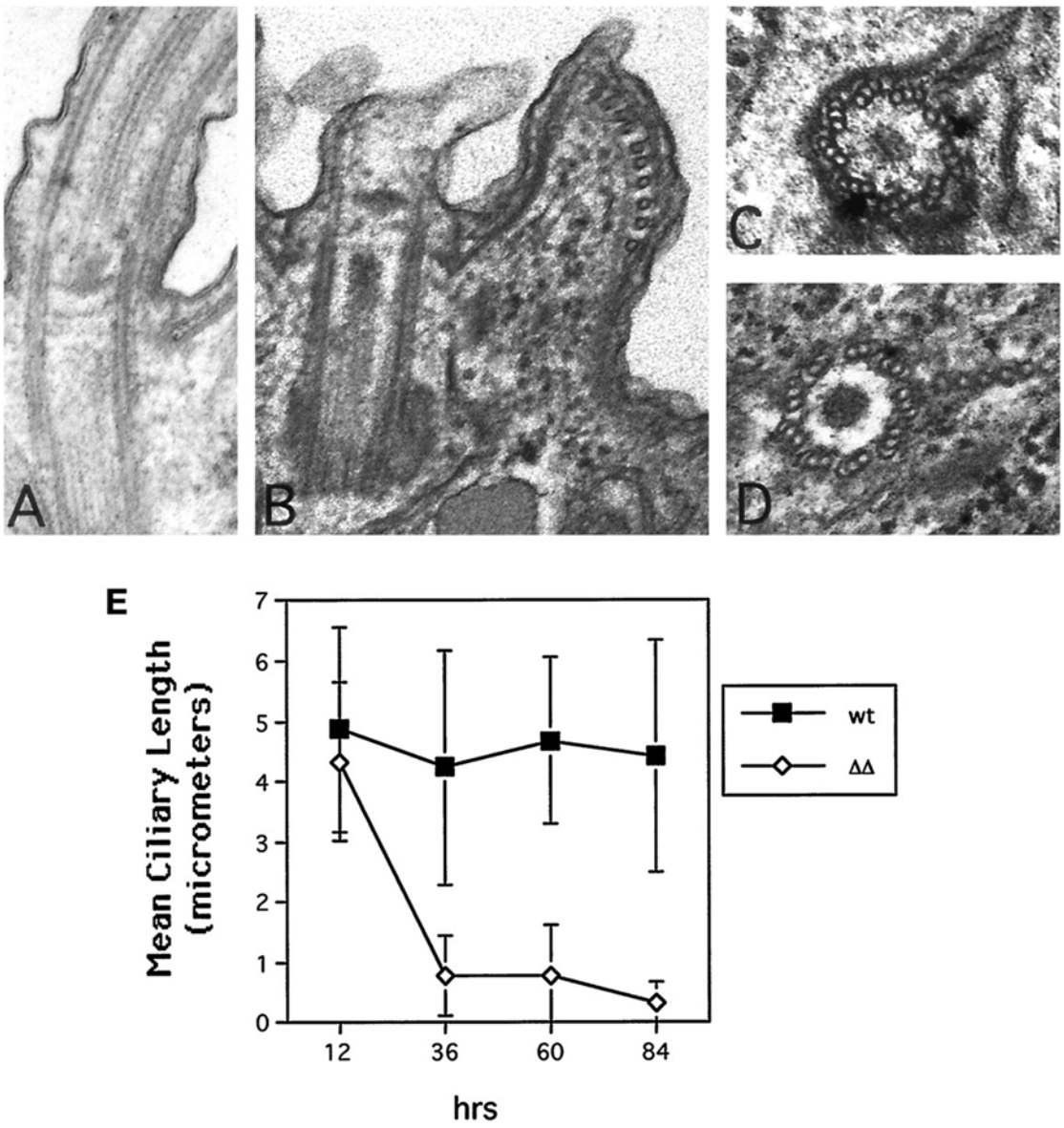
A
B
C
D
E
Mean Ciliary Length (micrometers)
0
1
2
3
4
5
6
7
12
36
60
84
hrs
wt
ΔΔ

Figure 3.4

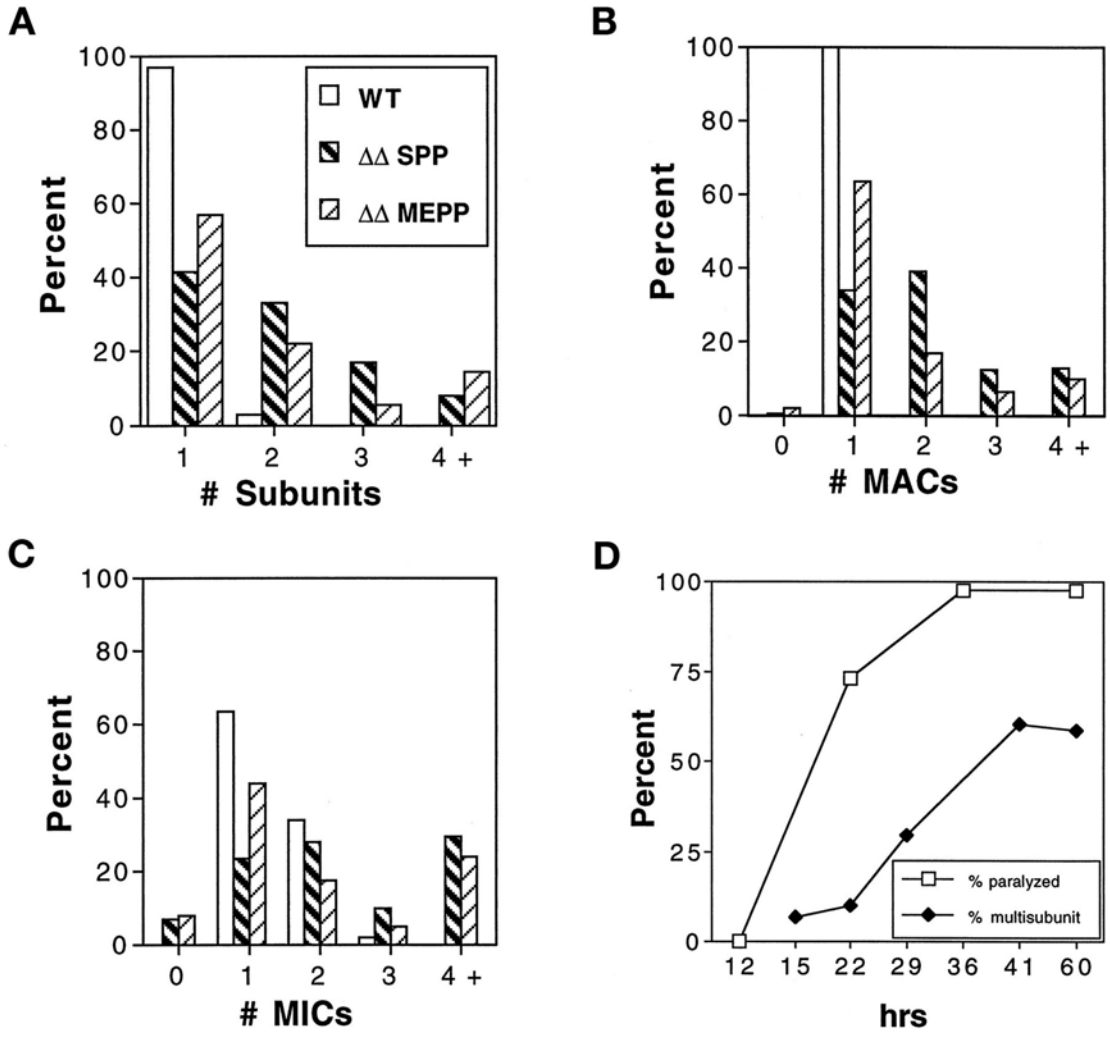
A
100
80
60
40
20
0
Percent
WT
ΔΔ SPP
ΔΔ MEPP
1
2
3
4 +
Subunits
B
100
80
60
40
20
0
Percent
0
1
2
3
4 +
MACs
C
100
80
60
40
20
0
Percent
0
1
2
3
4 +
MICs
D
100
75
50
25
0
Percent
% paralyzed
% multisubunit
12
15
22
29
36
41
60
hrs

Figure 3.5

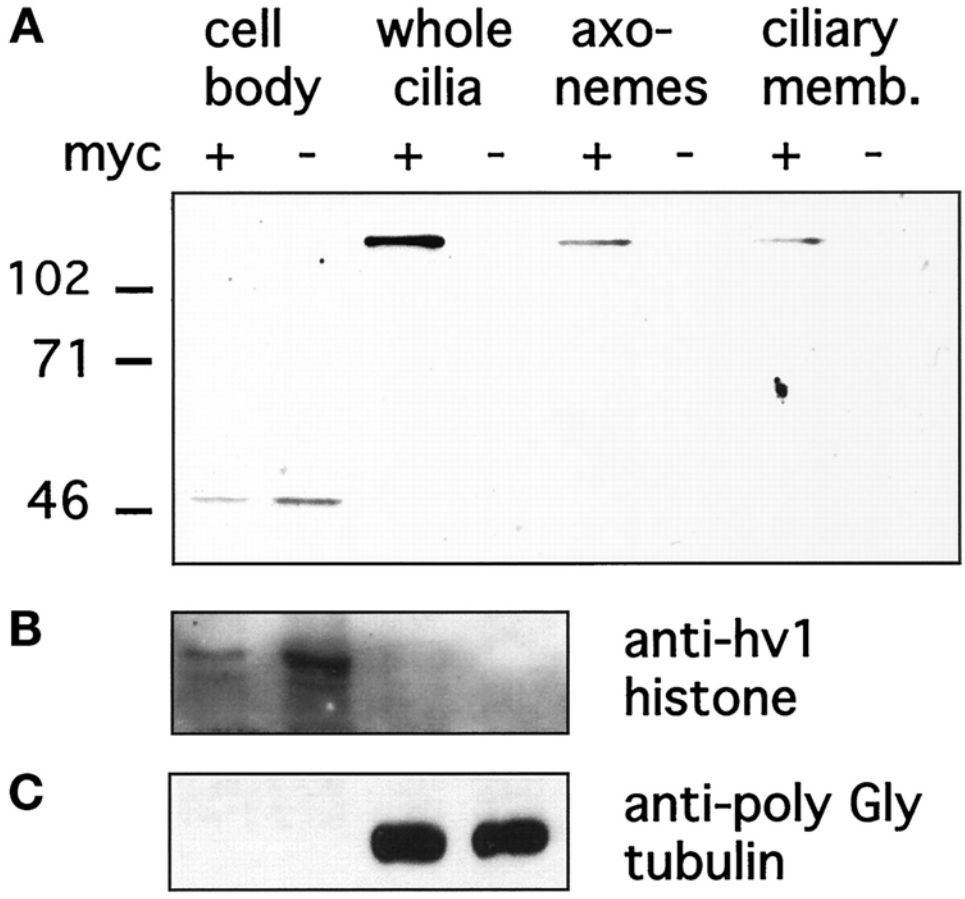
A
cell body
whole cilia
axo-nemes
ciliary memb.
myc + - + - + - + -
102
71
46
B
anti-hv1 histone
C
anti-poly Gly tubulin

Figure 3.6

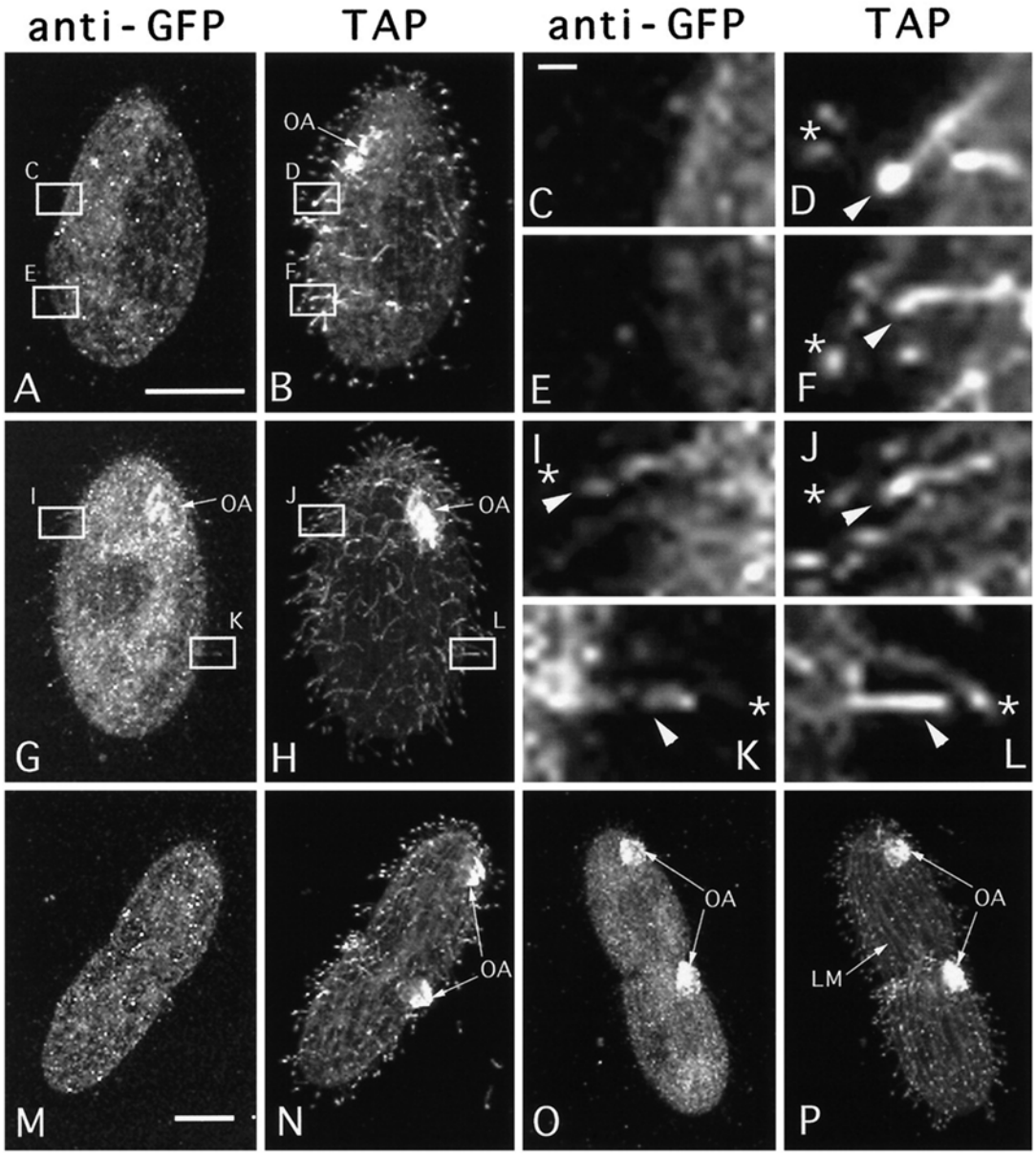
anti-GFP
TAP
anti-GFP
TAP
OA
C
D
E
F
A
B
C
D
E
F
I
J
K
L
G
H
I
J
K
L
M
N
O
P
OA
OA
OA
OA
LM

Figure 3.7

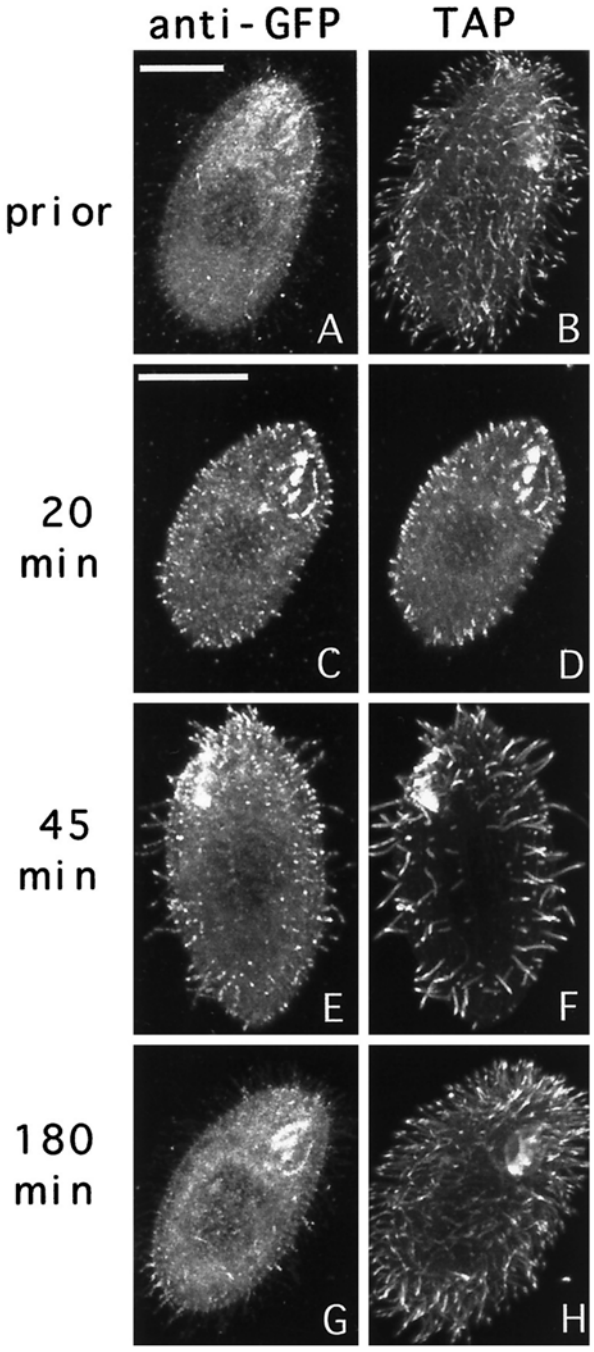

Figure 3.8

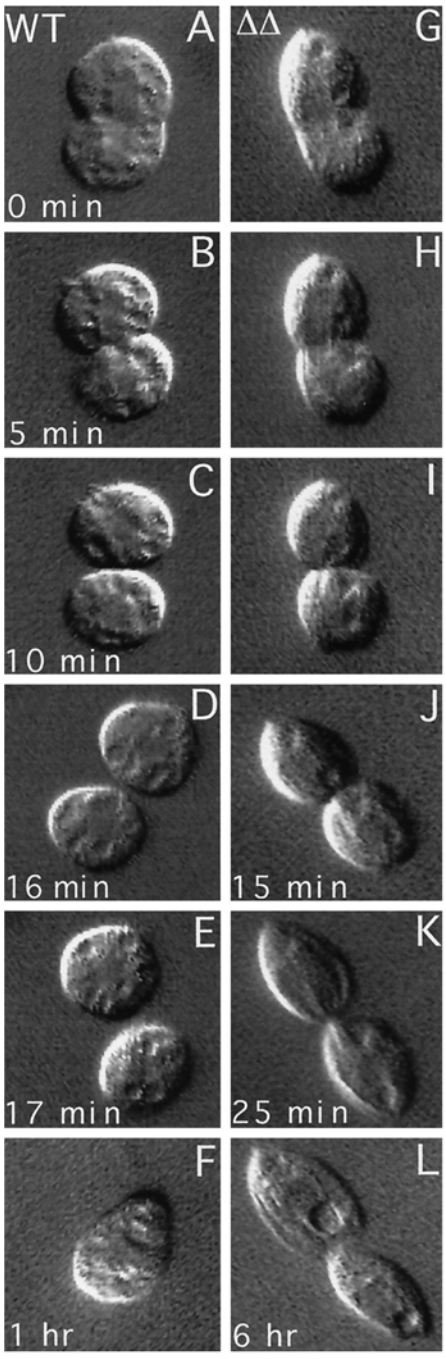
WT
A
0 min
ΔΔ
G
B
5 min
H
C
10 min
I
D
16 min
J
15 min
E
17 min
K
25 min
F
1 hr
L
6 hr

Figure 3.9

CHAPTER 4

ROTOKINESIS, A NOVEL PHENOMENON OF CELL LOCOMOTION -ASSISTED CYTOKINESIS IN THE CILIATE *TETRAHYMENA THERMOPHILA*[1]

ABSTRACT

The mechanism responsible for final cell separation at the end of cytokinesis is currently unknown. Knockout strains of the ciliate, *Tetrahymena thermophila* lacking the kinesin-II homologous molecular motors, Kin1p and Kin2p are paralyzed due to their complete loss of cilia and undergo frequent cytokinesis failures. Observations of live dividing cells revealed that cleavage furrow ingression is normal in kinesin-II double knockout cells until the final stage of cell separation (Brown, *et al*., 1999). During closer inspection of dividing cells using video DIC microscopy we found that wildtype cells undergo an extremely complex motile behavior near the end of cytokinesis. This process, which we have named rotokinesis, appears to facilitate the physical separation of daughter cells. Here we present recent work on *Tetrahymena* rotokinesis and review studies in other organisms which suggest that the use of cell locomotion in the completion of cytokinesis is a general phenomenon of motile cell types.

INTRODUCTION

During cytokinesis in animal cells and Protozoa, a cleavage furrow forms at the equator of the parental cell and begins to ingress, culminating in the complete segregation of the parental cell into two daughter cells (reviewed in Rappaport, 1996; Glotzer, 1997; Field *et al.*, 1999). Extensive molecular and structural evidence accumulated over the last several years has shown the central importance of a contractile ring of actin and myosin which forms at the leading edge of the cleavage furrow (Schroeder, 1972; De Lozanne and Spudich, 1987; Knecht and Loomis, 1987; Kitanishi-Yumura and Fukui, 1989; Sanger *et al.*, 1989; Ohba *et al.*, 1992). In the general model of contractile ring function, as myosin moves along membrane-anchored anti-parallel actin filaments, the ring contracts, pulling along the associated cell membrane and causing furrow ingression

(Rappaport, 1996, p. 180). While this model is adequate to explain the formation and ingression of the cleavage furrow, it is not sufficient to explain how cytokinesis leads to complete physical separation of the daughter cells. Since the entire machinery for cleavage furrow ingression is presumably on the cytoplasmic side of the plasma membrane, the contraction of an actin/myosin ring would be unlikely to cause the breakage of the cytoplasmic bridge connecting the daughter cells. In fact, in cleaving echinoderm eggs, the contractile ring disappears prior to the final separation of daughter cells (Schroeder, 1972). Our recent studies indicate that the mechanism of final cell separation can be surprisingly simple, based on breakage of the cytoplasmic bridge by coordinated locomotion of daughter cells. We present genetic evidence in support of this model in the ciliate *Tetrahymena thermophila* and review studies on other cell types which also implicate cell locomotion in the completion of cytokinesis.

MATERIALS AND METHODS

Cell Culture

Wildtype and kinesin-II double knockout cells were grown in SPP medium (Gorovsky, 1973) supplemented with antibiotics (SPPA) at 30℃ essentially as described (Brown *et al.*, 1999). Prior to immunofluorescence microscopy, wildtype and double knockout cells were grown in drops without shaking. Prior to video microscopy, wildtype cells were grown in 50 ml cultures with moderate shaking. For inhibition of whole cell motility, dividing cells were isolated into 9% methylcellulose in SPPA.

Microscopy

Tetrahymena cells were processed for immunofluorescence as previously described and were stained with antitubulin antibodies (SG antiserum) and DAPI (Brown *et al.*, 1999). Cells were visualized on a Zeiss Axioskop epifluorescence microscope with a Zeiss 100x Plan Neofluar (1.30 NA oil) objective lens and standard FITC and DAPI filter sets. A Zeiss MC100 spot 35 mm camera was used to capture images on Kodak T-max 400 black and white film. After processing, negatives were scanned on a Umax Powerlook 2000

scanner with Umax magicScan software v. 2.4.1 at a resolution of 1000 dpi. For video microscopy, cells were isolated into 6-10 μl of medium in a chamber created by slightly elevating a cover slip above the surface of a slide with double-sided tape. This chamber kept the drop from spreading and allowed free locomotion of swimming cells. Differential interference contrast video microscopy was performed on the Zeiss Axioskop microscope with a Zeiss 40x Plan Neofluar (0.75 NA) objective lens. Movies were collected using the DAGE-MTI (Michigan City, IN) DC330 charge-coupled device camera and were fed directly into the S-video input on a Macintosh G3/AV All-in-one computer. Movies were saved using Apple (Cupertino, CA) Video Player software. Single frames were copied into Adobe Photoshop from QuickTime movie player software. Photoshop was used to crop and resize images.

RESULTS

Rotokinesis in Tetrahymena thermophila

Our studies on the mechanism of ciliary assembly have unexpectedly led us to the discovery that cell locomotion plays an unrecognized role in cytokinesis in *Tetrahymena*. Our initial goal was to identify microtubule-dependent motors involved in the assembly of cilia in *Tetrahymena*. Mounting evidence from other organisms has implicated kinesin-II in the assembly of cilia and flagella. Kinesin-II is proposed to be an anterograde motor protein which moves ciliary subunits from the cell body to the tips of cilia during their assembly (Scholey, 1996; Rosenbaum *et al.*, 1999). We identified two *Tetrahymena* homologs of kinesin-II encoded by the *KIN1* and *KIN2* genes (Brown *et al.*, 1999). Gene knockout strains lacking either *KIN1* or *KIN2* showed only mild deficiencies in ciliary motility and cell growth. To address the possibility of overlapping or synergistic functions between *KIN1* and *KIN2*, we disrupted all copies of both genes in a single strain (Brown *et al.*, 1999). The most conspicuous phenotypic change in double knockouts was their complete loss of motility resulting from the inability to assemble and maintain cilia. Unexpectedly, about 60% of mutant cells had also failed to complete

cytokinesis, as revealed by the presence of multiple nuclei and multiple cortical subunits (Brown *et al.*, 1999, and Fig. 4.1). The phenotype of kinesin-II mutants could be explained in two ways. According to the first model, kinesin-II functions in two distinct pathways in *Tetrahymena* by transporting cargo required for both assembly of cilia and formation or ingression of the cleavage furrow. The second possibility is that the arrest in cytokinesis is induced by cell paralysis. In the second model kinesin-II plays an indirect role in cytokinesis by maintaining normal cell locomotion.

To explore these two models, we used immunofluorescence microscopy to study the intracellular localization of an epitope-tagged KIN1 protein (Kin1p). Most of Kin1p was found in cilia with only a small fraction in the cell body. In the cell body, Kin1p was detected as a diffuse signal with no association with the nuclei or the cleavage furrow in dividing cells. Moreover the cell body pool of Kin1p did not seem to undergo any rearrangements during the cell cycle (Brown *et al.*, 1999). Although the immunolocalization studies did not support a direct role for Kin1p in cytokinesis, it was still possible that either the cell body or the ciliary pool of kinesin-II plays a role in cytokinesis that does not require its close association with the cleavage furrow. For example, the motor complexes may be needed to deliver membrane vesicles to the growing cell surface during cytokinesis, but the membrane insertion sites may be localized to cilia. To test whether the absence of kinesin-II genes affects the course of cytokinesis, we analyzed live dividing cells using video microscopy (Brown *et al.*, 1999). Observation of dividing *Tetrahymena thermophila* cells is facilitated by their remarkably short generation time of about 180 minutes at 30°C. The cleavage furrow first appears only on one side of the cell at about 20 minutes before the end of cell division. We analyzed wildtype and kinesin-II-deficient, paralyzed mutants starting from the stage of unilateral furrowing. The rate of ingression of the cleavage furrow in mutant cells was nearly normal until the final segment of cytokinesis when the wildtype daughter cells split apart. At that stage daughter cells are connected only by a narrow cytoplasmic

bridge. Strikingly, many mutant cells failed to separate from each other, the cytoplasmic bridge expanded and the two daughters slowly integrated into one cell by gradual cortical integration (Brown *et al.*, 1999). Thus, kinesin-II is not required for the initiation and ingression of the cleavage furrow but it plays a role in the culmination of cytokinesis. To better understand this final stage of cytokinesis we carefully re-examined wildtype dividing cells. Unexpectedly, we discovered that dividing *Tetrahymena* cells undergo a very complex motile behavior near the end of cytokinesis (Brown *et al.*, 1999). During the final minutes before daughter cells separate, the posterior daughter cell undergoes multiple unidirectional (clockwise when viewed from posterior to anterior) rotations relative to the anterior daughter (Fig. 4.2A). The majority of the rotations occur within two minutes of final separation, with up to 46 rotations per cell. We named this phenomenon, rotokinesis. The motility associated with rotokinesis also includes periods when the posterior daughter cell appears to stop rotating and pulls briefly before continuing to rotate. In general, the completion of cytokinesis involved a pull and rotation of both daughter cells away from the equatorial plane of the dividing cell (Fig. 4.2B). It appears that *Tetrahymena* cells use this coordinated daughter cell locomotion to break the cytoplasmic bridge by force. The rotations may create a mechanical strain within the connecting bridge that can be easily severed by brief pulling (Fig. 4.2C). Due to their complete paralysis, double knockout cells were unable to undergo this motile behavior. Thus, the simplest explanation of the failure of kinesin-II deficient cells to divide is that they are unable to use mechanical force to separate at the end of cytokinesis (Brown *et al.*, 1999). To further test this model, we isolated dividing wildtype *Tetrahymena* cells into a highly viscous solution of methylcellulose. Under these conditions cells are nearly immobilized but undergo some uncoordinated movements of daughter cells. We previously found that cells isolated under similar conditions into standard medium completed cleavage furrow ingression and final separation via rotokinesis in under 20 min (Brown *et al.*, 1999). In 9% methylcellulose, division took

much longer and often involved the formation of an extremely long intercellular bridge (Fig. 4.3). Attempts to completely immobilize cells in concentrations of methylcellulose above 9% led to a halt in cytokinesis even at early stages of cleavage furrow ingression. This is consistent with earlier studies which showed that plating *Tetrahymena* cells on agar or gelatin led to cell death and abnormal cortical morphology (Hjelm, 1977).

DISCUSSION

All of the evidence supports the following simple model regarding the involvement of kinesin-II in cytokinesis in *Tetrahymena*. Kinesin-II appears to function solely in the assembly of cilia. The absence of kinesin-II leads to a failure to assemble and maintain cilia and results in cell paralysis. Lack of cell locomotion leads to arrests at cytokinesis due to the inability of mutant cells to use mechanical forces to split apart. This sequence of events is further supported by the timing of appearance of phenotypic defects. In phenotypically wildtype cells in which we induced the double knockout phenotype using the novel approach of knockout heterokaryons (Hai and Gorovsky, 1997), cells first lost cilia and became paralyzed before they underwent arrests at cytokinesis (Brown *et al.*, 1999). In fact, we have never observed a multinucleate/multisubunit kinesin-II null cell which was still motile. If our hypothesis is correct, in general, *Tetrahymena* mutants which are paralyzed due to the absence of cilia or ciliary paralysis but can still grow, should also show similar arrests at cytokinesis. Unfortunately, very few motility mutants have been isolated to date in *Tetrahymena*. A screen for temperature sensitive mutants with defects in both the regeneration of cilia after experimentally induced deciliation and in growth resulted in mutants falling within three complementation groups (Pennock *et al.*, 1988, groups 1, 3 and 5). The group 5 mutants undergo a cell cycle arrest prior to the beginning of cytokinesis (Pennock *et al.*, 1988) and therefore the phenotype of these mutants neither contradicts nor supports our hypothesis. However, the group 1 mutants arrest as doublets at a late stage of cytokinesis. These doublets had relatively few cilia which were also much shorter than

cilia of wildtype cells (Gitz *et al.*, 1993). In the original analysis of group 3 mutants, Pennock et al. found that cells ceased dividing and began to die some time between 5 and 24 hours after the shift to the restrictive temperature (Pennock *et al.*, 1988). Closer study of these mutants (renamed *oad1*) revealed that they fail to assemble cilia with a normal complement of outer dynein arms (Attwell *et al.*, 1992). Attwell et al. found that cells homozygous for the *oad1* mutation became nonmotile after 5-8 generations but grew as well as wildtype cells at the restrictive temperature (Attwell *et al.*, 1992). We reanalyzed the *oad1* mutants. After 24 hr following the shift to the restrictive temperature, *oad1* cells still retain some residual motility, although their movement was extremely slow. Thus, the *oad1* mutants are not completely paralyzed and may retain the ability to undergo motility-assisted cytokinesis. In fact, we did observe rotation of the posterior daughter cells in dividing *oad1* cells at the restrictive temperature (our unpublished observations). It will be important to isolate more mutants which lack ciliary function to see whether the close association between loss of motility and loss of normal cell division in *Tetrahymena* holds true.

Role of cell locomotion in cytokinesis in other cell types

There is substantial descriptive and in some cases experimental evidence in the literature supporting the role of cell locomotion in cytokinesis. Early observations of cell division in *Amoeba proteus* suggested that cell locomotion is used to split a parental cell into two daughters (Chalkley, 1935). Chalkley described a stage after mitotic prophase during which the dividing cell extends long pseudopodia which attach to the substrate and begin pulling on opposing sides of the mother cell. He states that, "this process continues until the increasing locomotor activity literally tears the daughter cells apart" (Chalkley, 1951). Later, Rappaport and Rappaport found that manipulations which prevented the movement of daughter cells did not prevent successful completion of division in this organism (Rappaport and Rappaport, 1986). While they found that motility was not essential, these authors confirmed that normal division generally

involves the opposing migration of daughter cells (Rappaport and Rappaport, 1986). Importantly, these researchers did not report the time required for immobilized *Amoeba* to divide and therefore it is possible that although not essential, cell motility may facilitate cell separation in *Amoeba*.

Adherent mammalian cells also appear to use motility in the completion of cell division. In an electron microscopic analysis of human sternal bone marrow cells, Mullins and Biesele distinguished two stages in the cytokinesis of metazoan cells (Mullins and Biesele, 1977). The first stage involves furrowing leading to the formation of a cytoplasmic bridge containing the midbody microtubules. The second stage involves severing of this intercellular bridge. In a process termed narrowing, localized loss of midbody microtubules was accompanied by a decrease in diameter of the corresponding region of the intercellular bridge. After the bridge narrowed to a certain threshold diameter, attachment-mediated movement of the daughter cells away from each other appeared to stretch the bridge until it was severed at its thinnest point (Mullins and Biesele, 1977). Recently, Burton and Taylor calculated the traction forces generated by dividing mammalian cells (Burton and Taylor, 1997). Swiss 3T3 fibroblasts were allowed to divide on elastic silicone sheets. By measuring the lengths of wrinkles created by cells dividing on these sheets and comparing them to wrinkles generated by externally applied forces of known strength, the forces exerted on the substrate by cells at different stages of cytokinesis could be measured. Near the completion of cytokinesis, daughter cells moved away from each other along the axis running through the cytoplasmic bridge. During this period, the force applied to the substratum increased and the silicone sheet became compressed between the daughter cells until they separated, at which point the silicone sheet recoiled, propelling the divided cells rapidly away from one another (Burton and Taylor, 1997). This study showed that motile mammalian cells can increase the force they apply to the intercellular cytoplasmic bridge specifically at the time when the bridge breaks and the daughter cells separate.

Cell locomotion appears to play a role in cytokinesis in the slime mold *Dictyostelium discoideum*. In this organism, myosin-II has been localized to the cleavage furrow (Yumura *et al.*, 1984). When myosin-II expression was prevented by disruption of the endogenous gene or by anti-sense RNA expression, cells were unable to grow in suspension culture and became multinucleate (De Lozanne and Spudich, 1987; Knecht and Loomis, 1987). Interestingly, cells lacking myosin-II were able to divide when they attached to a substrate. Huge multinucleate cells generated in suspension could divide when transferred to a solid substrate by tearing off parts of the cell in a process that is not coupled to mitosis. Since portions of the cell were able to survive if they contained a nucleus, this type of abnormal division was originally proposed to be the method of multiplication for myosin-II deficient *Dictyostelium* cultures on a substrate. (De Lozanne and Spudich, 1987). Neujahr et al. reexamined the course of division of myosin-II null cells on a solid substrate and found that mononucleated cells were able to undergo characteristic morphological changes associated with mitosis, including ingression of a cleavage furrow and ruffling at the distal edges of the cells (Neujahr *et al.*, 1997). However, constriction of the cleavage furrows in myosin null cells on a substrate was slower and less uniform than cells expressing myosin-II (Zang *et al.*, 1997). The final separation of either myosin-II null or wildtype *Dictyostelium* cells grown on a solid substrate appeared to be accomplished by migration of the daughter cells in opposite directions, to sever the narrow bridge remaining between them (Neujahr *et al.*, 1997; Neujahr *et al.*, 1997, http://www.unc.edu/depts/salmlab/bigrc.mov). This observation suggests that attachment of myosin-II deficient cells to a solid substrate may be important primarily for the final separation of daughter cells, but the results of Zang et al. do not support this conclusion. They found that myosin-II deficient cells grown in suspension, or on a hydrophobic surface to which they could not adhere, underwent relatively normal cell cycle-associated morphological changes prior to the time when wildtype cells elongate and form a cleavage furrow. At this stage, myosin-II null cells never elongated

or formed a cleavage furrow (Zang *et al.*, 1997). Thus, in the absence of myosin-II expression, attachment and motility of *Dictyostelium* cells may be important both for initiation of the cleavage furrow as well as completion of cytokinesis.

While myosin-II is not required for *Dictyostelium* cytokinesis on a substrate it does make the process more efficient (Neujahr *et al.*, 1997). This observation suggests that there may be at least two mechanisms of final cell separation whose activities are coordinated during normal cytokinesis. Zang et al. named these two mechanisms cytokinesis A for the myosin-dependent process and cytokinesis B for the myosin independent and presumably traction force mediated process (Zang *et al.*, 1997). Both mechanisms may be involved in cytokinesis of cells grown on a substratum. Cytokinesis-B of *Dictyostelium* resembles rotokinesis of *Tetrahymena* in some respects. Both cytokinesis-B and *Tetrahymena* rotokinesis may facilitate cell separation by increasing the force applied to the cytoplasmic bridge remaining after furrowing is complete. In addition, neither process is absolutely required for cell division. Cytokinesis-B is not required since wildtype *Dictyostelium* cells can divide in the absence of attachment which prevents traction forces **(**Neujahr *et al.*, 1997). Similarly, 40% of immotile kinesin-II null *Tetrahymena* cells displayed no evidence of cytokinesis failure (Brown *et al.*, 1999).

Unique features of Tetrahymena rotokinesis

Unlike the force generating events in amoeboid and mammalian cells, the motility associated with final daughter cell separation in *Tetrahymena* includes periods when the two presumptive daughter cells undergo movements that are unique to each daughter. As mentioned earlier, the posterior daughter rotates multiple times immediately prior to cell separation. During these rotations the anterior daughter does not rotate (Fig. 4.2). The independent movements of *Tetrahymena* daughter cells suggest that there must be a mechanism by which the two daughter cells independently regulate their movements. This unknown mechanism may trigger differential patterns of ciliary beating in both presumptive daughter cells. Interestingly, expression of calmodulin antisense RNA in

Dictyostelium led to cells that could form a cleavage furrow which ingressed to a thin intercellular bridge but was not able to complete division (Liu *et al.*, 1992). Calmodulin has been found associated with ciliary axonemes of ciliates (Satir and Barkalow, 1996) and is essential for the process of ciliary reversal in *Paramecium* (Naitoh and Kaneko, 1972). This raises the possibility that *Tetrahymena* locomotion-assisted cytokinesis is regulated by changes in cytosolic calcium. It is tempting to speculate that dividing *Tetrahymena* generate differences in the levels of free calcium between the daughter cells which enable rotations only in the posterior daughter.

ACKNOWLEDGEMENTS

This work was supported by the Public Health Service Grant GM-54017 from the National Institutes of Health to JG.

REFERENCES

Attwell GJ, Bricker CS, Schwandt A, Gorovsky MA, Pennock DG, 1992. A temperature-sensitive mutation affecting synthesis of outer arm dyneins in *Tetrahymena thermophila*. *J.Protozool.* **39**: 261-266.

Brown JM, Marsala C, Kosoy R, Gaertig J, 1999. Kinesin-II is preferentially targeted to assembling cilia and is required for ciliogenesis and normal cytokinesis in *Tetrahymena*. *In press*

Burton K, Taylor L, 1997. Traction forces of cytokinesis measured with optically modified substrata. *Nature* **385**: 450-454.

Chalkley HW, 1935. The mechanism of cytoplasmic fission in *Amoeba proteus*. *Protoplasma* **24**: 607-621.

Chalkley HW, 1951. Control of fission in *Amoeba proteus* as related to the mechanism of cell division. *Ann. N.Y. Acad. Sci.* **51**: 1303-1310.

De Lozanne A, Spudich JA, 1987. Disruption of the *Dictyostelium* myosin heavy chain gene by homologous recombination. *Science* **236**: 1086-1091.

Field C, Li R, Oegema K, 1999. Cytokinesis in eukaryotes: a mechanistic comparison. *Curr. Opin. Cell Biol.* **11**: 68-80.

Gitz DL, Eells JB, Pennock DG, 1993. The *dcc* mutation affects ciliary length in *Tetrahymena thermophila*. *J.Euk.Microbiol.* **40**: 668-676.

Glotzer M, 1997. The mechanism and control of cytokinesis. *Curr. Opin. Cell Biol.* **9**: 815-823.

Gorovsky MA, 1973. Macro- and micronuclei of *Tetrahymena pyriformis*: a model system for studying the structure and function of eukaryotic nuclei. *J.Protozool.* **20**: 19-25.

Hai B, Gorovsky MA, 1997. Germ-line knockout heterokaryons of an essential alpha-tubulin gene enable high-frequency gene replacement and a test of gene transfer from somatic to germ-line nuclei in *Tetrahymena thermophila*. *Proc. Natl. Acad. Sci. U.S.A.* **94**: 1310-1315.

Hjelm KK, 1977. Monstrous *Tetrahymena* with intraclonal variation in structure produced by hereditary modification of normal cells. *J. Protozool.* **24**: 420-425.

Kitanishi-Yumura T, Fukui Y, 1989. Actomyosin organization during cytokinesis: reversible translocation and differential redistribution in *Dictyostelium*. *Cell Motil. Cytoskeleton* **12**: 78-89.

Knecht DA, Loomis WF, 1987. Antisense RNA inactivation of myosin heavy chain gene expression in *Dictyostelium discoideum*. *Science* **236**: 1081-1086.

Liu T, Williams JG, Clarke M, 1992. Inducible expression of calmodulin antisense RNA in *Dictyostelium* cells inhibits the completion of cytokinesis. *Mol.Biol.Cell* **3**: 1403-1413.

Mullins JM, Biesele JJ, 1977. Terminal phase of cytokinesis in D-98S cells. *J. Cell Biol.* **73**: 672-684.

Naitoh Y, Kaneko H, 1972. Reactivated triton-extracted models of Paramecium: modification of ciliary movement by calcium ions. *Science* **176**: 523-524.

Neujahr R, Heizer C, Albrecht R, Ecke M, Schwartz J-M, Weber I, Gerisch G, 1997. Three-dimensional patterns and redistribution of myosin-II and actin in mitotic *Dictyostelium* cells. *J. Cell Biol.* **139**: 1793-1804.

Neujahr R, Heizer C, Gerisch G, 1997. Myosin II-independent processes in mitotic cells of Dictyostelium discoideum: redistribution of the nuclei, re-arrangement of the actin system and formation of the cleavage furrow. *J. Cell Sci.* **110**: 123-137.

Ohba H, Hirono M, Edamatsu M, Watanabe Y, 1992. Timing of formation of *Tetrahymena* contractile ring microfilaments investigated by inhibition with skeletal muscle actin. *Dev. Genet.* **13**: 210-215.

Pennock DG, Thatcher TH, Bowen J, Bruns PJ, Gorovsky MA, 1988. A conditional mutant having paralyzed cilia and a block in cytokinesis is rescued by cytoplasmic exchange in *Tetrahymena thermophila*. *Genetics* **120**: 697-705.

Pennock DG, Thatcher TH, Gorovsky MA, 1988. A temperature-sensitive mutation affecting cilia regeneration, nuclear development, and the cell cycle of *Tetrahymena thermophila* is rescued by cytoplasmic exchange. *Mol.Cell.Biol.* **8**: 2681-2689.

Rappaport. 1996. *Cytokinesis in animal cells*. 1 ed. Developmental and Cell Biology Series, eds. P. W. Barlow, J. B. L. Bard, P. B. Green, D. L. Kirk. Cambridge: Cambridge University Press

Rappaport R, Rappaport BN, 1986. Experimental analysis of cytokinesis in *Amoeba proteus*. *J. Exp. Zool.* **240**: 55-63.

Rosenbaum JL, Cole DG, Diener DR, 1999. Intraflagellar transport: the eyes have it. *J. Cell Biol.* **144**: 385-388.

Sanger J, Mittal B, Dome JS, Sanger JW, 1989. Analysis of cell division using fluorescently labeled actin and myosin in living ptk2 cells. *Cell Motil. Cytoskeleton* **14**: 201-219.

Satir P, Barkalow KL, 1996. Cilia: structure and molecular biology. In: K. Hausmann, P. C. Bradbury, ed. *Ciliates: cells as organism*. Gustav Fischer, Stuttgart. , 355-377.

Scholey JM, 1996. Kinesin-II, a membrane traffic motor in axons, axonemes, and spindles. *J.Cell Biol.* **133**: 1-4.

Schroeder TE, 1972. The contractile ring II. Determining its brief existence, volumetric changes, and vital role in cleaving *Arbacia* eggs. *J. Cell Biol.* **53**: 419-434.

Yumura S, Mori H, Fukui Y, 1984. Localization of actin and myosin for the study of ameboid movement in *Dictyostelium* using improved immunofluorescence. *J. Cell Biol.* **99**: 894-899.

Zang J-H, Cavet G, Sabry JH, Wagner P, Moores SL, Spudich JA, 1997. On the role of myosin-II in cytokinesis: division of *Dictyostelium* cells under adhesive and nonadhesive conditions. *Mol. Biol. Cell* **8**: 2617-2629.

FIGURE LEGENDS

Figure 4.1. Loss of cilia and arrests in cytokinesis in kinesin-II knockout cells. Cells were stained with the SG antiserum against total gel purified *Tetrahymena* ciliary tubulin and FITC conjugated goat anti-rabbit secondary antibodies (A, C, and E). Nuclei were visualized by staining with 4',6-diamidino-2-phenylindole (B, D, and F). A-B, A control cell. C-F, kinesin-II double knockout cells with multiple micro and macronuclei.

Figure 4.2. Observations of cell locomotion-assisted cytokinesis (rotokinesis) in *Tetrahymena* using video differential interference contrast (DIC) microscopy. (A) A series of time-lapse images showing a living dividing *Tetrahymena* cell a few minutes prior to final separation of daughter cells. All images shown in panel A cover a period of about 1 second of recording. Features visible on the cell surface are marked with an arrow (anterior daughter), an arrowhead and an asterisk (posterior daughter). The posterior daughter cell undergoes a rapid rotation in the direction shown by the arrow in the first panel (top, left). The structure marked with an arrowhead is invisible for two frames, but reappears on later images. The structure marked with an asterisk is lost from sight after it passes around the back side of the cell. Note the lack of rotation of the anterior daughter. (B) Five frames showing rotation away from the division plane which occurs immediately prior to the final separation. Cell surface markers are indicated by an arrowhead and an asterisk. Note rotation of markers relative to the line connecting the poles of the dividing cells. (C) Model of *Tetrahymena* locomotion-assisted cytokinesis. After ingression of the cleavage furrow to a thin intercellular bridge, rotation of the posterior daughter narrows the bridge which can then be broken at its weakest point by pulling and rotation away from the division plane.

Figure 4.3. A wildtype cell near the completion of cytokinesis was isolated into 9% methylcellulose in culture medium. Images were collected by video DIC microscopy every five minutes. (A) Dividing cell immediately after isolation from log phase culture. (B) Undivided cell twenty minutes after isolation into methylcellulose. (C) Fifty minutes after isolation, the daughter cells underwent uncoordinated movements and were connected by a very long intercellular bridge.

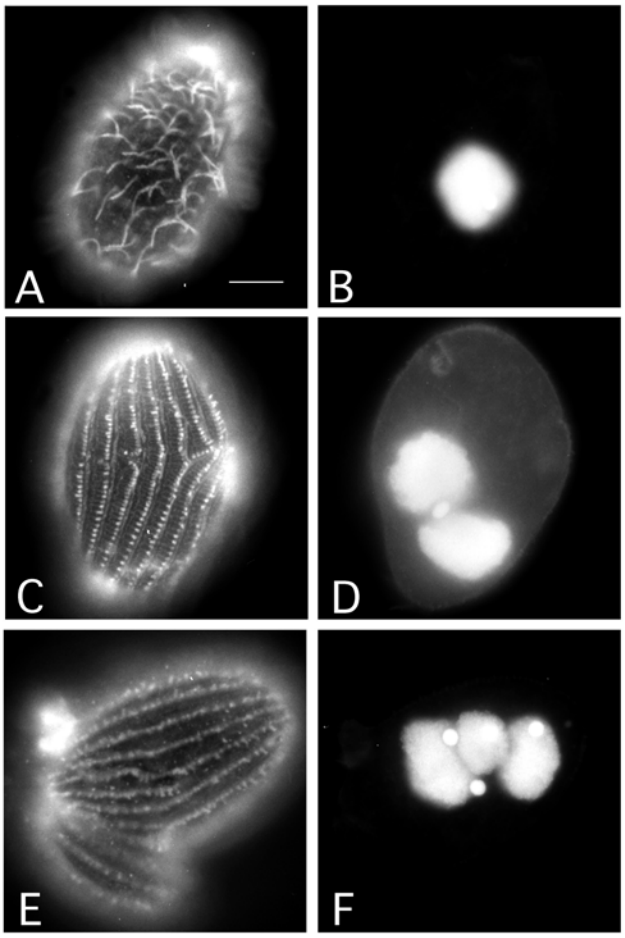

Figure 4.1

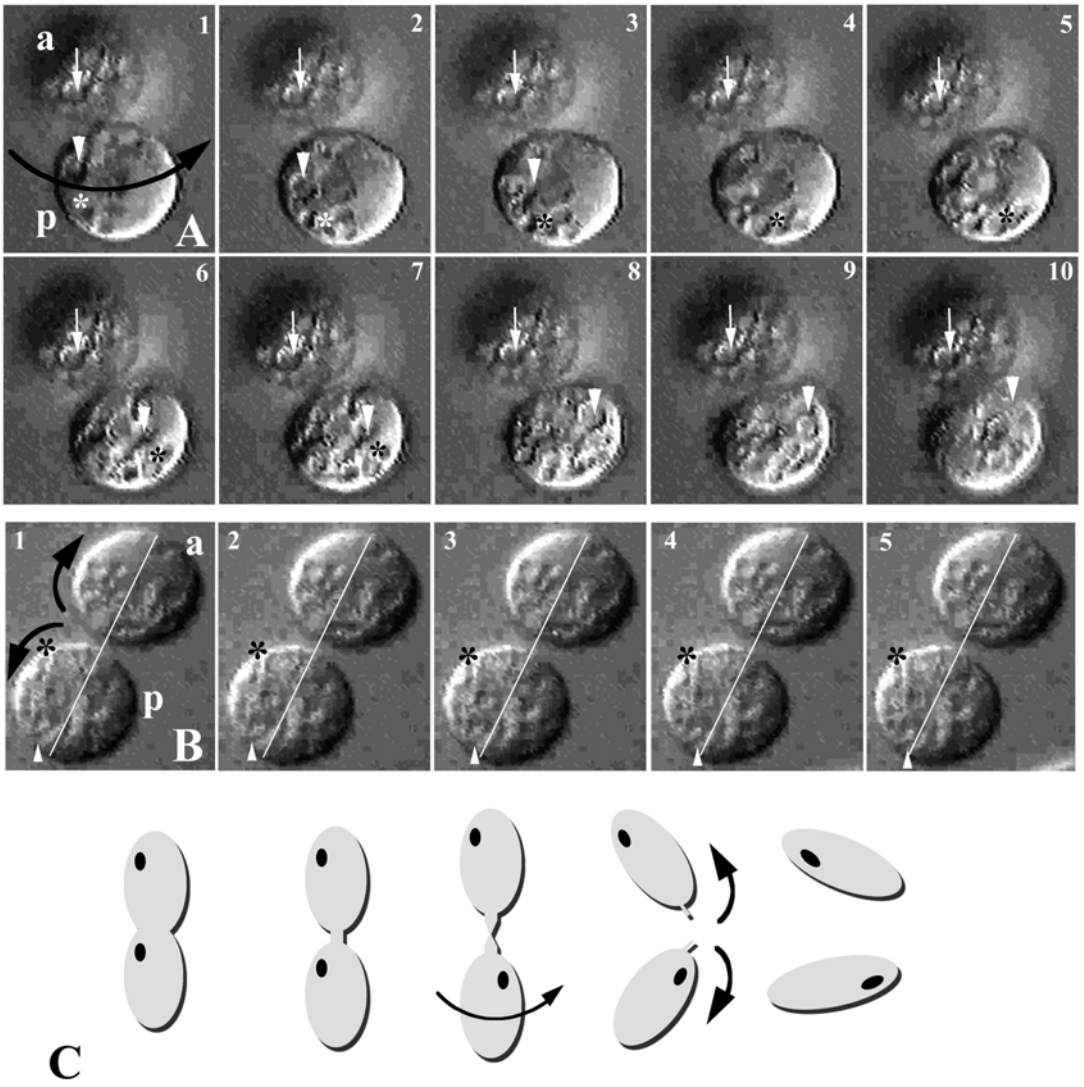

Figure 4.2

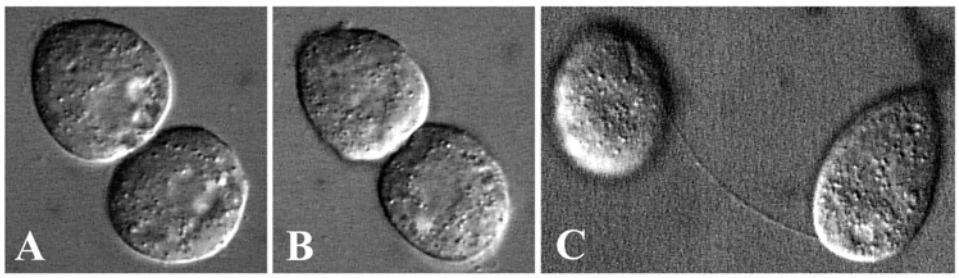

Figure 4.3

CHAPTER 5

SUPPRESSORS OF NULL MUTATIONS IN THE *TETRAHYMENA RFT1* IFT RAFT SUBUNIT GENE SUGGEST A SIGNALLING ROLE FOR RFT1 PROTEIN [1]

[1] Jason M. Brown, Yan Gao, Rupal Thazhath and Jacek Gaertig. To be submitted to The Journal of Cell Biology.

ABSTRACT

We cloned a *Tetrahymena thermophila* gene, *RFT1,* encoding a homologue of the *Chlamydomonas* intraflagellar transport (IFT) raft protein, IFT52. Disruption of *RFT1* led to a loss of cilia and cytokinesis failures, a combination of traits indistinguishable from the phenotype of mutants lacking subunits of kinesin-II, the known IFT motor protein. We provide further evidence that the cytokinesis failures in *Tetrahymena* IFT mutants result from a lack of cell movements during cytokinesis rather than from a direct involvement of IFT components in cytokinesis. Partial suppressor strains of the *RFT1* null phenotype spontaneously appearedwhich assemble short cilia. The partial suppressor cells can assemble long cilia at high cell density and resorb cilia at low cell density, suggesting that the mechanism of suppression involves signaling between cells. Co-culture experiments suggest that partial suppressor cells can respond to a signal which stimulates assembly of cilia. This signal, which may be a secreted factor, appears to be generated by nonsuppressed mutants as well as wildtype cells. Non-suppressed cells appear to be incapable of responding to the signal. A more complete suppressor subclone spontaneously appeared among the partial suppressor cells. This second suppressor had cilia with nearly normal length and structure, the maintenance of which was unaffected by cell density. High resolution 2D gel analysis of proteins revealed a single protein of about 35 kD greatly increased in the matrix/membrane fraction of cilia of suppressor cells. Although various connections have been made between IFT components and signal transduction, to our knowledge this is the first report to show that at least under certain conditions sustaining ciliary assembly and presumably IFT is dependent on signal transduction.

INTRODUCTION

Intraflagellar Transport (IFT) is a bidirectional motility that occurs within flagella as well as both motile and non-motile cilia (reviewed in Rosenbaum et al., 1999). During

IFT, large protein complexes known as rafts are transported between the cell body and the tips of axonemes (Kozminski et al., 1995). Mutants affected in either the anterograde or retrograde raft movement have been identified (Iomini et al., 2001). In the most extreme cases of IFT deficiency, flagella or cilia resorb and cannot reassemble, showing that IFT is required for both assembly and maintenance of these organelles (Kozminski et al., 1995; Pazour et al., 1999; Pazour et al., 1998; Porter et al., 1999).

Anterograde IFT is driven at least in part by kinesin-II motor proteins moving along outer doublet microtubules (Kozminski et al., 1995; Piperno et al., 1996). In *Chlamydomonas*, *Tetrahymena*, and mouse, loss-of-function mutations showed a requirement for kinesin-II in assembly of motile cilia and flagella (Brown et al., 1999b; Nonaka et al., 1998; Walther et al., 1994). Kinesin-II mutations also affected some non-motile cilia, including chemosensory neurons in of *Caenorhabditis elegans* and connecting cilia in mouse retinal rod cells (Marszalek et al., 2000; Shakir et al., 1993). In *C. elegans* a raft component, OSM-6, was shown to move in the anterograde direction at the same rate as the kinesin-II accessory subunit, KAP, supporting the hypothesis that kinesin-II transports rafts within cilia (Signor et al., 1999).

Members of the DHC1b class of dyneins are required for retrograde IFT. Dyneins are thus thought to be the motors that return rafts, kinesin-II, and perhaps other ciliary components to the cell body, where they are apparently recycled. In *Chlamydomonas*, the dynein light chain mutant, *fla14*, and the dynein heavy chain mutant, *dhc1b*, both result in extremely shortened flagella having tips filled with rafts, supporting the role of dynein in returning rafts to the cell body (Pazour et al., 1999; Pazour et al., 1998). In the *C. elegans che3* dynein mutant, IFT is specifically blocked in the ciliary portion of chemosensory neurons (Signor et al., 1999).

An elegant biochemical analysis in *Chlamydomonas* showed that raft particles are composed of complex A, containing 4 proteins, and complex B, containing 11 proteins (Cole et al., 1998). Many of the identified IFT polypeptides revealed sequence

homology with potential counterparts in other organisms, indicating strong evolutionary conservation of the IFT mechanism. For example, the complex B subunits p52, p88 and p172 of *Chlamydomonas* are homologous to the *C. elegans* proteins OSM-6, OSM-5 and OSM-1, respectively, all of which are required for normal structure and function of the nematode nonmotile chemosensory cilia (Cole et al., 1998). A mutation in the mouse homolog of *IFT88*, *Tg737*, is known to cause murine polycystic kidney disease, and the primary cilia in the kidney of *Tg737* mutant mice are shorter than in normal mice (Pazour et al., 2000).

Despite progress in the identification of the molecular players and strong evidence of their essential contribution to both IFT and the assembly state of axonemes, the specific molecular function of IFT and rafts has remained elusive. It has been hypothesized that anterograde transport carries axonemal structural components (tubulins, dyneins, radial spoke proteins, etc.) from the cell body to their sites of incorporation which are primarily at the tips of the growing axoneme (Reviewed in Marszalek and Goldstein, 2000 and Rosenbaum et al., 1999). The fundamental question is what is the ultimate critical "cargo" of IFT motors. Are rafts themselves the cargo, or do they act as platforms which carry structural components of axonemes? So far it has not been possible to make a strong direct connection between IFT rafts and axonemal components. Although FLA10 kinesin-II was shown to be required for the transport of axonemal inner dynein arms to their sites of incorporation, anterograde transport of outer dynein arms did not require FLA10. In addition, no convincing biochemical evidence has directly linked rafts and axonemal components. However, even if the primary function of IFT is to replenish structural components as they turn over in the axoneme, it is currently unclear how the transport mechanism is regulated.

In at least some organisms, a major function of IFT may be to transport proteins involved in sensory functions and signal transduction. In mouse, a retina-specific kinesin-II knockout selectively affected transport of opsin and arrestin through the

immotile cilium that connects retinal rod cell inner and outer segments, but inactivation of kinesin-II did not lead to disassembly of the connecting cilium, itself (Marszalek et al., 2000). However, in this study only one of the few kinesin-II gene products has been eliminated and our own data (see Chapter 3) show that loss of function of just one kinesin-II motor chain may not be sufficient for significant effect on assembly of cilia (Brown et al., 1999b). Prior to flagellar resorption in *Chlamydomonas fla10* mutants at the restrictive temperature, cells lose the ability to undergo fertilization, a process involving movement of signaling components from the cell body into flagella (Pan and Snell, 2000; Piperno et al., 1996). Both of these studies suggest that kinesin-II may be transporting signaling complexes to the tips of axonemes.

Tetrahymena thermophila is a genetically and biochemically tractable system with features complementary to other model organisms explored in studies on cilia and flagella. We have shown that knocking out two partly redundant *Tetrahymena* kinesin-II genes, *KIN1* and *KIN2* led to loss of existing cilia and inability to assemble new cilia. Unexpectedly, kinesin-II null cells also underwent frequent arrests in cytokinesis (Brown et al., 1999b). A number of reports have implicated other members of the kinesin superfamily in cytokinesis (Ohkura et al., 1997; Powers et al., 1998; Raich et al., 1998; Wiliams et al., 1995). Also, kinesin-II mutants gave synthetic cell cycle phenotypes with other mutations in *Chlamydomonas* (Lux and Dutcher, 1991). However, localization studies and observations of living cells lead us to propose that kinesin-II is not directly involved in cleavage furrow constriction in *Tetrahymena* (Brown et al., 1999b). Instead, we suggested that loss of motility in kinesin-II null mutants blocks the final separation of daughter cells, which as we found later, involves a series of rotational and pulling movements which facilitate cell fission (rotokinesis) (Brown et al., 1999a).

In the present study, we have cloned a *Tetrahymena* homologue of the raft protein genes *IFT52* /*OSM-6*. We describe the disruption of this gene, *RFT1*. Loss of *RFT1* led to a phenotype identical to the kinesin-II null phenotype, including disassembly of cilia

and cytokinesis defects. We show that the RFT1 protein is not localized to the cleavage furrow, consistent with an indirect role in cytokinesis. Surprisingly, we isolated a spontaneous suppressor of *RFT1* with very short cilia, which grow longer at higher cell densities. We suggest that this phenotype may be mediated by a factor secreted by cells to the medium, possibly acting in an autocrine manner. To our knowledge, this is the first report to suggest that an extracellular factor influences ciliary assembly in a way that involves a known IFT component. We propose that maintaining IFT is dependent on receiving extracellular signals and hypothesize that this property may be involved in regulation of size of cilia and flagella

MATERIALS AND METHODS

Culture Growth and Conjugation

Cells were grown in either SPP (1% proteose peptone, 0.2% glucose, 0.1% yeast extract, 0.003% EDTA·ferric sodium salt)(Gorovsky, 1973) or MEPP (2% proteose peptone, 2mM Na_3citrate·$2H_2O$, 1 mM ferric chloride, 12.5 μM cupric sulfate, 1.7 μm folinic acid, Ca salt) (Orias and Rasmussen, 1976) supplemented with 100 U/ml pennicilin, 100 μg/ml streptomycin, and 0.25 μg/ml amphotericin B. Culture growth and conjugation were done as described (Brown et al., 1999b).

Cloning and Sequence Analysis of RFT1

PCR was used to amplify a homolog of IFT52 from total *Tetrahymena* DNA. Degenerate primers were designed from published peptide sequence alignments (Cole et al., 1998). Primer OSM6AS, 5'-AA(T/C) AA(G/C/T) GA(T/C) (T/G)C(T/C) GT(T/C) (A/G)T(T/C) AGA-3' is a sense strand encoding the conserved peptide sequence N(N/K)D(A/S)V(I/V)RV(I/V)R. Primer OSM6CA, 5'-TTC (A/G)TC (A/T)A(A/G) (A/G)TC (A/G)AA (A/T)A(A/G) TTC-3' is an antisense strand of the sequence encoding ELFDLDE. These primers amplified a 750 bp fragment with an ORF showing homology to IFT52 and OSM6. A 3.4 kb HindIII fragment was subsequently cloned which encompasses about 1200 bp of *RFT1* coding region along with two introns and the 3'

end of the *RFT1* gene. A cDNA fragment was located in the *Tetrahymena* EST database identical to the coding sequence of *RFT1*. A complete coding sequence of cDNA clone (213) was kindly provided by Dr. R. Pearlman (York University) and was used for further sequence analysis. Multiple sequence alignments were prepared using the PILEUP program in the University of Wisconsin GCG software (UWGCG; Madison, WI). Shading was created with Boxshade software available online at www.ch.embnet.org/software/BOX_form.html using default settings. Sequence homologies were calculated using BESTFIT (UWGCG; Madison, WI).

Germline RFT1 Knockout

Disruption of *RFT1* was accomplished essentially as described (Brown et al., 1999b). The plasmid pRFT1-1, carrying the 3.4 kb genomic fragment of *RFT1*, was digested at the unique Bsu36I site near the N-terminal end of the coding region. Blunt ends were created using T4 DNA polymerase and the *neo2* disruption cassette (Gaertig et al., 1994) was inserted creating the pRFT1-1bsuneo2 plasmid. To prepare for disruption of the *RFT1* gene in the germline micronucleus (MIC), 15 μg of pRFT1-1bsuneo2 digested with HindIII to release the disrupted *RFT1* fragment was used to coat 6 mg of 1 μm gold particles (Biorad). CU428.1 and B2086.1 cells that had been allowed to conjugate for 3-4.5 hr were bombarded with DNA coated particles using the biolistic gun (Biorad). Bombarded cells were incubated in SPPA medium at 30°C and selected with 120 μg/ml paromomycin 5.5 hr after the last shot. A single transformant heterozygous in the germline for *RFT1::neo2* was brought to homozygosity as described (Cassidy-Hanley et al., 1997). To reveal the phenotype of homozygous *RFT1* deficiency, two resulting heterokaryon strains of different mating types (strains 7G5 and 7G6) were induced to conjugate and individual mating pairs were isolated into MEPP medium for subsequent growth.

Construction of GFP-tagged RFT1 Fragment and Rescue Transformation

In an attempt to construct a cadmium inducible system for expression of *RFT1*, the RFT1 cDNA was amplified with addition of HindIII and BamHI sites to the 5' and 3' ends of the RFT1 coding region, respectively. Primers used were RFT15'HIIIPCR, 5'-GAG TGA AGC TTG ATG AGT GGA GAA TAC AGC A-3' and NewRFT13'Bam, 5'-TGG GAT CCT TAT ACA AAA TAC ATA CAT AGT-3'. The resulting fragment was used to replace the coding region in the plasmid pMTTG1 (Shang et al., 2001 and Y. Gao and J. Gaertig, personal communication) creating pMTTRFT1B2. In pMTTRFT1B2, the cadmium-inducible metallothionein promoter (Shang et al., 2001 and Y. Gao and J. Gaertig, personal communication) is connected to the *RFT1* coding region flanked by the 5' and 3' UTRs of the *Tetrahymena* BTU1 gene, allowing insertion of the fragment in the endogenous BTU1 locus by homologous recombination as described (Gaertig et al., 1999). To create a GFP-tagged *RFT1*, PCR was used to add a HindIII site to the 5' end and MluI, NcoI, and BamHI sites to the the 3' end of the RFT1 cDNA coding region. Primers were pRFT15'HIIIPCR and RFT1-3'PCR3enz, 5'-ACT ACG GAT CCT CAC CCC ATG GCA CCT ACG CGT CTG AGC TTC TTG AAA TTT A-3'. The resulting fragment was digested with HindIII and BamHI and inserted into pMTTG1 as described above to create pMTTRFT1-3enz which was subsequently digested with MluI and NcoI. A MluI-NcoI flanked GFP fragment was inserted into digested pMTTRFT1-3enz to create pMTTRFT1GFP which encodes a chimeric protein with a GFP tag at the C-terminus of the RFT1 protein (Rft1p). RFT1Δ cells growing in MEPP were biolistically bombarded in the macronucleus (MAC) with the 3.4 kb genomic RFT1 fragment released from pRFT1-1, the 5'Btu1-RFT1-3'Btu1 released from pMTTRFT1B2, or the 5'Btu1-MTT-RFT1-3'Btu1 fragment released from pMTTRFT1GFP. No drug selection was required since only transformants recovered motility and normal cytokinesis.

Immunocytochemistry and Electron Microscopy

Cells were prepared for confocal analysis essentially as described (Brown et al., 1999b). Briefly, cells were isolated into drops of 10 mM Tris pH 7.5 on poly-L-lysine coated coverslips. For staining with SG serum against total *Tetrahymena* tubulin (Guttman and Gorovsky, 1979), cells were simultaneously fixed and permeabilized and were then air dried at 30°C. For staining with anti-GFP rabbit polyclonal antibodies (Clontech, Palo Alto, CA), cells were permeabilized briefly in the presence of protease inhibitors (0.5 μg/ml leupeptin, 10 μg/ml E-64, 10 μg/ml chymostatin, 12.5 μg/ml of antipain) and 1 μM paclitaxel followed by fixation with an equal volume of 2% paraformaldehyde and air drying at 30°C. Nuclei were stained with either propidium iodide or DAPI. A Biorad MRC 600 confocal microscope was used for imaging of stained cells. Ciliary lengths were measured on individual confocal sections using Scion Image**.** For consistency of analysis, cilia were measured on the image including the widest section through the nucleus for a given Z-series. Scion Image was also used to measure the total length of the cell periphery on the section from which ciliary lengths were measured by using the freehand tool to trace the cell periphery and the Measure Accumulated Perimeter macro. The total number of measurable cilia was divided by length of cell periphery to calculate measurable cilia/μm.

For electron microscopy, cells were washed with 10 mM Tris, pH 7.5 and fixed in 4% glutaraldehyde in 10 mM Tris buffer at 4°C for 1 hr, washed 3 times with 10 mM Tris and postfixed in 4% osmium tetroxide for 1 hr at 4°C. Cells were embedded in Epon after dehydration in graded steps from 30-100% ethanol. Sections were stained with uranyl acetate and lead citrate and were visualized on a JEOL 100CXII transmission electron microscope.

Phenotypic Analysis

For dilution series experiments, RFT1Δsm1 cells actively growing in MEPP with shaking at 160 rpm at 30°C were washed and resuspended in fresh MEPP at a concentration of

$3x10^5$/ml. Serial dilutions were then prepared from this stock and cells were incubated in 10 ml on Petri plates (10 cm diameter) with or without gentle shaking (30 rpms) either at 30°C or at room temperature. Cells were scored on an inverted microscope using 10 X objective (100X total magnification) for motility and presence of the multiple subcells indicative of cytokinesis failures. Cells were scored as motile if there was clear active displacement of the cell body. To determine the effect of slower growth rate on ciliary assembly, cells were diluted in modified versions of MEPP containing between 2% and 0.1% proteose peptone. In order to account for growth of cells without successful cytokinesis, average number of subcells (cortical components of multinucleated cells) per ml was calculated. First, average number of cells per 10X field on an inverted microscope was converted to cells per ml by calibrating the microscopic counts using a Coulter Electronics (Hialeah, FL) model ZF cell counter. Average cortical subcells per cell was calculated and multiplied by average cells/ml to obtain subcells/ml. Stimulation of ciliary assembly between strains was addressed by mixing wildtype and RFT1Δsm1 cells or RFT1Δ10 or wildtype cells (OC21-12) cells in different proportions. For stimulation by mutant cells, motility was quantitated as described above. For stimulation by cells with wildtype cilia, cilia were only measured on the RFT1Δsm1 cells which were identified by the presence of multiple cortical subcells. This method allows the clear identification of RFT1Δsm1 cells. However, we are likely to underestimate the extent of stimulation of ciliary assembly in the RFT1Δsm1 cells since recovery of near wildtype motility would be expected to help prevent cytokinesis defects. Statistical significance of differences in means was assessed by performing paired one- and two-tailed t-tests using Microsoft Excel software. For shaking experiments, a 2 proportion z-test was performed to assess the significance of the observed differences.

Cell Fractionation and Two-dimensional Gel Analysis

About $3x10^8$ cells from one liter of strain RFT1Δmov1 or CU428 (a wildtype strain) were pelleted and washed with 200 ml of 10mM Tris (pH 7.5). Cilia were prepared using the

"Calcium Shock" method (Gibson and Asai, 2000). The ciliary pellet was washed once with 10 ml of HME buffer [10 mM HEPES, 2 mM $MgCl_2$, 1 mM EGTA, pH 7.5, with protease inhibitors (as described above) and 1mM DTT]. To extract membrane and soluble proteins, cilia were resuspended in 1 ml of HME buffer with 10 mM ATP, 10 mM $MgCl_2$, and 0.1% NP-40, and incubated on a rotator for 30 minutes. After centrifugation at 14000 g for 10 minutes, the supernatant (membrane/matrix) or pellet (axoneme) was applied on a Centricon YM-10 column (Millipore) and concentrated to about 3 mg/ml. For 2D analysis of proteins, the IPGphor system from Amersham Pharmacia was used for isolelectric focusing . About 25-200 μg of ciliary membrane plus matrix or axoneme proteins was loaded on a pH 4-7 or pH 3-10, 18 cm IPGphor gel strip, and focused for about 80000 Vhs. After incubationin equilibration buffer for 15 minutes, each IEF gel strip was applied to the second dimension 7.5 % SDS-PAGE. To visualize protein spots, either silver staining using "Hoefer Processor Plus" from Amersham Pharmacia or GelCode Blue staining from Pierce was used.

RESULTS

Cloning of RFT1, a Tetrahymena homologue of the IFT raft complex subunit IFT52

To identify potential IFT52 homologues in *Tetrahymena*, total genomic DNA was amplified by PCR using degenerate primers designed to recognize conserved portions of IFT52 coding regions from other organisms. A 750 bp sequence with similarity to IFT52 was amplified and used to clone a 3.4 kb genomic fragment containing a partial ORF encoding the putative gene, named *RFT1*. Soon thereafter, a complete cDNA sequence of the *RFT1* gene was identified in the *Tetrahymena* EST project performed on a full-length cDNA library constructed by the laboratory of Dr. Aaron Turkewitz (University of Chicago, IL). The *RFT1* cDNA clone was kindly provided by Dr. R. Pearlman (York University, Canada). According to the cDNA sequence, the *RFT1* coding region encodes a predicted protein, Rft1p, of 434 amino acids with calculated MW and pI of 49 kDa and

4.99, respectively. The predicted Rft1p protein sequence is 48% identical to IFT52 of *Chlamydomonas* and 35% identical to OSM-6 of *C.elegans* (Fig. 5.1A).

Cells lacking RFT1 do not assemble or maintain cilia and are unable to complete cytokinesis normally

We created knockout heterokaryon strains with disrupted copies of *RFT1* in the germline MIC and wildtype copies in the somatic MAC (Fig. 1B and C). These heterokaryons maintain a wildtype phenotype during vegetative growth, since only the genes in the MAC are expressed. When heterokaryons are crossed with each other the resulting progeny develop a new MAC from the old MIC, thus expressing the phenotype conferred by mutated micronuclear genes. Strikingly, the progeny (RFT1Δ) lost cilia with very similar temporal kinetics to the loss of cilia in our previously reported kinesin-II double knockouts. Immunofluorescence microscopy of cells revealed that most cells had completely lost cilia by 30 hrs (Fig. 5.2). As for the previously described kinesin-II mutants (Brown et al., 1999b), RFT1Δ mutants died on the standard SPP medium but could be grown in the enriched MEPP medium which bypasses the requirement for phagocytosis, which is dependent on beating of oral cilia in normal cells. In addition, many mutants had multiple sets of nuclei and consisted of multiple cortical subcells (Fig. 5.2), showing that *RFT1* knockouts undergo multiple cytokinesis failures. This phenotype is essentially identical in both the temporal progression and terminal morphology to the phenotype of cells lacking kinesin-II motor subunits that we previously described (Brown et al., 1999b). Thus, kinesin-II and Rft1p function in the same pathway in *Tetrahymena*.

GFP-tagged RFT1 localizes primarily to cilia and does not colocalize with the cleavage furrow

We prepared a chimeric *RFT1* gene encoding an Rft1p-GFP fusion protein. We placed the Rft1p-GFP coding gene under the control of the cadmium inducible MTT promoter and targeted the whole fragment into the BTU1 locus using negative paclitaxel selection as described (Shang et al., 2001). Surprisingly, RFT1Δ cells could be rescued

with the MTT-RFT1 or MTT-RFT1-GFP fragments with or without the addition of cadmium to the growth medium. Extensive washing and incubation of rescued cells in buffer or ultrapure water never resulted in a loss of motility. These data suggest that a low level of expression of Rft1p-GFP controlled by the MTT promoter occurred even in the absence of exogenous cadmium. It is likely that a very small amount of Rft1p protein is sufficient for assembly of cilia.

Staining of Rft1p-GFP expressing cells with polyclonal anti-GFP antibodies revealed a predominant localization of Rft1p-GFP to cilia (Fig. 5.3). In cells double stained with anti-centrin antibodies (which mark the basal bodies in ciliates) the most intense Rft1p-GFP labeling was immediately above the centrin (data not shown). In dividing cells there was no colocalization of Rft1p-GFP with the cleavage furrow region in either live dividing cells by GFP-autofluorescence (not shown) or in fixed-stained cells (Fig. 5.3D-O).

During the initial stages of elongation of the mitotically dividing MIC, short oral cilia or basal bodies in the posterior daughter cell were already intensely labeled, suggesting that as for kinesin-II, raft particle proteins are localized to cilia in the initial phase of assembly (Fig. 5.3 D-F). At a slightly later stage of cell division, a zone of intense ciliary labeling was present just posterior to the cleavage furrow (Fig. 5.3 G-I). Previous studies described a wave of ciliation that moves posteriorly beginning at the cleavage furrow (Frankel et al., 1981). Our results suggest that Rft1p is involved in establishing this wave.

Cytokinesis failures in RFT1 knockouts are rescued by growth in shaking cultures

The striking similarity of cytokinesis defects observed for the *RFT1* and kinesin-II knockouts suggested that either the IFT pathway is directly involved in cytokinesis, or in both cases the phenotype could be a secondary effect caused by loss of motility. In our studies on kinesin-II we described an elaborate type of whole cell motility called rotokinesis, that appears to help wildtype cells complete cytokinesis (Brown et al.,

1999a). As in kinesin-II mutants, *RFT1* knockout cells are unable to undergo rotokinesis due to cell paralysis. In order to further test the importance of whole cell motility for the completion of cytokinesis in *Tetrahymena*, we grew immotile *RFT1* knockouts with and without shaking for 48 hours. As we had observed previously, cells grown without shaking were often polynucleated indicating cytokinesis failures (Fig. 5.4C and D). On the other hand, while cells grown with shaking did not recover motility, they had dramatically fewer cytokinesis failures (Fig. 5.4A and B). This result suggests that shear forces in the shaking culture may have replaced the motility associated with rotokinesis. These results further confirm that the cytokinesis defects observed in ciliary assembly mutants are not directly related to the function of IFT proteins but are an indirect consequence of lack of rotokinesis.

Isolation of spontaneous partial suppressors of the RFT1Δ phenotype

All of the mutant strains with a knockout of *RFT1* used in this study were generated by mating two parental heterokaryons with genetically identical genomes derived by a parthenogenetic pathway known as genomic exclusion (Orias and Bruns, 1976). Thus, we expected that progeny cells from isogenic parents would show the same phenotype. To our surprise, about 3% (n=96) of the progeny from the same parental strains showed a partial suppression of the RFT1Δ phenotype. In these clones, designated as RFT1Δsm (semi-motile), the majority of cells had functional oral cilia and produced food vacuoles, had very short and scattered locomotory cilia, and some cells were capable of limited movements. To determine to what extent the suppressed cells were able to assemble cilia, we fixed and stained cells for fluorescence microscopy with anti-tubulin antibodies. The RFT1Δ10 cells only had 0.07 cilia per μm of cell periphery in confocal sections, compared with 0.28 cilia per μm in wildtype cells. In the partial suppressor strain RFTΔsm, there was a dramatic increase in the density of measurable cilia compared with the original mutant population. In the semi-motile RFT1Δsm cells there were 0.21 cilia per μm. While the measurable cilia on RFT1Δsm cells were slightly

longer (mean length 1.2 μm, p=0.000012) than RFT1Δ10 cilia (mean length 0.83 μm), these cilia were still much shorter than wildtype cilia (mean length 4.2 μm) (Fig. 5.5A-C and E).

During an extended period of growth (~130 generations) an even more complete suppression of the mutant phenotype appeared spontaneously in one of the RFT1Δsm clones (RFT1Δsm1). We established a clonal line resulting from this apparent second suppression event called RFT1Δmov1 (for moving RFT1Δ). Immunofluorescent analysis of RFT1Δmov1 revealed that these cells recovered wildtype ciliary density (0.29 per μm) and the measurable cilia were of intermediate length (2.9 μm) between wildtype and RFT1Δsm1 cells ($p=2.6x10^{-20}$, Fig. 5.5D and E). Even though the RFT1Δmov1 cells appeared among the original RFT1Δsm1 cells, reisolation produced stable clones which for many generations maintained either the RFT1Δsm or RFT1Δmov phenotype, Thus, the apparent second suppression event did not occur in all RFTΔsm1 cells.

Thin section EM revealed that most basal bodies in RFT1Δ cells completely lacked cilia (Fig. 5.6A). While some basal bodies did have associated short cilia, these cilia uniformly lacked a central pair (Fig. 5.6B and C). The semi-motile suppressor strain RFT1Δsm1 had fewer naked basal bodies, but cilia were short with most still lacking a central pair (Fig. 5.6 E and Table 5.I). Interestingly, 13% of basal bodies on RFT1Δsm1 cells had evidence of a central pair, suggesting that these cilia may be primarily responsible for the partial recovery of motility in these cells. The further suppression in RFT1Δmov1 cells is correlated not only with an increase in ciliary length, but also with a dramatic increase in the assembly of normal 9+2 axonemes (Fig 5.5D, Fig. 5.6G, and Table 5.I). Thus, it is clear that relatively frequent suppression events allow cells to assemble cilia without Rft1p protein.

Maintenance of cilia in RFT1Δsm cells is cell density- and temperature-sensitive

During sub-culturing of the RFT1Δsm1 strain, a surprising aspect of the suppressed phenotype became evident. The RFT1Δsm1 cells grow with shaking at 30°C

to a maximal cell density of about 3-5x10^5 cells per ml, which is considerably lower than WT cells. When a growing semi-motile culture is diluted more than ~10x, to below 3x10^4 cells/ml, there is a reproducible, progressive loss of motility (Fig. 5.7). This effect was especially striking 9.5 hrs after dilution in cells diluted 20-100x (1.5x10^4 – 3x10^3 cells/ml). Cultures initially diluted to 3x10^3 cells/ml completely lost motility by 9.5 hr post-dilution and remained completely immobile at 21.5 hr. As cell density increased in these diluted cultures over time, motility returned. In further support of the importance of cell motility in *Tetrahymena* cytokinesis, even after cells recovered some motility with increased cell density, dilutions that initially led to the most severe loss of motility had many more cells with evidence of cytokinesis defects (Fig. 5.7D).

Immunofluorescence analysis of RFT1Δsm1 cells 21.5 hr after dilution revealed that the loss of motility was due to a dilution-dependent shortening of cilia (Fig 5.8 and Table 5.II). Cells from a culture with an initial density of 1.5x10^5 cells/ml were covered with scattered short cilia (Fig. 5.8A). Cells diluted to between 3x10^4 and 6x10^3 cells/ml maintained many short cilia which often appeared to be concentrated near the anterior end and oral apparatus of the cell (Fig. 5.8B and C). The fact that cells at these intermediate dilutions lost some motility and had drastic cytokinesis defects suggests that these short cilia are non-functional. The complete but reversible loss of motility in cells that were diluted to 3x10^3 cells/ml and maintained at 30°C was apparently due to a drastic reduction in ciliary length (Fig. 5.8D and E). In these cells the density of measurable cilia was only 60% of the density in the culture that was 50x more concentrated. The measurable cilia were also short, their mean length being only 48% of the mean length of cilia from cells diluted to 1.5x10^5 ($p=8.5x10^{-32}$, Table 5.II).

To test the temperature effect on this process, we diluted RFT1Δsm1 cells to 3x10^3 cells/ml and grew them at 22°C. Unlike cells diluted to the same concentration and grown at 30°C, cells grown at the lower temperature maintained cilia and had an accompanying return to normal cytokinesis (Fig. 5.8F and Table 5.II). Thus maintenance

of cilia in RFT1Δsm cells is both cell density dependent and temperature sensitive. While the dilution effect is very pronounced at 30°, at 22° cilia are less dependent on cell density.

Imbalance between rapid growth rate and slow ciliary assembly does not appear to account for the cell density dependent RFT1Δsm phenotype

The increased ciliation in the RFT1Δsm cells at lower temperatures and higher cell densities raised the possibility that mutants are able to maintain longer cilia only under conditions when their growth rate is reduced. If the suppression was due to upregulation of an RFT1-like protein with less efficiency than Rft1p itself, rapid cell growth might give insufficient time between cell divisions for the suppressor protein to allow complete ciliary assembly. To address this possibility, we diluted cells to $3x10^3$/ml and grew them in several modifications of the MEPP medium containing progressively lower concentrations of proteose peptone. While reducing the proteose peptone concentration drastically slowed the growth of RFT1Δsm1 cells (Fig. 5.9A), it had no effect on the loss of motility. Cells in all media showed the same dilution-dependent loss of cilia and cytokinesis defects. In fact, at later times, the cells grown at higher concentration of peptone had more motility. This could be explained by the faster growth rate which leads to higher cell density. The simplest explanation of these data is that the stimulation of ciliation is dependent on increased cell density, suggesting that a cell-cell signaling pathway may be involved.

Wildtype and RFT1Δ cells can stimulate ciliary assembly in the RFT1Δsm1 strain

We attempted to detect the putative secreted factor in several ways. First, spent medium from RFT1Δsm1 cells grown at high density did not stimulate assembly of cilia in the cells at low cell density. Also, spent medium from wildtype and RFT1Δmov1 cells did not have an effect. In contrast, we observed that any kind of spent medium decreased motility compared to fresh medium. One possible explanation for these data is that the signal may be a secreted factor that acts locally and may be extremely unstable.

We attempted to determine whether the RFT1Δsm1 cells secreted a factor that acts highly locally in an autocrine manner. To this end we grew RFT1Δsm1 cells on a plate at low density at room temperature, either without shaking or with very gentle shaking. The purpose of gentle shaking was to introduce enough mixing of the medium so that the putative factor could be swept away from the cell, but at the same time not to help cells with completing cytokinesis, since the cell division defects are useful as a diagnosis of ciliary function. Strikingly, unshaken cells grew at higher rate and had fewer cytokinesis defects and more motility (Fig. 5.10A). A different result was obtained when the same experiment was repeated at 30°C. Here we observed that shaken cells had fewer cytokinesis defects compared to unshaken cells. However, there was still a great difference in the proportion of motile cells. More motile cells were present in the unshaken culture compared to the shaken culture (Fig. 5.10A). This result can be explained if we assume that at 30°C, increased membrane fluidity allows even gentle shaking to help cells complete cytokinesis by bypassing rotokinesis. This would explain why shaken cells showed less multinucleation. Thus, the results of shaking at 30°C are very striking. Even though the culture that was shaken grew to higher cell density, these cells did not recover robust motility, unlike cells grown at the same temperature without shaking. These results suggest that gentle shaking either equalizes a locally secreted factor or prevents direct cell-cell contacts.

To further test whether cell communication is involved in maintaining cilia in RFT1Δ cells, we performed mixing experiments to test for stimulation by other strains. When we mixed RFT1Δsm1 cells diluted to a concentration that causes resorption of cilia in controls with a high concentration of WT cells, motility was clearly stimulated in the semi-motile suppressor. However, in this experiment recovery of complete motility was difficult to quantify since cells that recover wildtype motility should be indistinguishable from wildtype. To overcome this problem, we measured cilia on fixed and stained cells. In order to be sure we were measuring cilia only on mutant cells, we chose only cells that

showed clear arrests in cytokinesis (Fig. 5.10 B-D). Clearly, this method prevents us from measuring cilia on cells that recover near wildtype assembly and motility. Even so, we found that cilia on identifiable RFT1Δsm1 cells were 39% longer when diluted and mixed with wildtype ($p= 8.69x10^{-39}$, Fig. 5.10 C and E) than when they were only diluted (Fig. 5.10 B and E). On the other hand, *RFT1* null cells were unable to respond to the assembly-promoting signal generated by wildtype cells (Fig. 5.10 D and E). This result suggests that *RFT1* null cells may be deficient in the part of the pathway involved in responding to the signal. Preliminary results also suggest that RFT1Δ10 cells are capable of stimulating RFT1Δsm1 cells (data not shown). So while *RFT1* null cells may be capable of generating the assembly-promoting signal, they are clearly unable to respond to the signal. Therefore, the mechanism of suppression in RFT1Δsm1 cells is likely due to an increased ability to respond to the signal, possibly by overproduction of a receptor or signal transduction component.

The data presented so far suggest some type of cell-cell interaction but do not distingusih between direct contact and a mechanism mediated by a secreted soluble factor. To distinguish between these two possibilities, we performed co-culture experiments in which diluted RFTΔsm1 cells were grown on filters immersed in other cells. Under these conditions, direct cell contact is prevented between strains, but soluble factors can pass freely. While these methods need further refinement to be reliable, preliminary results from these experiments suggest that diluted RFT1Δsm1 cells may recovered more motility when grown over concentrated RFTΔsm1 cells compared to growth over pure medium (data not shown). If these data prove to be reproducible, they would strongly support the hypothesis that a secreted factor is responsible for transmitting the assembly-promoting signal between cells.

A protein is reproducibly upregulated in suppressor cells

Taken together, the above results suggest that suppression of the *RFT1* null phenotype may involve a mechanism whereby some factor is produced in the suppressor

cells that is involved in signaling between cells at high cell densities and that this factor is unstable at higher temperatures. Such a mechanism would also necessitate the action of a receptor for the proposed factor. To begin the search for the proposed factor or its receptor, we performed two-dimensional gel analysis of ciliary proteins from wildtype and RFT1Δmov1 cells. We find that one protein of about 35 kD is reproducibly upregulated in the suppressor cells compared to wildtype, suggesting that this protein could be involved in the mechanism of suppression. This protein was found in the fraction of cilia containing NP-40 extractable proteins (Fig. 5.11 compare B and D with A and C, respectively). We estimate that this protein is increased at least 10-fold compared to WT cells (Fig. 5.11 A and C). In contrast, no difference was found in the proteins of the axonemal compartment (Fig. 5.11 compare E and F). These data suggest that the 35 kD protein is part of the suppression mechanism. Its presence in the NP-40 soluble fraction is consistent with its potential role as a receptor for an extracellular signal. Peptide sequencing of this protein is under way.

DISCUSSION

We show that the ciliated protozoan *Tetrahymena* has a gene, *RFT1* that is homologous to the IFT52 component of rafts, Osm-6 of *C.elegans*, and predicted proteins from *Drosophila* and mammals. We also show that knocking out the *RFT1* gene leads to loss of cilia and defects in cytokinesis. This phenotype is essentially identical to the phenotype of *Tetrahymena* cells lacking motor subunits of kinesin-II (Brown et al., 1999b). These results establish the requirement for Rft1p protein for ciliary assembly and maintenance and are fully consistent with Rft1p being a cargo of kinesin-II that is essential for ciliary assembly. We are now also more convinced that the cytokinesis defect in the *RFT1* and kinesin-II mutants is not the result of direct involvement of IFT components in cytokinesis. This is supported by the fact that Rft1p localizes exclusively to cilia and as in the case of kinesin-II does not appear in the cleavage furrow area (Brown et al., 1999b). Furthermore, the cytokinesis defects of *RFT1* mutants could be

almost completely suppressed by vigorous shaking, indicating that the cleavage furrow progresses almost to completion so that cell fission can be accomplished by a simple mechanical stress without damaging cells. In addition to a role in ciliary assembly, we previously described an indirect function for *Tetrahymena* kinesin-II in cell division. Kinesin-II mutants in this organism not only lose cilia, but also frequently fail to complete cytokinesis. Several lines of evidence suggested that the loss of a novel type of whole cell motility, called rotokinesis, was sufficient to explain the cytokinesis defects in kinesin-II mutants. Rotokinesis involves the persistent, unidirectional rotation of only the posterior daughter cell around an axis passing through the cytoplasmic bridge connecting the daughter cells. We have proposed that the torque generated by rotokinesis may help to weaken the cytoplasmic bridge between presumptive daughter cells, thereby increasing the likelihood that cytokinesis will be successful (Brown et al., 1999a). A similar mechanism appears to operate in amoeboid cell types, called cytokinesis B, in which presumptive daughter cells crawl away from the cytoplasmic bridge, using traction forces to tear the cytoplasmic bridge apart (Zang et al., 1997). Although unlikely, a possibility still exists that both kinesin-II and Rft1p are involved directly in ciliary assembly and cytokinesis, and that the involvement in cytokinesis is independent of ciliary motility and does not require accumulation of either kinesin-II or raft particles near the cleavage furrow. An ultimate test for requirement of ciliary motility in rotokinesis will be to eliminate a protein that leads to paralysis of cilia but not to their disassembly and is unrelated to the kinesin-II and IFT pathway. Experiments are underway with the PF16 homolog of *Tetrahymena* recently discovered in an EST search which is known to be required for central pair stability and flagellar motility in *Chlamydomonas* (Dutcher et al., 1984; Smith and Lefebvre, 1996).

It was more surprising that spontaneous partial suppressor cells were identified at a relatively high frequency (~3%) of pairs isolated from crosses of the *RFT1* knockout heterokaryons. The result was very surprising because both the suppressing and non-

suppressing strains were derived from crosses of the same parental strains that were produced by a technique of genomic exclusion which makes genomes of both mating parents fully homozygous and identical (Orias and Bruns, 1976). However, we should keep in mind that when a new macronucleus is produced in the progenies, the genome undergoes extensive rearrangement, which involves deleting about 10% of micronucleus-specific DNA, and chromosome fragmentation. Importantly, these genome-processing events are not always reproducible. In some cases, deletions occur at alternative sites sometimes, separated by considerable distance (Blackburn et al., 1985). It has never been reported that such alternative gene processing could affect protein-coding genes. However, our results suggest that the alternative genome processing may have contributed to the suppression in the original *RFT1Δ* strain. Alternatively, it is possible that assembling partial cilia in the absence of RFT1 is possible without a genetic change, by physiological upregulation of certain proteins, and that these events have a certain probability of occurring. Clearly, cells belonging to the same clone are not physiologically identical, the asynchronous cell cycle in clones being a prime example of such variation. Given that the partial suppression phenotype appeared with such high frequency and after only a few generations, it is unlikely that it was caused by random spontaneous mutations. The fact that cilia of the more advanced suppressor cells have a single protein in the membrane/matrix fraction that is several-fold increased in abundance compared to WT cells suggests that this putative alternative processing event could have affected the level of expression of this or perhaps additional proteins which compensated for the absence of Rft1p.

The most surprising result however, was the observation that the phenotype of intermediate suppressor cells was strongly dependent on cell density, with higher cell density stimulating assembly of longer cilia. We showed that it is unlikely that the observed effect was caused by particular growth conditions, and rather appears to be mediated by a factor in the medium, possibly acting in an autocrine manner. We found

that wildtype cells could stimulate ciliary assembly in the intermediate suppressors, but the null cells were unable to respond to this signal. Preliminary results also suggested that *RFT1* null cells may be able to generate the assebly-promoting factor. Therefore, it appears that the suppressor strains have an increased ability to respond to the signal compared to null cells. We still do not have evidence that wildtype cells use the factor to stimulate assembly of their own cilia. In fact, on the surface this concept may not even seem reasonable since wildtype cells swim rapidly and therefore would likely leave a secreted factor behind. However, our shaking experiments indicate that the factor acts rapidly and appears to be very unstable. Also, it is widely known among *Tetrahymena* researchers that most ciliary assembly occurs just prior to cell division and during this period cells are less motile and often found at the bottom of culture dishes. Thus, it is possible that ciliary assembly is under extracellular control even in wildtype cells. However, it is important to note that we are unaware of any evidence that wildtype cells grown in shaking culture have shorter cilia than the same cells grown without shaking as we would predict if the secreted factor is important for ciliary maintenance in wildtype cells. It is possible that the factor is only important for ciliary assembly in the context of the suppressor strain or that functional Rft1p makes wildtype cells so sensitive to low levels of the proposed factor that cell movement and growth in shaking cultures do not affect ciliary assembly. Which brings us back to the initial question of what function the factor could have in wildtype cells. We can propose a model for the role of Rft1p to help guide future experiments. One possibility is that when a raft complex enters the tip of the cilium, an extracellular factor may mediate modification of Rft1p, possibly via a tip-specific receptor, and only such a modified raft complex can be reused for another round of IFT. In the suppresor strain, the mechanism of suppresion could be based on overproduction of such membrane ciliary receptor so that increased activation of additional raft components could allow for increase ciliary assembly. Alternatively, the suppression may be based on overproduction of another component of raft complexes

which can be activated by the same receptor. The remaining question is why cells would evolve such a mechanism for control of assembly of cilia via a secreted factor. One possibility is that this mechanism is used not only to stimulate assembly of cilia but also to ensure equality of their length. We can hypothesize that all cilia compete for the limited quantity of this factor, and shorter cilia have some advantage in capturing the factor. This could be a simple consequence of tips of shorter cilia being closer to the cell surface, where the factor could be released.

ACKNOWLEDGMENTS

We are especially grateful to Dr. Ronald Pearlman (York University) for providing the *RFT1* cDNA (*Tetrahymena* EST project clone 213). Thanks also to Dr. Joel Rosenbaum (Yale University) and Dr. Doug Cole(University of Idaho) for helpful discussions. We also sincerely thank Dr. Mark Farmer, Dr. John Shields, and Patrick Brown (Center for Advanced Ultrastructural Research, University of Georgia) for their assistance with confocal and electron microscopy. We thank Dr. Marty Gorovsky for providing the SG antiserum and Dr. Aaron Turkewitz for the GFP construct. In addition, we are truly grateful to UGA graduate students Krzysztof Rogowski and Chengbao Liu for helpful discussion and insight. This work was supported by an American Cancer Society grant to J.G.

REFERENCES

Blackburn, E.H., P. Challoner, M. Cherry, E. Howard, T. Ryan, and E.A. Spangler. 1985. Genome rearrangements in macronuclear development of Tetrahymena. *In* UCLA Symp. Mol. Cell Biol. M. Simon and I. Herskowitz, editors. 191-203.

Brown, J.M., C. Hardin, and J. Gaertig. 1999a. Rotokinesis, a novel phenomenon of cell locomotion-assisted cytokinesis in the ciliate Tetrahymena thermophila. *Int. Cell Biol. Rep.* 23:841-848.

Brown, J.M., C. Marsala, R. Kosoy, and J. Gaertig. 1999b. Kinesin-II is preferentially targeted to assembling cilia and is required for ciliogenesis and normal cytokinesis in *Tetrahymena*. *Mol. Biol. Cell*. 10:3081-3096.

Cassidy-Hanley, D., J. Bowen, J. Lee, E.S. Cole, L.A. VerPlank, J. Gaertig, M.A. Gorovsky, and P.J. Bruns. 1997. Germline and Somatic Transformation of Mating *Tetrahymena thermophila* by Particle Bombardment. *Genetics*. 146:135-147.

Cole, D.G., D.R. Diener, A.L. Himelblau, P.L. Beech, J.C. Fuster, and J.L. Rosenbaum. 1998. *Chlamydomonas* kinesin-II-dependent intraflagellar transport (IFT): IFT particles contain proteins required for ciliary assembly in *Caenorhabditis elegans* sensory neurons. *J. Cell Biol.* 18:993-1008.

Dutcher, S.K., B. Huang, and D.J. Luck. 1984. Genetic dissection of the central pair microtubules of the flagella of *Chlamydomonas reinhardtii*. *J Cell Biol.* 98:229-36.

Frankel, J., E.M. Nelsen, and L.M. Jenkins. 1981. Development of the ciliature of *Tetrahymena thermophila*. II. Spatial subdivision prior to cytokinesis. *Dev. Biol.* 88:39-54.

Gaertig, J., Y. Gao, T. Tishgarten, T.G. Clark, and H.W. Dickerson. 1999. Surface display of a parasite antigen in the ciliate *Tetrahymena thermophila*. *Nat. Biotech.* 17:462-465.

Gaertig, J., L. Gu, B. Hai, and M.A. Gorovsky. 1994. High frequency vector-mediated transformation and gene replacement in *Tetrahymena*. *Nucleic Acids Res.* 22:5391-5398.

Gibson, T.M., and D.J. Asai. 2000. Isolation and characterization of 22S outer arm dynein from Tetrahymena cilia. *Methods Cell Biol.* 62:433-40.

Gorovsky, M.A. 1973. Macro- and micronuclei of *Tetrahymena pyriformis*: a model system for studying the structure and function of eukaryotic nuclei. *J.Protozool.* 20:19-25.

Guttman, S.D., and M.A. Gorovsky. 1979. Cilia regeneration in starved *Tetrahymena*: an inducible system for studying gene expression and organelle biogenesis. *Cell.* 17:307-317.

Iomini, C., V. Babaev-Khaimov, M. Sassaroli, and G. Piperno. 2001. Protein particles in *Chlamydomonas* flagella undergo a transport cycle consisting of four phases. *J.Cell.Biol.* 153:13-24.

Kozminski, K.G., P.L. Beech, and J.L. Rosenbaum. 1995. The Chlamydomonas kinesin-like protein FLA10 is involved in motility associated with the flagellar membrane. *J.Cell Biol.* 131:1517-1527.

Lux, F., III, and S.K. Dutcher. 1991. Genetic interactions at the FLA10 locus: suppressors and synthetic phenotypes that affect the cell cycle and flagellar function in Chlamydomonas reinhardtii. *Genetics*. 128:549-561.

Marszalek, J.R., and L.S. Goldstein. 2000. Understanding the functions of kinesin-II. *Biochemica et Biophysica Acta*. 1496:142-150.

Marszalek, J.R., X. Liu, E.A. Roberts, D. Chui, J.D. Marth, D.S. Williams, and L.S. Goldstein. 2000. Genetic evidence for selective transport of opsin and arrestin by kinesin-II in mammalian photoreceptors. *Cell*. 102:175-187.

Nonaka, S., Y. tanaka, Y. Okada, S. Takeda, A. harada, Y. Kanai, M. Kido, and N. Hirokawa. 1998. Randomization of left-right asymmetry due to loss of nodal cilia generating leftward flow of extraembryonic fluid in mice lacking KIF3B motor protein. *Cell*. 95:829-837.

Ohkura, H., T. Torok, G. Tick, J. Hoheisel, I. Kiss, and D.M. Glover. 1997. Mutation of a gene for a Drosophila kinesin-like protein, KLP38B, leads to a failure of cytokinesis. *J. Cell Sci.* 110:945-954.

Orias, E., and P.J. Bruns. 1976. Induction and isolation of mutants in Tetrahymena. *In* Methods in Cell Biology. Vol. 13. D.M. Prescott, editor. Academic Press, New York. 247-282.

Orias, E., and L. Rasmussen. 1976. Dual capacity for nutrient uptake in tetrahymena. IV. growth without food vacuoles. *Exp. Cell Res.* 102:127-137.

Pan, J., and W.J. Snell. 2000. Signal transduction during fertilization in the unicellular green alga, *Chlamydomonas*. *Curr. Opin. Microbiol.* 3:596-602.

Pazour, G.J., B.L. Dickert, Y. Vucica, E.S. Seeley, J.L. Rosenbaum, G.B. Witman, and D.G. Cole. 2000. *Chlamydomonas* IFT88 and its mouse homologue, polycystic kidney disease gene Tg737, are required for assembly of cilia and flagella. *J.Cell.Biol*. 151:709-718.

Pazour, G.J., B.L. Dickert, and G.B. Witman. 1999. The DHC1b (DHC2) isoform of cytoplasmic dynein is required for flagelar assembly. *J. Cell. Biol*. 144:473-481.

Pazour, G.J., C.G. Wilkerson, and G.B. Witman. 1998. A dynein light chain is essential for the retrograde particle movement of intraflagellar transport (IFT). *J. Cell Biol.* 141:979-992.

Piperno, G., K. Mead, and S. Henderson. 1996. Inner dynein arms but not outer dynein arms require the activity of kinesin homologue protein KHP1(FLA10) to reach the distal part of flagella in Chlamydomonas. *J. Cell Biol.* 133:371-379.

Porter, M.E., R. Bower, J.A. Knott, P. Byrd, and W. Dentler. 1999. Cytoplasmic dynein heavy chain 1b is required for flagellar assembly in Chlamydomonas. *Mol. Biol. Cell*. 10:693-712.

Powers, J., O. Bossinger, D. Rose, S. Strome, and W. Saxton. 1998. A nematode kinesin required for cleavage furrow advancement. *Current Biology*. 8:1133-6.

Raich, W.B., A.N. Moran, J.H. Rothman, and J. Hardin. 1998. Cytokinesis and midzone microtubule organization in *Caenorhabditis elegans* require the kinesin-like protein ZEN-4. *Mol. Biol. Cell*. 9:2037-2049.

Rosenbaum, J.L., D.G. Cole, and D.R. Diener. 1999. Intraflagellar transport: the eyes have it. *J. Cell Biol.* 144:385-388.

Shakir, M.A., T. Fukushige, H. Yasuda, J. Miwa, and S.S. Siddiqui. 1993. C. elegans osm-3 gene mediating osmotic avoidance behaviour encodes a kinesin-like protein. *Mol. Neurosci.* 4:891-894.

Shang, Y., X. Song, J. Bowen, Y. Gao, J. Gaertig, and M.A. Gorovsky. 2001. A robust inducible-repressible promoter greatly facilitates somatic and germiline gene Knockouts, conditional expression and overexpression of homologous and

heterologous genes in Tetrahymena thermophila. *Proc. Natl. Acad. Sci. U.S.A.* In Press.

Signor, D., K.P. Wedaman, J.T. Orozco, N.D. Dwyer, C.I. Bargmann, L.S. Rose, and J.M. Scholey. 1999. Role of a class DHC1b dynein in retrograde trasnport of IFT motors and IFT raft particles along cilia but not dentrites, in chemosensory neurons of living *Caenorhabditis elegans*. *J. Cell. Biol*. 147:519-530.

Smith, E.F., and P.A. Lefebvre. 1996. PF16 encodes a protein with armadillo repeats and localizes to a single microtubule of the central apparatus in *Chlamydomonas* flagella. *J.Cell.Biol*. 132:359-70.

Walther, Z., M. Vashistha, and J.L. Hall. 1994. The *Chlamydomonas FLA10* gene encodes a novel kinesin-homologous protein. *J.Cell Biol.* 126:175-188.

Wiliams, B.C., M.F. Riedy, E.V. Wiliams, M. Gatti, and M.L. Goldberg. 1995. The Drosophila kinesin-like protein KLP3A is a midbody component required for central spindle asembly and initiation of cytokinesis. *J. Cell Biol.* 129:709-723.

Zang, J.-H., G. Cavet, J.H. Sabry, P. Wagner, S.L. Moores, and J.A. Spudich. 1997. On the role of myosin-II in cytokinesis: division of *Dictyostelium* cells under adhesive and nonadhesive conditions. *Mol. Biol. Cell*. 8:2617-2629.

TABLES

Table 5.1. Quantitative EM analysis of axonemal structure in RFT1 and suppressor strains.

Strain	Naked Basal Bodies	Short Axonemes Lacking Central Pair	9 + 2 Axonemes
RFT1Δ	66	18	0
RFT1ΔSm1	35	63	15
RFT1ΔMov1	0	20	55

Longitudinal sections through basal bodies were scored for the presence or absence of an associated axoneme and axonemes were scored for the presence or absence of a central pair. Numbers in table are raw numbers of basal bodies and axonemes in each category.

Table 5.2. Analysis of ciliary length and density for suppressor strain dilution series.

Initial Cell Density (per ml)	Culture Temp (°C)	Cilia per μm Cell Periphery	Avg. Length of Measurable Cilia μm +/- SEM (n)	P-value
1.5×10^{5}	30	0.25	2.9 +/- 0.089 (236)	N/a
3.0×10^{4}	30	0.16	2.0 +/- 0.112 (100)	1.0×10^{-5}
6.0×10^{3}	30	0.17	1.1 +/- 0.051 (169)	2.4×10^{-30}
3.0×10^{3}	30	0.15	1.4 +/- 0.051 (256)	8.5×10^{-32}
3.0×10^{3}	22	0.25	2.7 +/- 0.076 (256)	0.018

Growing RFT1Δsm cells were washed and resuspended in fresh MEPP at the indicated concentrations. After 21.5 hrs, cells were fixed and stained for IF with anti-tubulin antibodies. Cilia were counted and measured on single confocal sections corresponding to the widest section through the macronucleus for a given z-series. Data are from a single representative experiment among many that were performed with very similar loss of motility in diluted cells. P-values were generated using paired two-tailed t-tests comparing means for all other dilutions to the mean for 1.5×10^{5} cells/ml.

FIGURE LEGENDS

Figure 5.1. Sequence analysis and disruption of *RFT1*. Genbank accession numbers for sequence data used in comparisons are indicated in parentheses. (A) Rft1p (BF845521) is homologous to the known IFT proteins *C. elegans* OSM-6 (CAA03975) and *Chlamydomonas* IFT52 (AAL12162), as well as mouse NGD5 (AAA96241), human CGI53 (NP_057088) and *Drosophila* CG9595 (AAF52401). Multiple sequence alignment was performed using the PILEUP program of the University of Wisconsin GCG package. Shaded output was produced using the Boxshade software at (www.ch.embnet.org/software/BOX_form.html). Black shading indicates 50% or greater identity at a given position and gray shading indicates similarity. (B and C) Southern blot analysis of germline *rft1::neo2* transformants. (B) Left panel, Southern blot of total genomic DNA digested with EcoRI and Bsu36I and probed with a radiolabeled 3.4 kb genomic HindIII fragment of *RFT1*. Right panel, diagram of the *RFT1* locus. Lane 1, wildtype control strain; Lanes 2 and 3, independent germline transformants. Arrow in right panel, site susceptible to EcoRI star activity 1.2 kb upstream of the 3' EcoRI site. The wildtype locus gives fragments of 1.3 and 4.5 kb. A knockout is expected to yield a single 7.2 kb fragment and a 3' integration will give 1.3 and 9.3 kb fragments. The 4.5 kb band is present in all lanes indicating that the germline transformants are heterozygous for *RFT1/rft1::neo2*. Fragments generated by EcoRI star activity are indicated with asterisks. A 5.8 kb fragment likely generated by digestion of wildtype DNA with only EcoRI is indicated by δ. (C) Left panel, Southern blot of total genomic DNA digested with PstI and XbaI and probed with the same fragment as in B. Right panel, diagram of *RFT1* locus. Lanes 1-3 are as in B. The wildtype locus gives fragments of 2.0 and 5.2 kb. A knockout is predicted to give 0.6, 2.8, and 5.2 kb fragments. A 3' integration should give 0.6, 2.0, 4.2, and 5.2 kb fragments. Only the fragments larger than 0.6 kb are visible. Due to heterozygosity, the 2.0 kb fragment is present in the knockout strain.

Figure 5.2. Cytological analysis of RFT1Δ cells. The phenotype was induced by conjugation of knockout heterokaryon strains 7G5 and 7G6. Conjugation progeny were grown in MEPPA and stained with anti-tubulin antibodies (SG) and propidium iodide. Conjugation progeny were prepared for confocal microscopy 30-31 hours after isolation of conjugating pairs. (A and B) Wildtype control cells prior to and during division, respectively. (C) RFT1Δ mutant cell nearing the end of cytokinesis. (D) Mutant cell in an early stage of cytokinesis failure. Two MACs are evident. (E and F) Mutants after additional cytokinesis failures forming multilobed cells. Bar, 25 μm

Figure 5.3. Localization of *rft1-GFP*. RFT1Δ cells rescued with a *BTU1-MTT-RFT1-GFP-BTU1* fragment (see Materials and Methods) were grown in SPPA medium in the absence of cadmium. Cells were fixed and stained for confocal IF microscopy with polyclonal anti-GFP antibodies and DAPI. Left column, anti-GFP signal; middle column, DAPI signal; right column, merged images. (A-C) Interphase cell. Rft1p-GFP is primarily in cilia. (D-F) Cell in very early stage of micronuclear division. Posterior oral apparatus has short cilia in which Rft1p-GFP is highly concentrated. (G-I) Early stage of macronuclear elongation showing a zone of intense ciliary anti-GFP labeling immediately posterior to the developing cleavage furrow. (J-O) Later stages of macronuclear division and cleavage furrow ingression showing ciliary labeling but no accumulation in the cleavage furrow or cytoplasm. Bar, 10 μm

Figure 5.4. RFT1Δ cells were grown with (A and B) or without (C and D) shaking in MEPPA medium. After 48 hours, cells were prepared for IF microscopy as in Figure 2. Shown are merged grayscale images of the anti-tubulin and propidium iodide signals.

Figure 5.5. Cytological analysis of suppressor strains. Cells were grown in MEPPA medium and prepared for confocal imaging by staining with anti-tubulin antibodies as in

figure 2. (A) Wildtype control strain. (B) RFT1Δ10 (C) RFT1Δsm1 (D) RFT1Δmov1 (E) Quantitation of mean ciliary length (+/- standard error of the mean) using the measurement macro of Scion image software. For uniformity, portions of cilia visible on a single confocal section were measured for the widest cross section through the MAC in a particular Z-series. Only cilia that extended beyond the cell periphery were measured. P-values above each category were generated with a paired two-tailed t-test with the follwing null hypotheses: WT=RFT1 null; RFT1 null=RFT1 sm; RFT1 sm=RFT1 mov.

Figure 5.6. Electron microscopic analysis of suppressor strains. Cells prepared for EM were isolated from cultures actively growing in MEPPA. (A and B) Longitudinal sections through RFT1Δ10 basal bodies. In B a short cilium lacking a central pair is evident. (C) Cross section through three RFT1Δ10 axonemes lacking central pairs. (D and E) Longitudinal sections through RFT1Δsm1 basal bodies and short cilia. Some cilia in this strain have a central pair (D) whereas some do not (E). (F) Cross sections through several RFT1Δsm1 cilia showing different degrees of completeness of central pairs. (G) Longitudinal, cross and oblique sections through RFT1Δmov1 cilia showing that cilia are longer than in RFT1Δ10 and RFT1Δmov1 cells and most contain central pairs.

Figure 5.7. Analysis of dilution-dependent loss of motility in RFT1Δsm1 cells. Exponentially growing cells (3-5x10^5/ml) were washed and resuspended in fresh MEPPA at final dilutions of 0x (undil), 2x, 10x, 20x, and 100x. Cells were maintained at 30°C without shaking and live cells were scored on an inverted microscope for presence or absence of motility and for gross evidence of cytokinesis defects or normal cell shape. (A) 3.5 hr (B) 9.5 hr (C) 21.5 hr and (D) 33.5 hr after dilution.

Figure 5.8. Cytological analysis of RFT1Δsm1 dilution series and temperature shift experiment. Cells grown in MEPPA were washed in fresh media and resuspended at

$3x10^5$/ml. These cells were then diluted (A) 2x ($1.5x10^5$/ml), (B) 10x ($3x10^4$/ml), (C) 50x ($6x10^3$/ml), and (D and E) 100x ($3x10^3$/ml). (F) Cells diluted 100x as in D and E were grown at 22 degrees. After 21.5 hours, cells were fixed and stained as in figure 1.

Figure 5.9. Slowing growth rate does not allow cilia to form in highly dilute cultures. RFT1Δsm1 cells were diluted to ~ $3x10^3$/ml in modified MEPPA media containing varying concentrations of proteose peptone. (A) Growth rate decreased in media containing less than 2% proteose peptone. White bars, inoculum at t=0 and dilutions at 20.5 hr post-dilution; black bars, dilutions at 44 hr post-dilution. (B) Although all cells lose motility as observed previously, some slight shaking was present. Live cells were scored for the presence or absence of this shaking and for evidence of cytokinesis defects or normal cell shape. Slowing the growth rate decreased the likelihood that cells were observed shaking.

Figure 5.10. Evidence for involvement of cell communication. (A) RFT1Δsm1 cells were diluted to $3X10^3$/ml and grown at 22°C with or without gentle shaking or were diluted to $3X10^4$/ml and grown at 30°C with or without gentle shaking. Cells were scored for motility using a 10X objective on an inverted microscope. P-values were generated for comparison of proportions using a 2-proportion z-test with H_0: shaken=nonshaken and H_a: shaken≠non-shaken (n= 62 for unshaken at 30°C and 22°C, 50 for shaken at 30°C, and 70 for shaken at 22°C). (B-D) RFT1Δsm1(B and C) or RFT1Δ10 (D) cells were diluted to $3X10^3$/ml and incubated at 30°C without shaking and either with (C and D) or without (B) $7.5X10^4$ A*CAM (WT) cells/ ml. Cells were prepared for IF as in figure 2 and confocal sections representative of those used for scoring cilia lengths in E are shown. (E) Cilia lengths (+/- standard error of the mean) were measured on single confocal sections collected from cells prepared for B-D (n_{cells}=20 for RFT1Δsm1 and n_{cells}=10 for RFT1Δ10. Numbers of individual cilia

measured were 1187 for sm, 1058 for sm+ WT, 126 for null, and 136 for null+WT). Indicated p-values are from paired two tailed t-tests with H_0: sm=sm+WT and H_0: null=null+WT.

Figure 5.11. A single protein is predominantly upregulated in RFT1Δmov1 cells. NP-40 extractable membrane/matrix (A-D) or axonemal (E and F) proteins were subjected to two-dimensional gel electrophoresis. The first dimension (horizontal) was either a pH 3-10 (A and B) or a pH 4-7 (C-F) isoelectric focusing gel. The second dimension (vertical) was a 7.5% SDS polyacrylamide gel. Gels were silver stained to visualize protein spots. One protein, marked with an asterisk, was reproducibly upregulated in the suppressor strain.

A

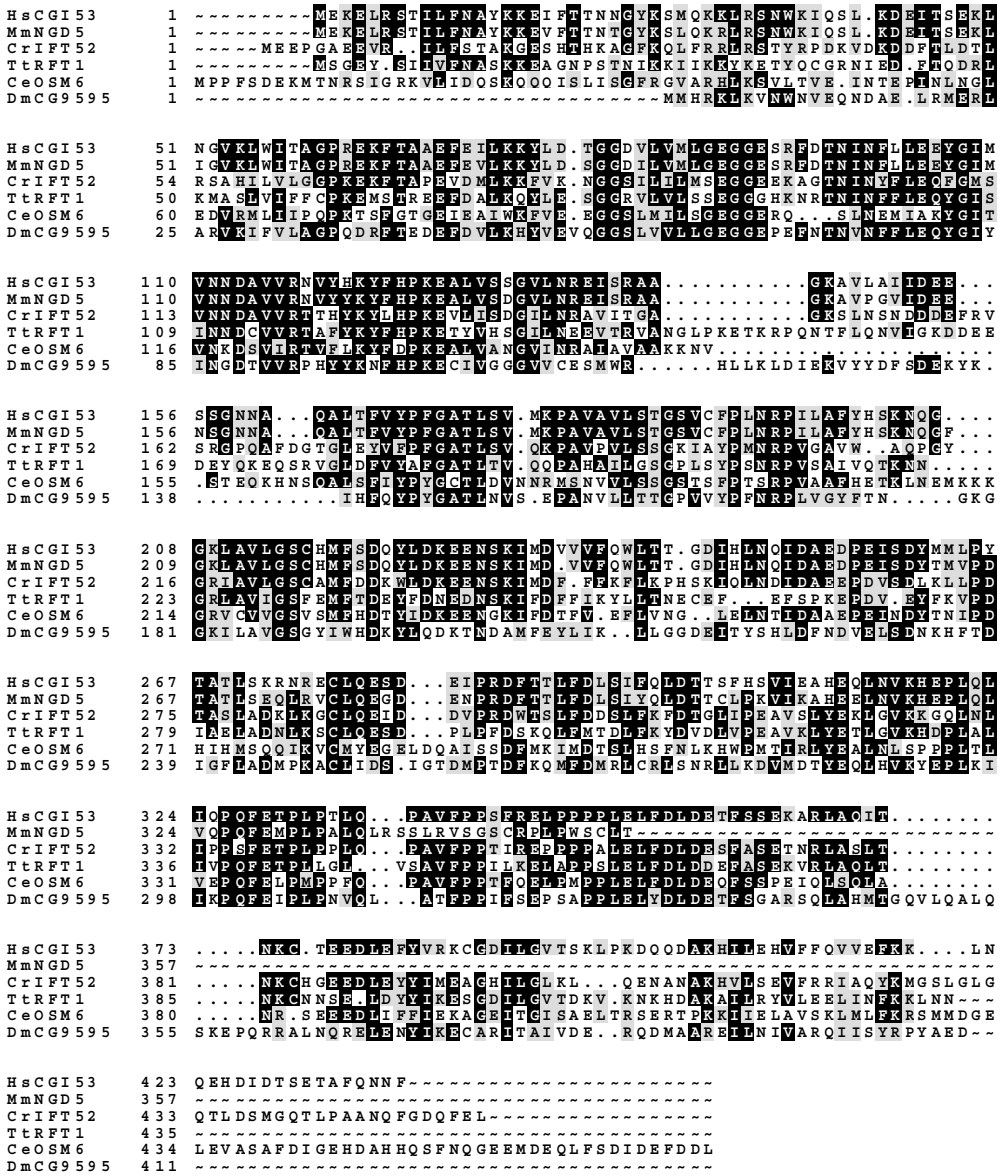

Figure 5.1

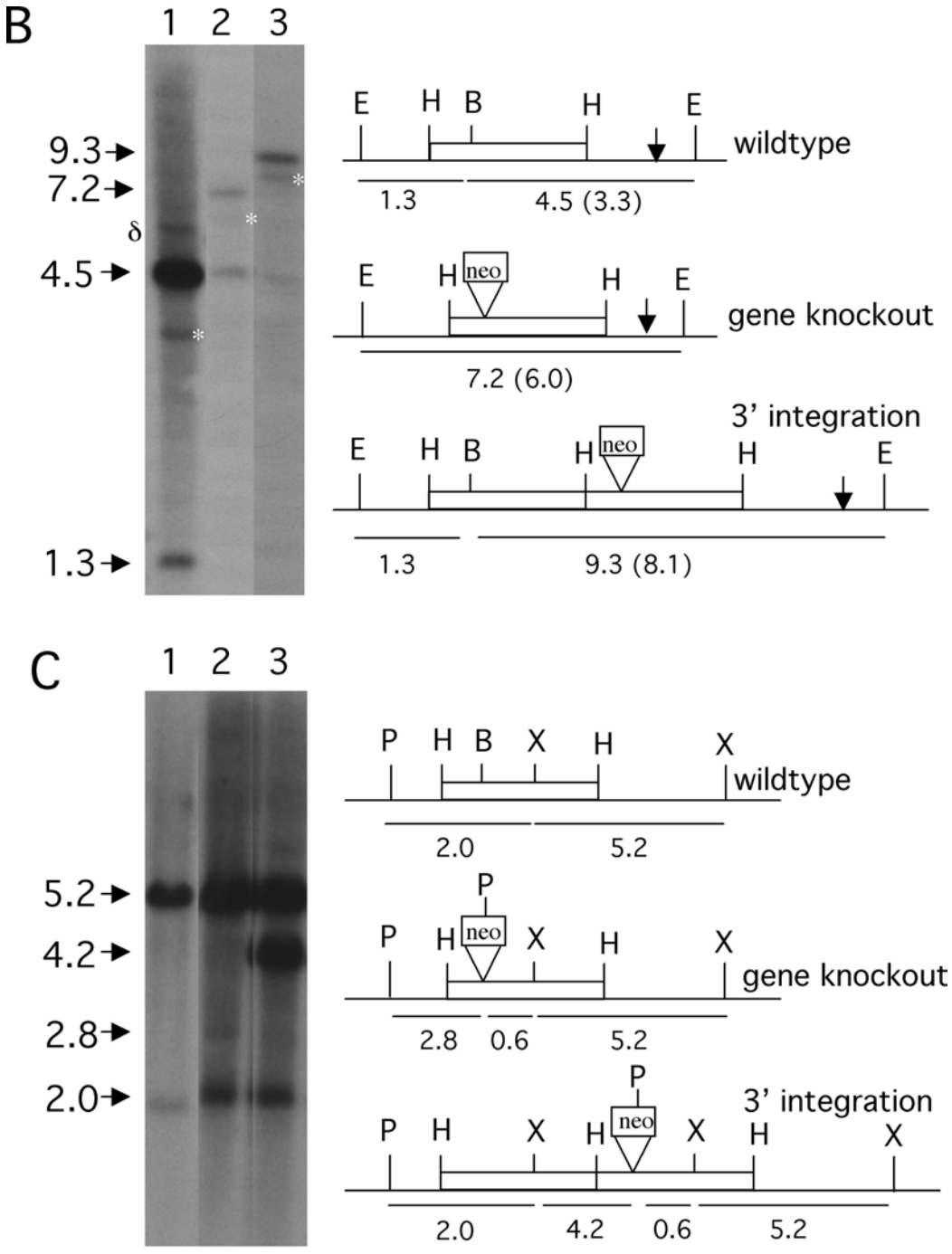
B
1 2 3
9.3
7.2
δ
4.5
1.3
E H B H E
wildtype
1.3 4.5 (3.3)
E H neo H E
gene knockout
7.2 (6.0)
3' integration
E H B H neo H E
1.3 9.3 (8.1)
C
1 2 3
5.2
4.2
2.8
2.0
P H B X H X
wildtype
2.0 5.2
P
P H neo X H X
gene knockout
2.8 0.6 5.2
P
3' integration
P H X H neo X H X
2.0 4.2 0.6 5.2

Figure 5.1

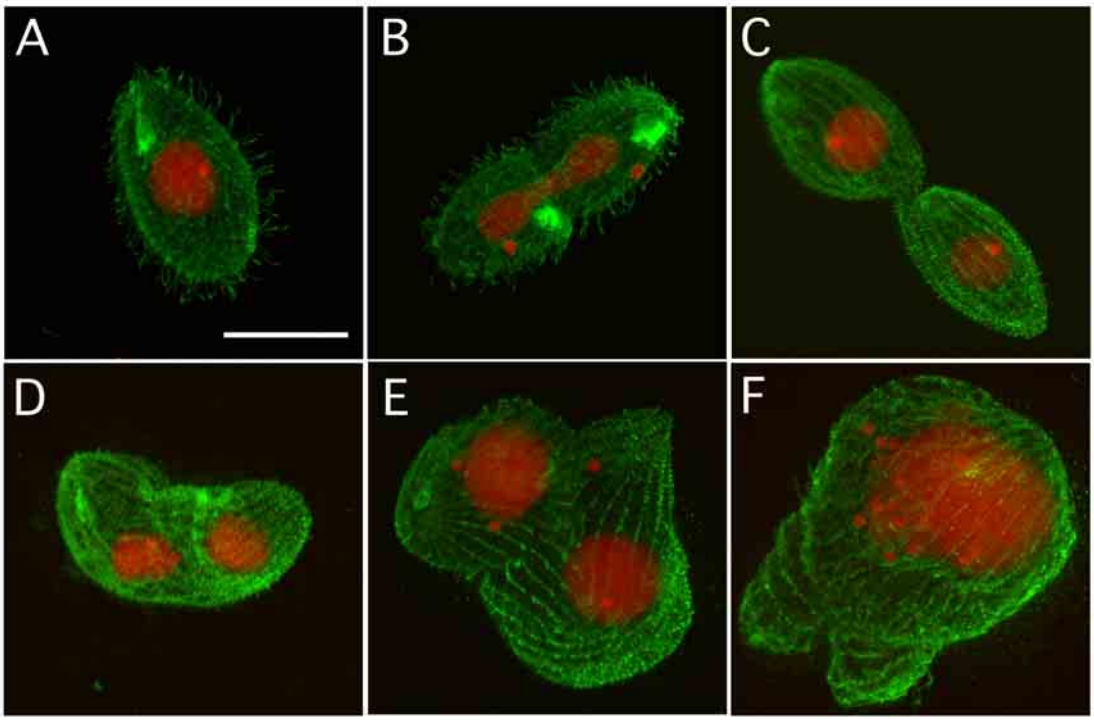

Figure 5.2

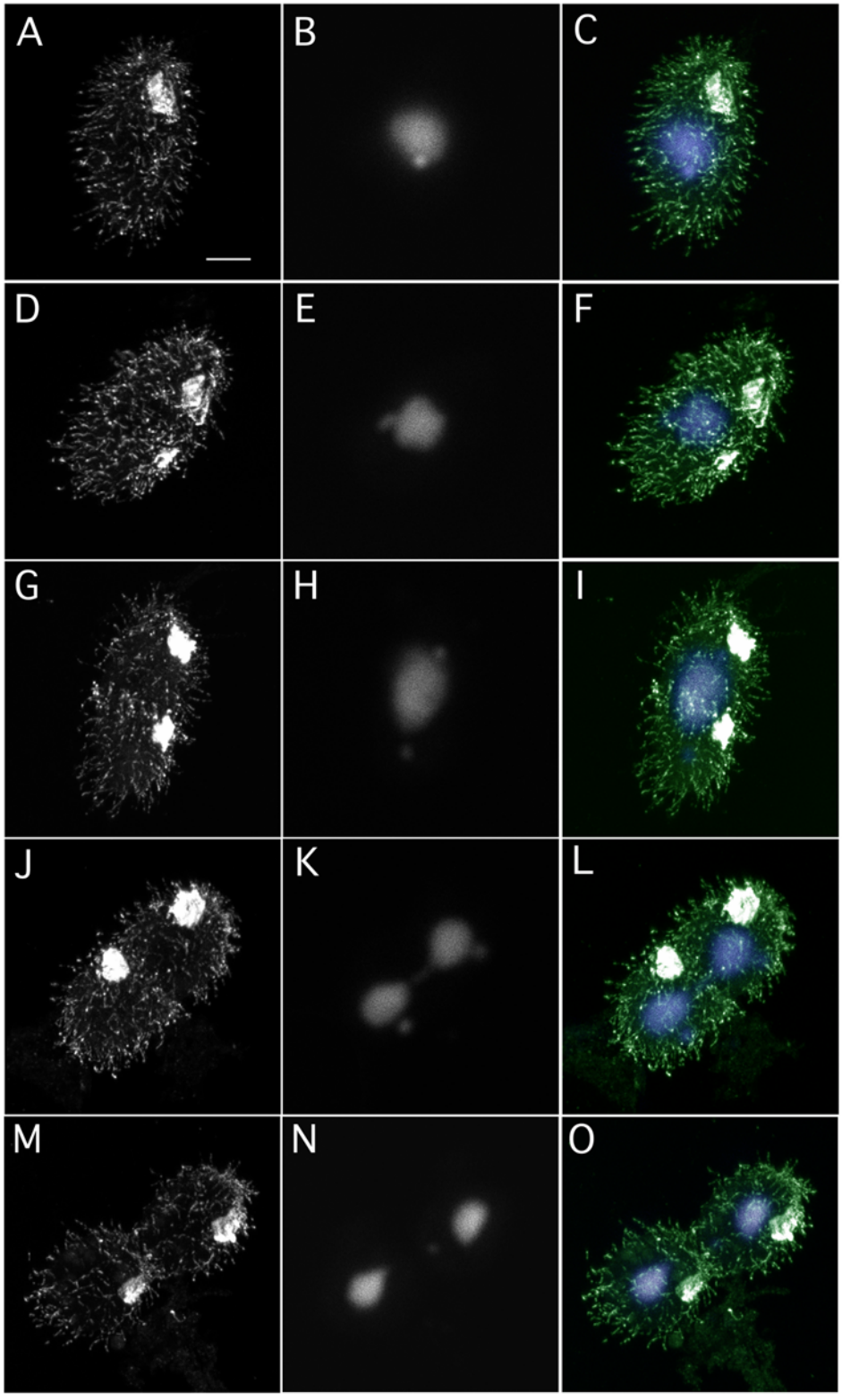

Figure 5.3

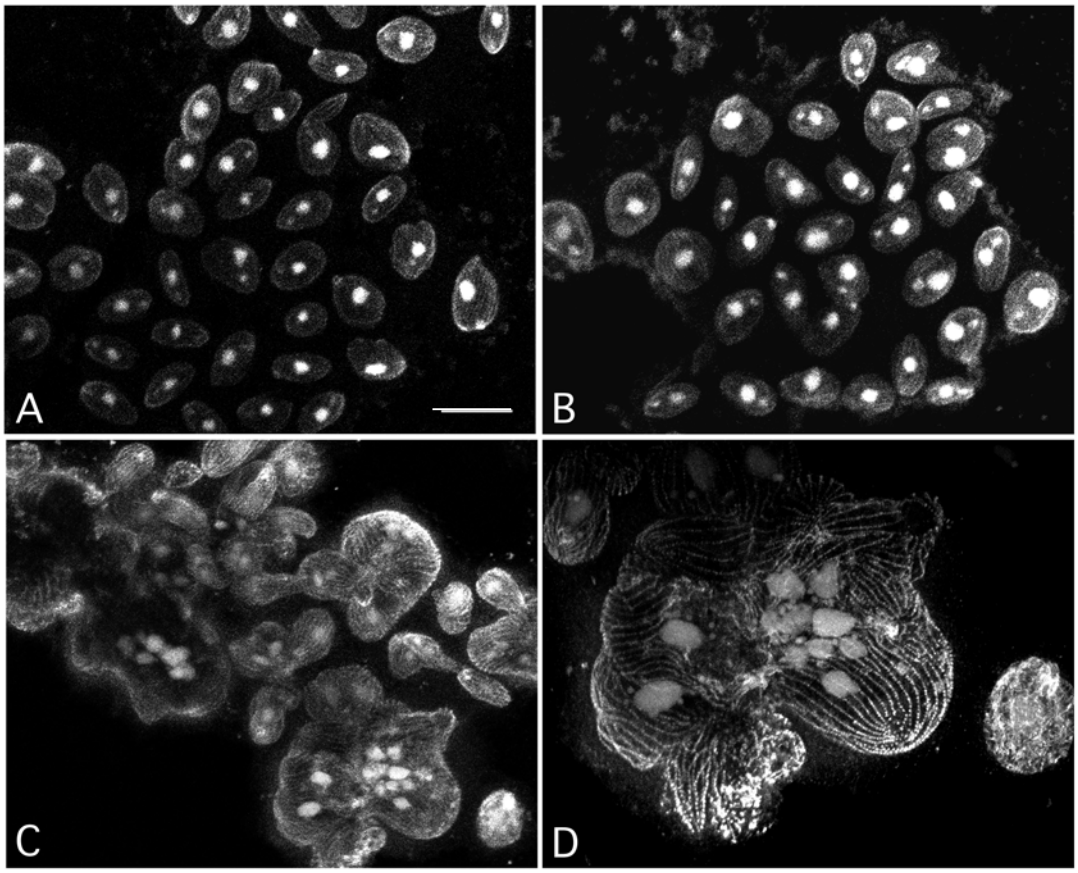

Figure 5.4

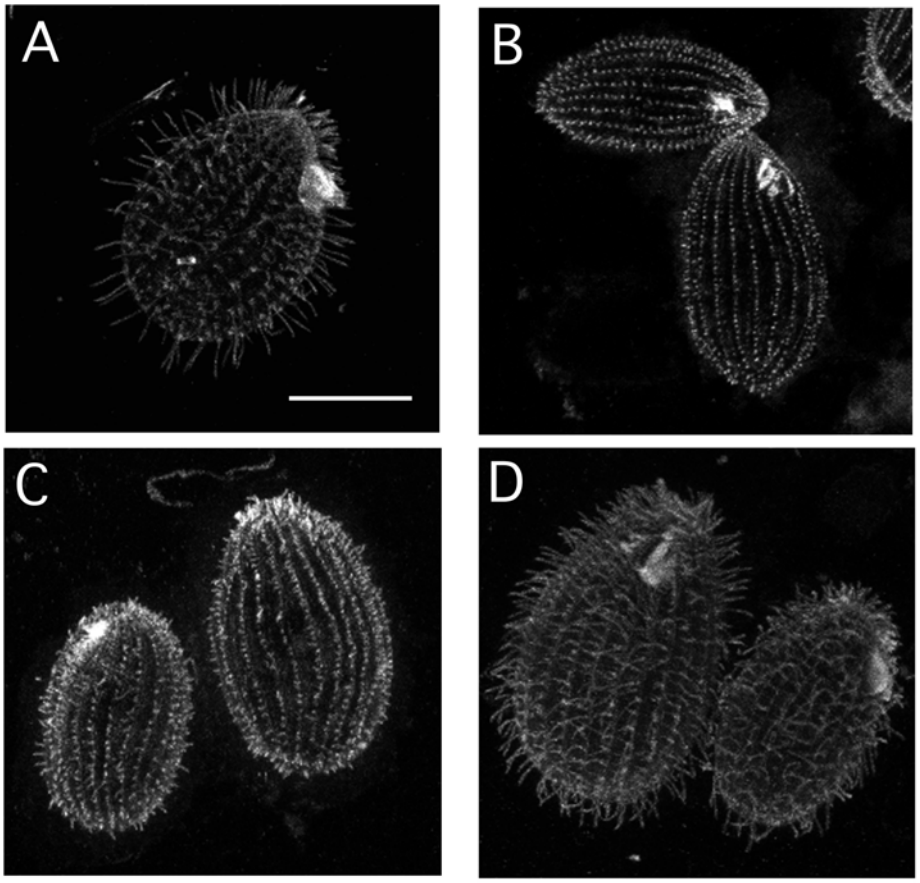
A
B
C
D

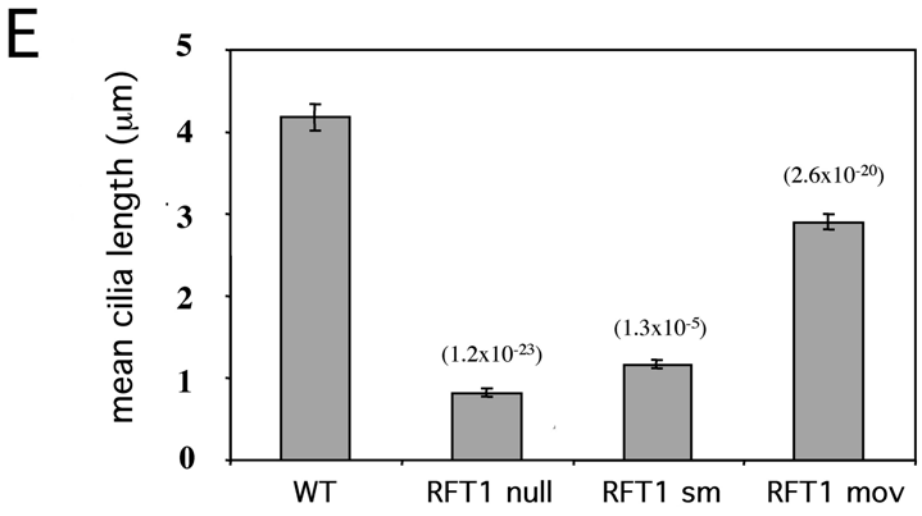
E
mean cilia length (μm)
5
4
3
2
1
0
(1.2x10-23)
(1.3x10-5)
(2.6x10-20)
WT
RFT1 null
RFT1 sm
RFT1 mov

Figure 5.5

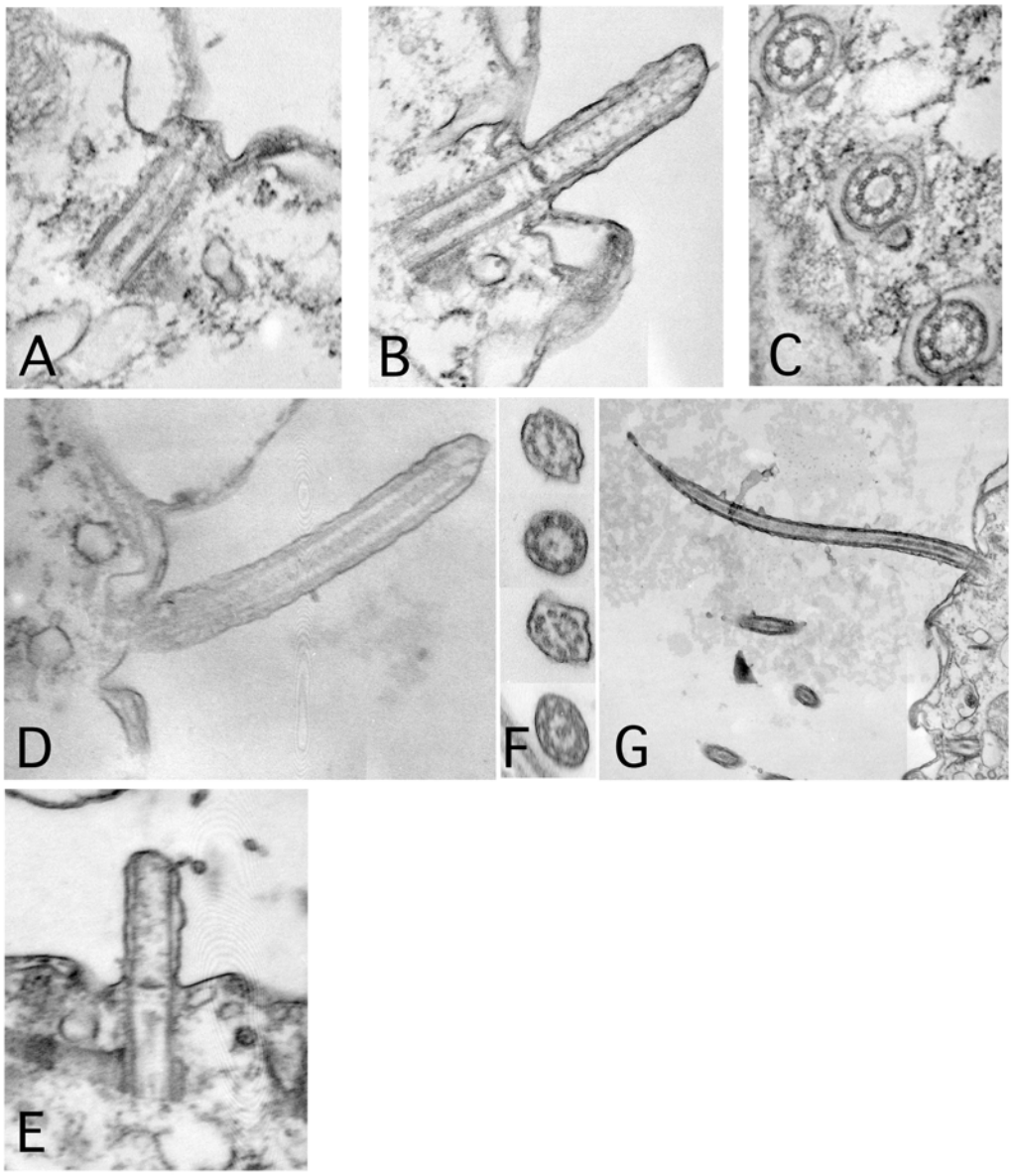

Figure 5.6

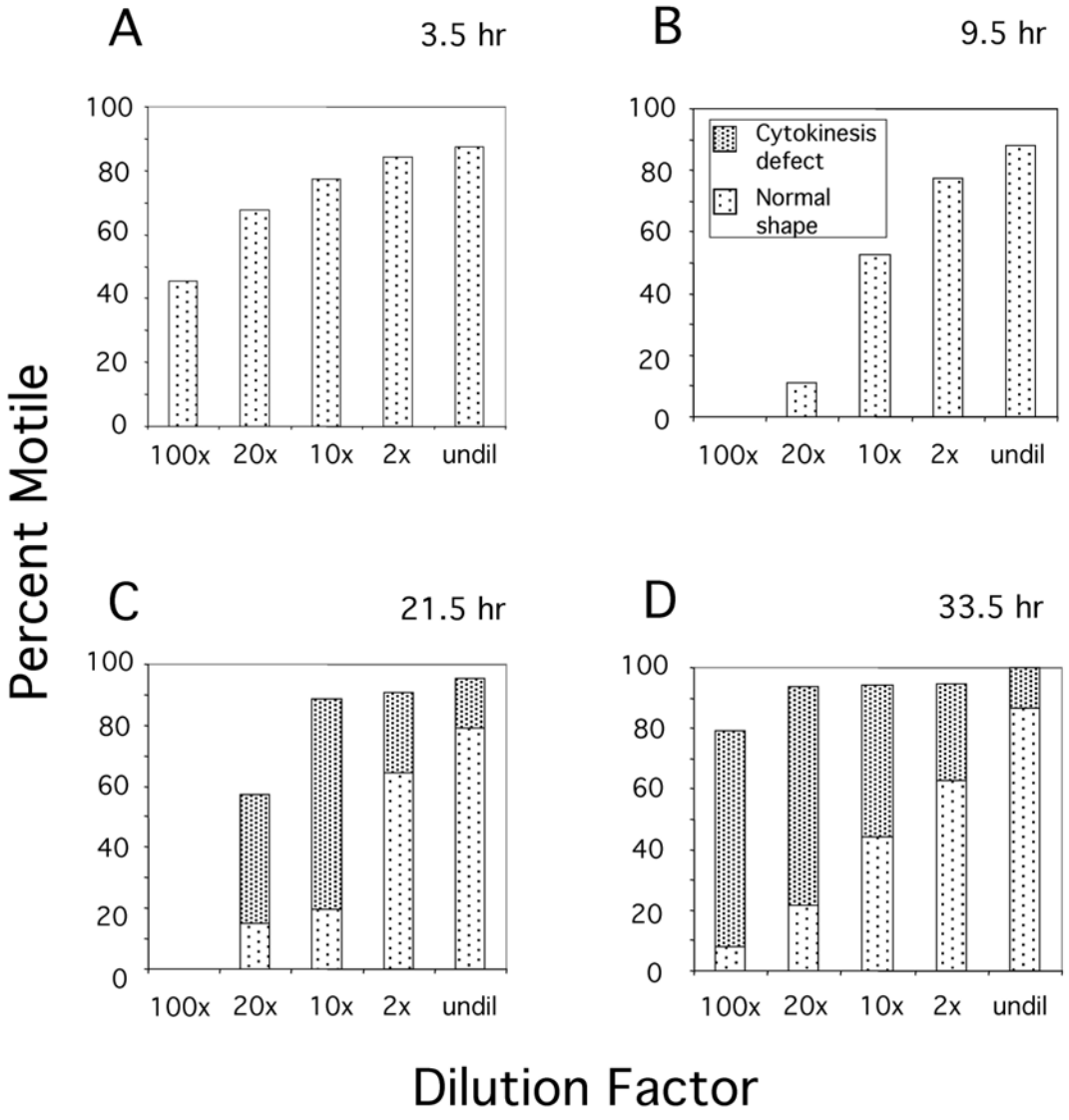
A
3.5 hr
B
9.5 hr
C
21.5 hr
D
33.5 hr
Cytokinesis defect
Normal shape
Percent Motile
Dilution Factor
100
80
60
40
20
0
100x
20x
10x
2x
undil

Figure 5.7

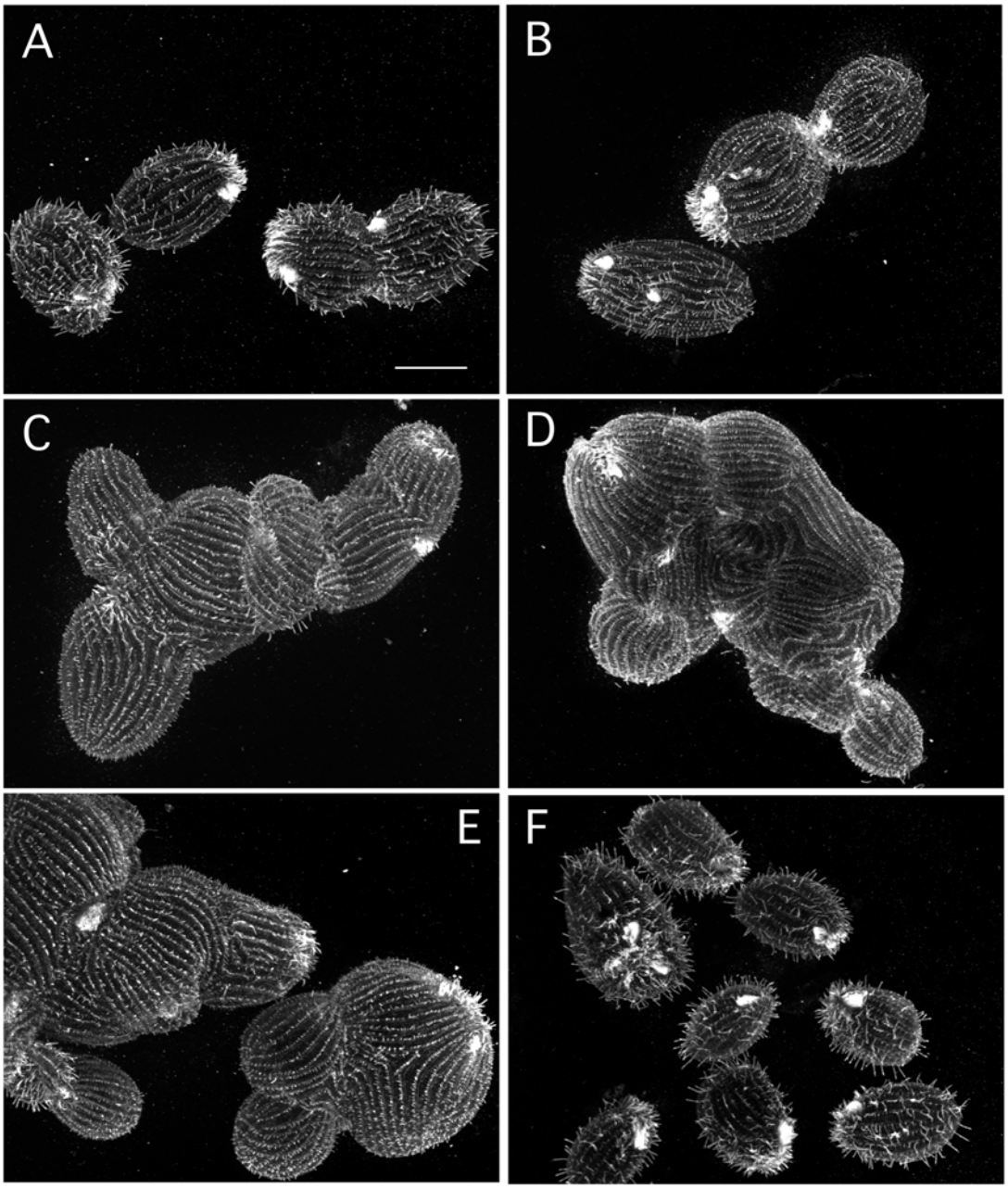

Figure 5.8

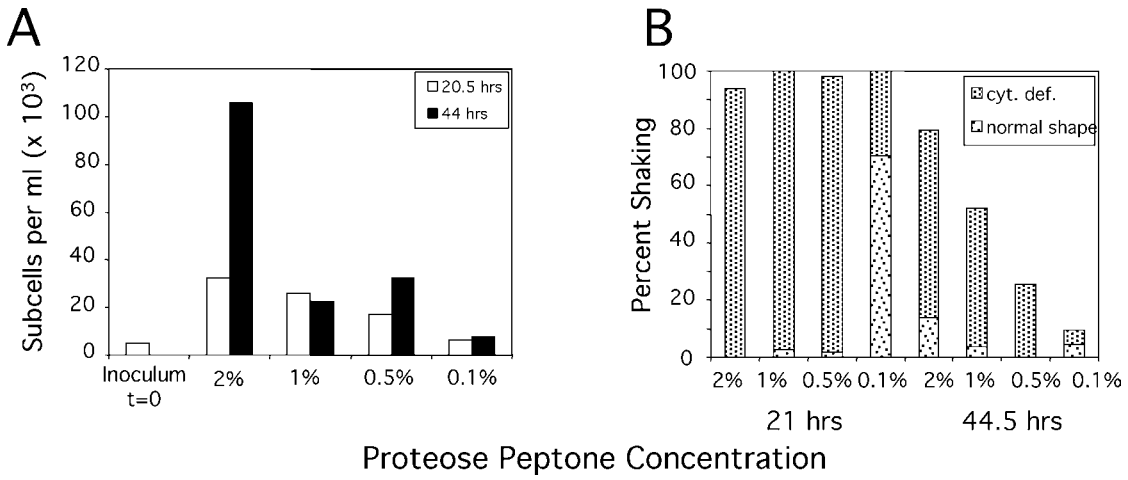
A
Subcells per ml (x 10³)
120
100
80
60
40
20
0
20.5 hrs
44 hrs
Inoculum t=0
2%
1%
0.5%
0.1%
B
Percent Shaking
100
80
60
40
20
0
cyt. def.
normal shape
2% 1% 0.5% 0.1% 2% 1% 0.5% 0.1%
21 hrs
44.5 hrs
Proteose Peptone Concentration

Figure 5.9

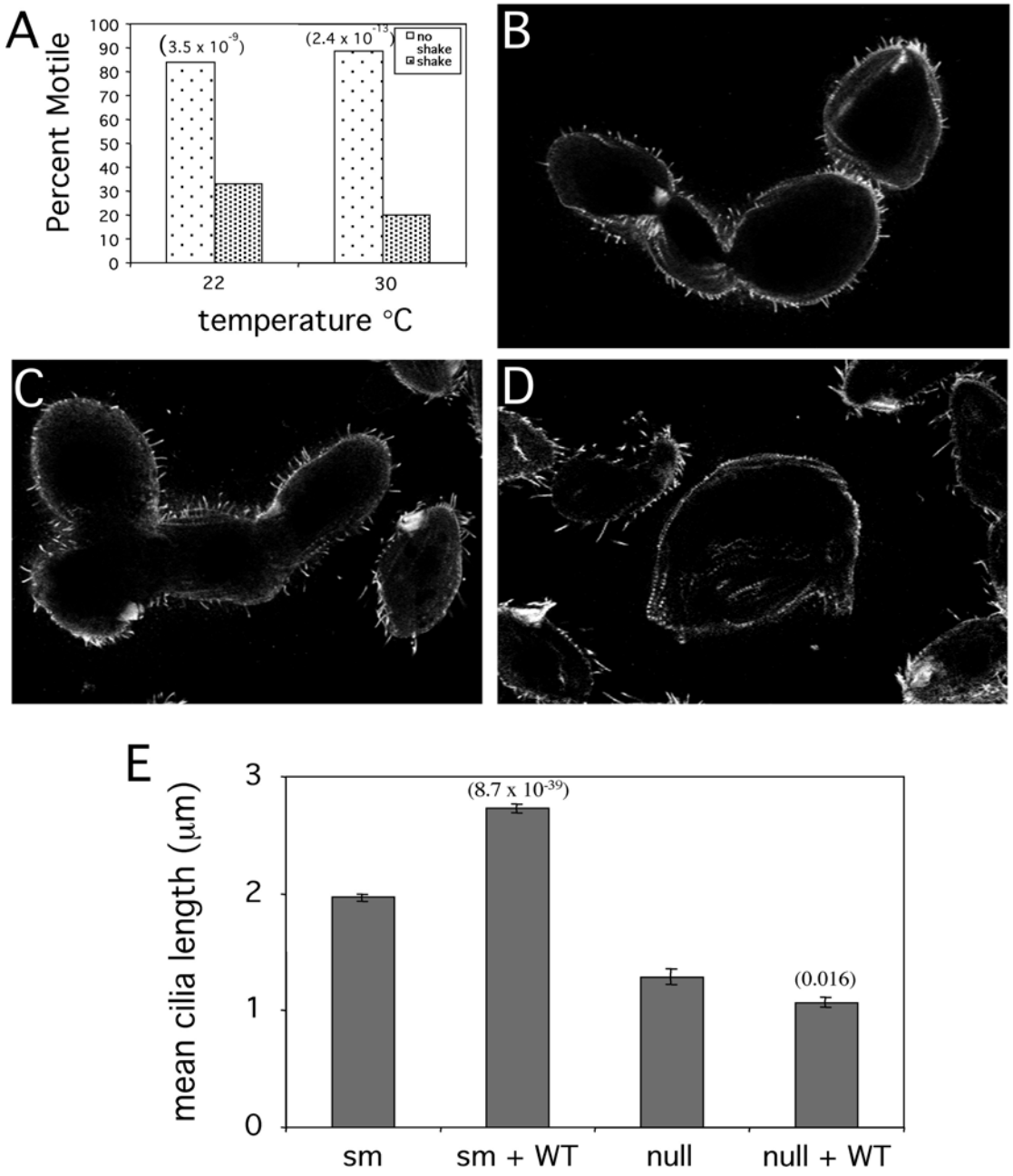
A
Percent Motile
100
90
80
70
60
50
40
30
20
10
0
(3.5 x 10-9)
(2.4 x 10-13)
no shake
shake
22
30
temperature °C
B
C
D
E
mean cilia length (μm)
3
2
1
0
(8.7 x 10-39)
(0.016)
sm
sm + WT
null
null + WT

Figure 5.10

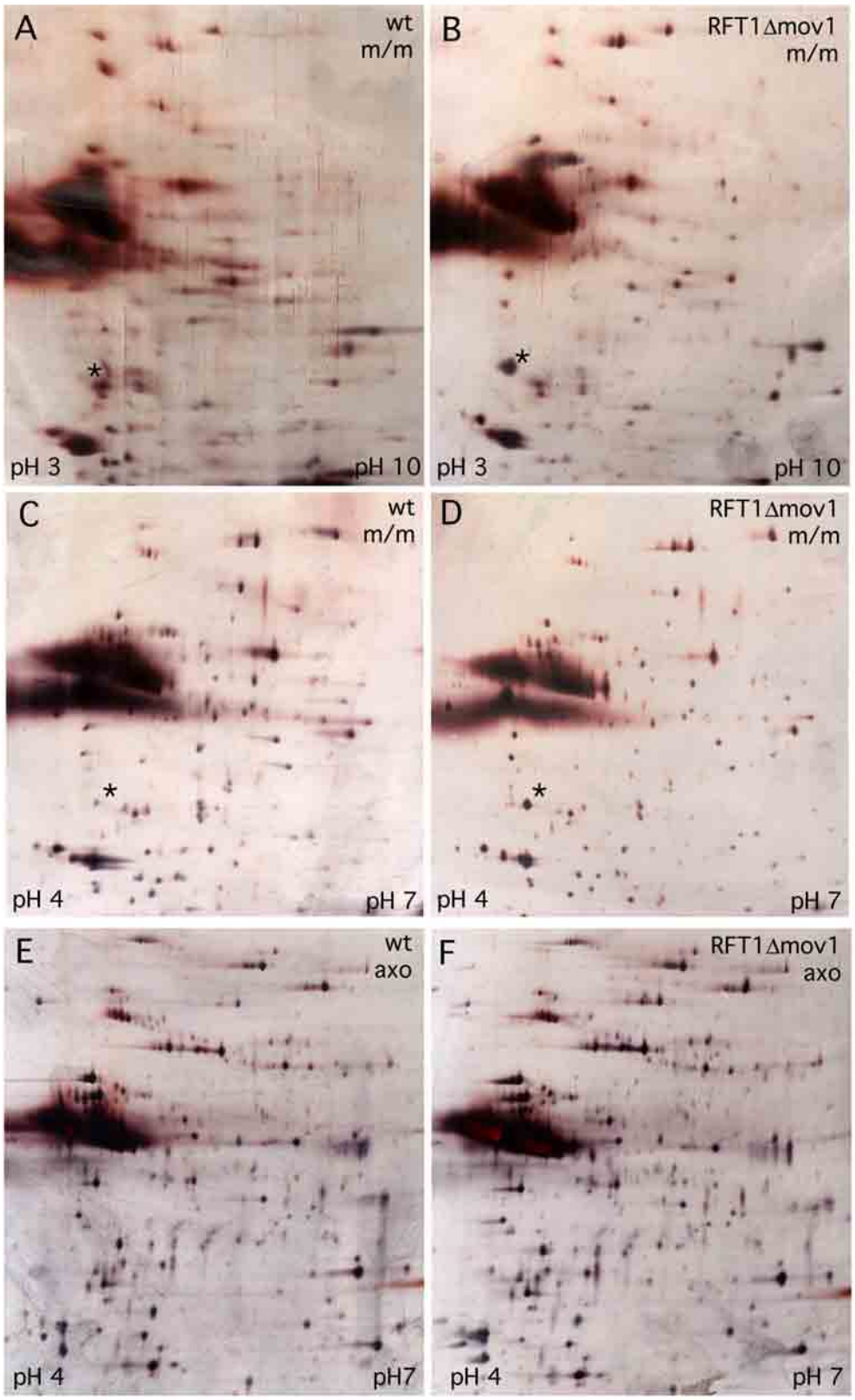
A
wt
m/m
pH 3
pH 10
B
RFT1Δmov1
m/m
pH 3
pH 10
C
wt
m/m
pH 4
pH 7
D
RFT1Δmov1
m/m
pH 4
pH 7
E
wt
axo
pH 4
pH7
F
RFT1Δmov1
axo
pH 4
pH 7

Figure 5.11

CHAPTER 6

CONCLUSION

My dissertation project began as an analysis of mutants in the putative ciliary kinesin-related protein, kinesin-II. Early on in the project, my interest shifted to a broader analysis of the mechanism of ciliary assembly and the significance of cilia for *Tetrahymena* cells. *Tetrahymena* has been used for many years to study processes related to ciliary beating, and as mentioned in Chapter 2, was actually the first organism from which axonemal dynein was extracted and analyzed. During the course of the studies presented here, we have confirmed our suspicion that recently developed techniques for germline transformation and gene replacement can be used to great advantage in the study of ciliary *assembly* in *Tetrahymena*.

Initially we cloned and disrupted two genes, *KIN1* and *KIN2*, coding for members of the kinesin-II family of molecular motors in *Tetrahymena*. Based on early studies of kinesin-II function in *Chlamydomonas,* suggesting a role in flagellar assembly (Kozminski et al., 1995), it was somewhat surprising that a disruption of either of the *Tetrahymena* genes lead to a relatively subtle phenotype. In neither case did the knockout phenotype lead to a loss of cilia. However, a closer analysis of the knockout cells showed that *KIN1* is more important for ciliary assembly, whereas *KIN2* is more important for normal cell growth. While the single kinesin-II knockouts had subtle defects, disruption of both genes simultaneously yielded a much more dramatic phenotype including three obvious defects. First, after induction of the mutant phenotype by mating double-knockout heterokaryon cells, isolated progeny exhibited a progressive loss of motility. Second, double-knockout cells were not viable on a standard growth medium and lacked food vacuoles, suggesting the possibility that they had non-functional

oral apparatuses. Third, before double-knockouts lost viability they began to form "monster" cells which appeared to result from defects in cytokinesis.

Once we described the gross phenotype of the *KIN1/KIN2* double knockouts, additional studies were aimed at determining whether the multiple phenotypic defects indicated that kinesin-II is multifunctional in *Tetrahymena*. This was an important question for several reasons. First, kinesin-II is the only kinesin known to be formed in part by heterodimerization of two similar, but non-identical motor subunits (Marszalek and Goldstein, 2000). This combined with the fact that in *Tetrahymena*, as well as in mouse (Yang and Goldstein, 1998) and *C. elegans* (Signor et al., 1999), at least three kinesin-II motor subunits are present raises the possibility that different motor subunits could mix and match in different combinations to form motors with varied functions. Second, as mentioned above, *KIN1* and *KIN2* single-knockouts had different phenotypes. Third, immunolocalization studies in both *Chlamydomonas* (Vashishtha et al., 1996)and sea urchin (Henson et al., 1995)and genetic studies in *Chlamydomonas* (Lux and Dutcher, 1991) suggested a possible function for kinesin-II in cell division. Therefore a critical aspect of the kinesin-II analysis was to address the hypothesis that kinesin-II is directly involved in multiple functions within the cell. To address the question of why the double knockouts lost motility, I performed confocal and EM analysis. Confocal analysis revealed that loss of motility was due to a nearly complete loss of locomotory cilia. Further analysis by EM confirmed that many basal bodies completely lacked associated axonemes. These results established for the first time that *Tetrahymena* has IFT components which are required for ciliary assembly. Interestingly, to my knowledge, this was also the first *Tetrahymena* mutant described which lacked cilia. Confocal analysis also confirmed our suspicions that the monster cells were formed by failures in cytokinesis, since the monsters, unlike wildtype cells, contained multiple MACs and MICs.

In an attempt to understand the cause of inviability of double knockouts on the standard growth medium, I tested the hypothesis that cells fail to survive simply because they lack oral cilia, rendering them unable to feed by the normal use of their oral apparatus. In 1975 Orias and Rasmussen showed that a *Tetrahymena* strain lacking an oral apparatus could be grown on an enriched medium known as MEPP. We reasoned that if the kinesin-II double knockouts die because they have a non-functional oral apparatus, then MEPP should rescue the growth of these cells as well. In fact, I found that this was the case. As mentioned above, when double-knockout heterokaryons are mated and pairs are isolated into drops of standard medium, the progeny divide only a few times and then lose viability. On the other hand, conjugation progeny from pairs isolated into MEPP medium could be grown indefinitely and actually maintained a reasonable growth rate when transferred to shaking culture. Thus, the loss of viability in standard medium was a secondary effect of the null mutations caused by loss of cilia. This discovery has turned out to be an important technological breakthrough for the study of IFT mutants in *Tetrahymena* and may explain why mutants completely lacking cilia have not been isolated in previous phenotypic screens designed to select for paralyzed cells.

In order to further address the function of kinesin-II, we performed localization studies. When immunolocalization of a myc epitope-tagged Kin1p failed, I created a *KIN1-GFP* fusion construct which rescued the loss of motility in the double KIN mutants. Immunolocalization with polyclonal anti-GFP antibodies revealed that kinesin-II is found at low levels in the cell body, but is primarily localized to cilia. Interestingly, we found that short cilia undergoing active assembly also appeared to have a higher level of GFP-Kin1p staining per unit length than longer cilia. This suggested that kinesin-II preferentially accumulates in cilia which undergo active assembly. A similar result has recently been described for the raft protein IFT52 in *Chlamydomonas* (Marshall and Rosenbaum, 2001). These authors also found that total IFT52 content was constant for

long and short flagella, yielding a higher concentration of IFT52 in short flagella. We did not address the total concentration of kinesin-II in short vs. long cilia, but it is possible that a similar mechanism could explain the apparent accumulation in *Tetrahymena* cilia.

Another aspect of the kinesin-II double-knockout phenotype that could be addressed with localization studies was the possible direct role in cell division. Staining of dividing cells expressing GFP-Kin1p with anti-GFP antibodies did not reveal any colocalization with the cleavage furrow or apparent relocalization during cell division except for the intense labeling of both anterior and posterior oral apparatuses. This result suggested that the kinesin-II cytokinesis phenotype may not indicate a direct role for kinesin-II in cell division. In order to further address the possibility of a direct function for kinesin-II in cell division, we observed live mutant and wildtype cells during formation and ingression of the cleavage furrow. We found that the initial stages of cleavage furrow ingression in the mutants were essentially indistinguishable from wildtype cells, but that mutants were defective in the final severing of the cytoplasmic bridge connecting the daughters.

Our observations of live dividing cells raised the intriguing possibility that mutant cells might fail to separate at the end of cytokinesis because they lack motility. Alternatively, kinesin-II may deliver some cargo that is necessary for the final separation of the daughter cells, and either the site of delivery is in the cilia, or if the site of delivery is in the cleavage furrow, accumulation of Kin1p at that site was below our level of detection. One keen observation by an undergraduate working on a class project under my direction helped begin to resolve these alternative hypotheses and led me into the second phase of my dissertation work. While collecting images of live cells during cytokinesis, Frank Hardin noticed that one of the daughter cells appeared to rotate just prior to cell division. When we made a detailed analysis of this motility, it became clear that most wildtype cells rotate prior to division, a motility that we named “rotokinesis”. In addition, rotokinesis involved a persistent unidirectional rotation of only the posterior

daughter cell and periods when rotation stopped and the two daughter cells appeared to pull apart before beginning to rotate again. It is hard to watch rotokinesis occurring without becoming convinced that the torque generated by the rotations help in the process severing the cytoplasmic bridge, which would support the hypothesis that kinesin-II double mutants fail to divide because of their lack of motility. In an effort to challenge this hypothesis, I isolated dividing wildtype cells into a highly viscous methyl-cellulose-containing medium. Under these conditions, motility of the dividing cells was greatly reduced and rotokinesis could not occur. Interestingly, division took more than twice as long in methylcellulose as in standard medium and a long cytoplasmic bridge formed between the daughters before division as both daughter cells underwent apparently uncoordinated movements. The involvement of whole cell motility in the completion of cytokinesis is not without precedent. In fact, in amoeboid cell types the crawling of daughter cells in opposite directions to break the cytoplasmic bridge may be a general phenomenon (Burton and Taylor, 1997; Zang et al., 1997). It is important to note that rotokinesis has features that are quite different from cell motility-assisted cytokinesis in these amoeboid cells, however. Namely the behavior of each daughter cell is distinct, with only the posterior daughter rotating. This raises the possibility that the two daughter cells have a mechanism to independently regulate their motility.

The work presented in Chapter 5 was initiated with two distinct purposes in mind. First, by cloning and disruption of a single subunit of the IFT raft complex, I hoped to be able to generate a partial phenotype that could provide some insight into the specific function of IFT. Previous studies, including our own indicated that kinesin-II-driven IFT is required for ciliary and flagellar assembly, but a critical question is what is the molecular mechanism by which IFT promotes assembly and maintenance of cilia. Are the rafts the true cargo for kinesin-II? In other words, do individual raft components have important direct roles in ciliary maintenance or do the rafts simply act as platforms to carry cargo in the form of ciliary structural components to the plus ends of the ciliary

microtubules? The second important aspect of the disruption of an IFT subunit was to further test the rotokinesis hypothesis. The rationale was that if the IFT mutants ended up lacking cilia and displayed normal cytokinesis, then we could hypothesize that kinesin-II plays a role in cytokinesis that is independent of its association with rafts. On the other hand, if the raft protein knockout lacked cilia, but also failed to divide normally then we could say that either our rotokinesis hypothesis is supported or kinesin-II and one of the raft proteins are both directly involved in cytokinesis. Of course, one other possibility was that a protein with homology to raft subunits in other organisms would not be required for ciliary assembly in *Tetrahymena*.

In order to address the questions presented above, I cloned and disrupted the *Tetrahymena* gene coding for a homologue of the *Chlamydomonas* IFT raft protein, IFT52. We named this gene *RFT1* for ciliary RaFT protein number 1. Disruption of *RFT1* lead to a phenotype that was indistinguishable from the kinesin-II double-knockout phenotype, placing the motor and its "cargo" in the same pathway. Once the knockouts were complete and the overall phenotype was documented, I began working with these cells to try to further test the rotokinesis hypothesis. I constructed a GFP-tagged *RFT1* construct with expression of the fusion gene driven by the cadmium-inducible *Tetrahymena* MTT promoter with the intention of performing localization studies in a tightly controllable system of inducible ciliary assembly. Interestingly, I was able to rescue *RFT1* null mutants with the construct both in the presence and in the absence of cadmium, although in the presence of high levels of cadmium the expression of the GFP fusion was increased dramatically. These results indicate that while expression of Rft1p-GFP from the MTT promoter is cadmium-responsive, it is not cadmium-dependent. GFP autofluorescence produced by expression of Rft1p-GFP in the absence of cadmium indicated that Rft1p localized specifically to cilia. In an effort to increase the sensitivity of detection we also performed immunolocalization with anti-GFP antibodies. These studies showed that indeed, Rft1p-GFP localized exclusively to cilia and never

accumulated in the cleavage furrow even at very late stages of cytokinesis. Thus, while a direct role in cytokinesis for both Rft1p and Kin1p was still possible, our inability to detect any cell-division-associated relocalization of either protein fused to GFP made it seem unlikely. We had previously noticed that when kinesin-II mutants were grown in shaking culture they appeared to form fewer monster cells than cells grown without shaking. This observation supported our hypothesis that cell motility is important for completion of cytokinesis and raised the question of whether the *RFT1* mutant would behave in the same way. In experiments designed to test this idea, we found that *RFT1* mutants have dramatically fewer arrests in cytokinesis in shaking culture than in non-shaking culture. These observations indicate clearly that whole cell motility is sufficient to separate daughter cells once the cleavage furrow has ingressed to a thin bridge. Of course the formal possibility remains that both Kin1p and Rft1p are directly involved in completion of cytokinesis. However, if a mutant with paralyzed flagella in a non-IFT protein coding gene was constructed, such a mutant should allow these two possiblities to be distinguished. Creation of such a mutant is currently underway by disrupting the function of a homologue of pf16, a gene mutation of which in *Chlamydomonas* leads to paralyzed flagella.

In the second portion of the *RFT1* study, we discovered that the loss of motility in *RFT1* null cells is partially suppressed at a relatively high frequency. By confocal and EM analysis we found that the partial recovery of motility in suppressed cells is due to the presence of very short axonemes, some of which lack a central pair. Interestingly, during continuous subculturing of these semi-motile suppressors (RFT1Δsm1) a second suppression event occurred to generate a population of cells (RFT1Δmov1) with further enhanced, although not wildtype, motility. These cells had longer cilia with much more frequent presence of central pairs. Thus, functional Rft1p is apparently not required for the assembly of cilia in the suppressor strains.

The most exciting aspect of my dissertation work has resulted from the isolation of these suppressor strains. Surprisingly, we found that the RFT1Δsm1 cells maintain their motility as well as the presence of cilia only under very specific conditions. We found that the maintenance of cilia was dependent on high cell density at 30°C whereas at 22°C cilia could be maintained at a lower cell density. This raised the exciting possibility that in the suppressor strain cells need to communicate with each other in order to maintain motility. There are several critical implications of this hypothesis. First, if the hypothesis is correct, there would need to be a signaling pathway to carry the information from one cell to another and then to the ciliary assembly machinery in the cell receiving the signal. Second, either cells would need to come in contact with one another, or there would need to be a soluble factor secreted by the cells. According to our results, such a soluble factor would be expected to be active over a relatively short distance and would be highly labile at 30°C. Specifically, growth of RFT1Δsm1 cells with shaking showed that moderate shaking was able to prevent the maintenance of motility in diluted cells. This result suggests that shaking sweeps away the soluble factor from the cell surface. Alternatively, this shaking may prevent cell-cell contact, but at the concentrations used in these experiments, cell-cell contact was unlikely even in non-shaken culture. Finally, our results suggest that loss of functional Rft1p in null mutants leads to an inability to respond to the secreted factor. This was shown by co-culture experiments in which wildtype cells were able to stimulate RFT1Δsm1 cells to grow longer cilia. Preliminary results also indicated that RFT1Δ10 cells can stimulateRFT1Δsm1 cells. The *rft1Δ* result indicates that the null mutant cells may in fact be able to communicate with the suppressor cells, likely through the proposed soluble factor. The results with wildtype cells show that the proposed signaling mechanism may have significance in a wildtype genetic background. Further experiments will need to be carried out to address the significance for wildtype cells. One simple experiment which is currently underway is to deciliate wildtype cells and allow them to regenerate cilia at different cell densities. If

the factor is important for ciliary assembly in wildtype cilia then at higher cell densities, ciliary assembly should occur more rapidly. The observation that RFT1Δ10 cells appear to be able to promote ciliary assembly in RFT1Δsm1 cells but are unable to assemble cilia themselves suggests that they are unable to respond to the signal promoting ciliary assembly. This was confirmed by mixing RFT1Δ cells with wildtype cells in the same experiment in which the wildtype cells could stimulate the semi-motile suppressor. In this experiment, the RFT1Δ cells were unable to respond to the signal produced by wildtype cells.

Our results suggest that loss of Rft1p function in null mutants leads to a loss of the ability to respond to a secreted signal promoting ciliary assembly. In the two suppressed strains, there could be a partial recovery of the ability to respond to the signal, perhaps by increased expression or hyperactivation of another component of the proposed signaling pathway. This protein could be a membrane receptor or another component of the raft particles. To work toward identification of such an upregulated protein, two-dimensional gel analysis of ciliary membrane fractions was performed and excitingly, a single polypeptide is reproducibly more abundant in membrane/matrix fractions from RFT1Δmov1 cells compared to wildtype. Sequencing of peptides generated from this protein is currently underway. We expect that if our hypothesis is correct, this upregulated protein may be a membrane receptor for the secreted signal.

While my dissertation project revealed important aspects of IFT function and regulation, many important questions remain. One question regarding kinesin-II function is what is the significance of the heterodimerization of the motor subunits. *Tetrahymena* will be a useful organism in which to address this question since three kinesin-II motor subunit genes have been identified. We currently do not know the phenotype of a *KIN5* knockout, but it may be important to create all possible combinations of double knockouts with *KIN1, KIN2,* and *KIN5*. Also, if these knockouts do not reveal the subunit composition of kinesin-II complexes it may be possible to determine subunit

interactions biochemically. This may turn out to be quite difficult, however. I spent some time attempting to affinity purify Kin1p and any associated proteins with very limited success. In addition, some of our collaborators tried to purify kinesin-II complexes from *Tetrahymena* and determined that they were present in extremely low quantities. As mentioned previously, while it seems unlikely, the possibility still remains that our rotokinesis hypothesis is incorrect and that both raft proteins and kinesin-II may play a direct role in *Tetrahymena* cytokinesis. Disruption of the *Tetrahymena* pf16 homologue may shed some important light on this problem.

The RFT1 study presented in Chapter 5 raises many important questions for understanding IFT function and regulation. Probably the most important question is why would cells need to invoke a soluble factor to control ciliary assembly. As we suggested in Chapter 5 (see Discussion), a soluble factor could be used to regulate ciliary length if it is released near the cell body and is recognized by a receptor located at the ciliary tip. Such an arrangement (Figure 6.1) would allow short cilia to outcompete long cilia for a relatively labile extracellular factor. Another critically important question is whether signaling is the sole purpose of raft complexes or whether direct transport of ciliary components is another function for the rafts. Clearly, results from several organisms suggest that axonemal components may be transported by rafts, but in general these results only show that IFT is required for transport of certain components. It is certainly possible that the signaling function of rafts may control the transport of axonemal components by as-yet unidentified transport mechanisms. The most likely scenario at this point appears to be that rafts bind directly to and carry some axonemal components, but that there are signaling components of rafts, such as Rft1p that control the activation state of the rafts and thereby control transport of the ciliary components. My results provide an important piece of the IFT puzzle and lay the groundwork for future studies of IFT in *Tetrahymena*.

REFERENCES

Burton, K., and L. Taylor. 1997. Traction forces of cytokinesis measured with optically modified substrata. *Nature*. 385:450-454.

Henson, J.H., D.G. Cole, M. Terasaki, D. Rashid, and J.M. Scholey. 1995. Immunolocalization of the heterotrimeric kinesin-related protein KRP(85/95) in the mitotic apparatus of sea urchin embryos. *Dev.Biol.* 171:182-194.

Kozminski, K.G., P.L. Beech, and J.L. Rosenbaum. 1995. The Chlamydomonas kinesin-like protein FLA10 is involved in motility associated with the flagellar membrane. *J.Cell Biol.* 131:1517-1527.

Lux, F., III, and S.K. Dutcher. 1991. Genetic interactions at the FLA10 locus: suppressors and synthetic phenotypes that affect the cell cycle and flagellar function in Chlamydomonas reinhardtii. *Genetics*. 128:549-561.

Marshall, W.F., and J.L. Rosenbaum. 2001. Intraflagellar transport balances continuous turnover of outer doublet microtubules: implications for flagellar length control. *J Cell Biol.* 155:In Press.

Marszalek, J.R., and L.S. Goldstein. 2000. Understanding the functions of kinesin-II. *Biochemica et Biophysica Acta*. 1496:142-150.

Signor, D., K.P. Wedaman, L.S. Rose, and J.M. Scholey. 1999. Two heteromeric kinesin complexes in chemosensory neurons and sensory cilia of Caenorhabditis elegans. *Mo. Biol. Cell*. 10:345-360.

Vashishtha, M., Z. Walther, and J.L. Hall. 1996. The kinesin-homologous protein encode by the *Chlamydomonas FLA10* gene is associated with basal bodies and centrioles. *J. Cell Sci.* 109:541-549.

Yang, Z., and L.S.B. Goldstein. 1998. Characterization of the KIF3C neural kinesin-like motor from mouse. *Mol. Biol. Cell*. 9:249-261.

Zang, J.-H., G. Cavet, J.H. Sabry, P. Wagner, S.L. Moores, and J.A. Spudich. 1997. On the role of myosin-II in cytokinesis: division of *Dictyostelium* cells under adhesive and nonadhesive conditions. *Mol. Biol. Cell*. 8:2617-2629.

FIGURE LEGENDS

Figure 6.1 Speculative model of ciliary assembly and IFT in light of my dissertation studies. (1) Ciliary structural subunits may associate with IFT rafts near the basal bodies. Only a subset of rafts may be activated either for motor binding or binding to tubulins, radial spokes, dynein arms, etc. (2) Activated rafts are transported to the ciliary tip and deposit there cargo which may inactivate the rafts. (3) An extracellular signaling molecule could be secreted near the base of cilia and (4) a receptor could locate in the ciliary tip membrane. (A) Tips of shorter cilia would be more competitive than longer cilia (B) for binding to a short range highly labile extracellular factor. (5) Binding of the extracellular molecule to the receptor may activate rafts through Rft1p. (6 and 7). When rafts return to the cell body, only rafts with activated Rft1p can be recycled.

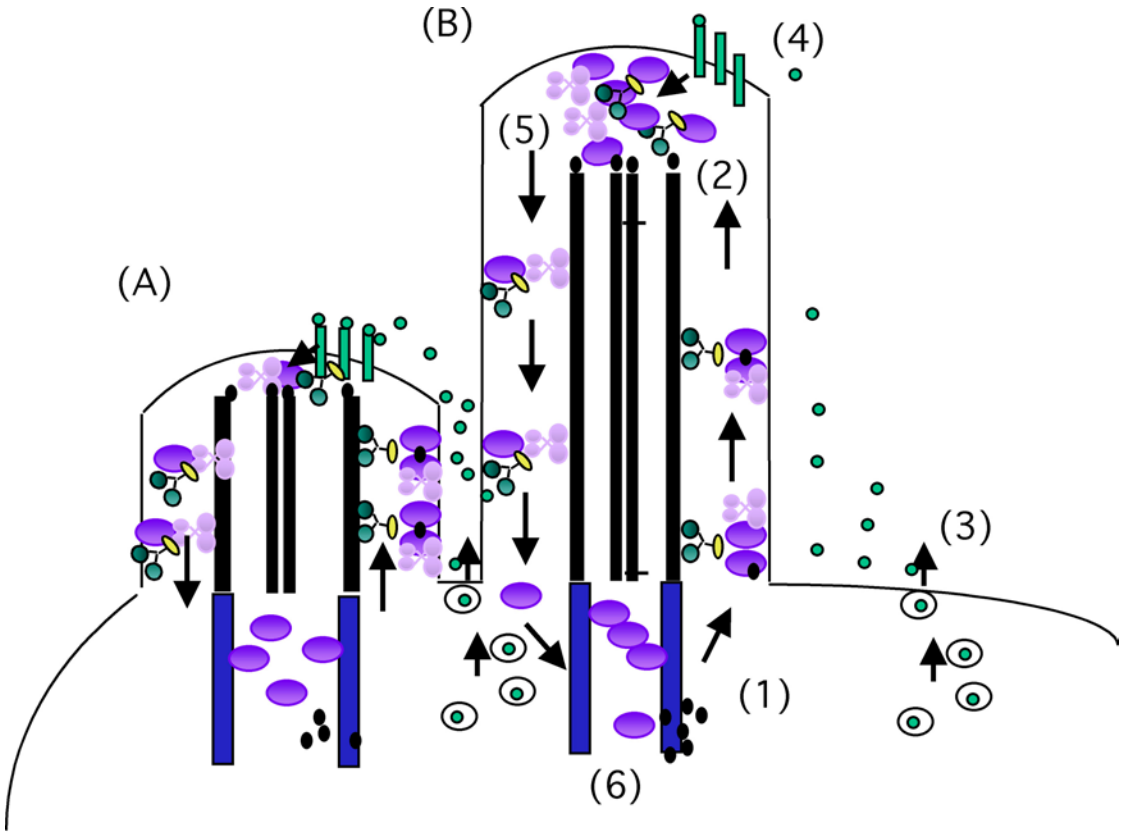

Figure 6.1